

**ESTUDIO DE LA DINAMICA ESTOCASTICA
MEDIANTE TIEMPOS DE PRIMER PASO**

Memoria de la Tesis Doctoral presentada por
Laureano Ramírez de la Piscina y Millán

y dirigida por José M. Sancho Herrero

Junio 1990

D. José María Sancho Herrero
Catedrático de Física de la Materia Condensada

CERTIFICA: Que la presente memoria titulada *Estudio de la Dinámica Estocástica mediante Tiempos de Primer Paso* ha sido realizada bajo su dirección en el Departamento de Estructura y Constituyentes de la Materia, y corresponde a una Tesis para optar al grado de Doctor en Ciencias Físicas.

Barcelona a 18 de Junio de 1990



Quisiera expresar en primer lugar mi más sincero agradecimiento al Dr. Jose María Sancho por la dirección y la ayuda que me ha brindado durante la realización de esta tesis, y por haberme introducido en esta rama de la Mecánica Estadística.

También la colaboración con los doctores F.J. de la Rubia, F. Sagués, y A. Hernández, así como con K. Lindenberg y G.P. Tsironis, de la Univ. de California.

Un recuerdo especial a J. Casademunt, con quien siempre tuve la ocasión de clarificar ideas, y a J.I. Jiménez, quien siempre me mostró su amistad y entusiasmo.

Quisiera agradecer finalmente a los compañeros del Dep. de Estructura y Constituyentes de la Materia de la U.B., y del Dep. de Física Aplicada de la U.P.C., y muy especialmente a C. Auguet, la amistad y ayuda en todo momento.

INDICE

I.	Introducción	
I.1	Contexto	I.1
I.2	Ruidos y Procesos	I.6
I.3	Caracterización de la Dinámica del Sistema .	I.11
I.4	Tiempos de Paso en Sistemas Markovianos Unidimensionales	I.14
I.5	Tiempos de Paso en Sistemas con Ruido de Color	I.20
I.6	Simulación	I.27
I.7	Esquema del Trabajo	I.30
I.8	Conclusiones, Resultados Originales y Perspectivas	I.42
	Referencias	I.50
II.	First Passage Time for a Bistable Potential Driven by Colored Noise	
II.1	General Remarks	II.1
II.2	A Lower Bound for the Critical Noise of the Fluctuating Potential Approximation	II.24
II.3	Highly Colored Noise	II.32
II.4	New Aspects of the Bistable Problem	II.41
III.	First Passage Times for a Marginal State Driven by Colored Noise	
IV.	Stochastic Dynamics of the Chlorite-Iodine Reaction	

I. INTRODUCCION

I.1

I.1 CONTEXTO

El estudio de sistemas fuera del Equilibrio constituye una de las ramas más interesantes de la Física Moderna. Sin duda, ha sido en este tipo de sistemas donde se ha encontrado la más rica fenomenología, y donde más interrelación tiene la Física con otras áreas de la Ciencia.

Sin embargo, al contrario de lo que se encuentra en la Física del Equilibrio, en estos problemas se carece de una formulación general y unificada para su tratamiento. Más bien se ha desarrollado en cada sistema sólo aspectos parciales, adoptando en cada caso la metodología que parece más apropiada. Básicamente, el origen de la carencia de tal formulación radica en la gran complejidad de los sistemas involucrados. La proyección de la evolución de todas las variables sobre unas pocas variables relevantes suele conducir a ecuaciones de evolución (que muchas veces sólo han podido ser obtenidas de forma fenomenológica) no lineales, de difícil tratamiento. Son estas ecuaciones las que describen el diagrama de fases y bifurcaciones del sistema. Sólo soluciones estacionarias en ciertas condiciones particulares de estas ecuaciones corresponden a estados de equilibrio, y pueden ser tratados por la teoría Termodinámica usual.

Además, la propia dinámica de los grados de libertad olvidados induce fluctuaciones en el comportamiento de las

I.2

variables relevantes que no aparecen contempladas en sus ecuaciones deterministas. Estas fluctuaciones son importantes por el hecho de que van a hacer posible toda una variedad de procesos nuevos como la evolución entre diversos atractores, o la formación de estructuras disipativas.^{1,2} El tratamiento de estos procesos requiere, pues, un punto de vista en el que la evolución de los sistemas en el espacio de fases es estocástica. Todo esto nos sitúa en el marco de los Procesos Estocásticos, que constituye el contexto del presente trabajo.

Un sistema estocástico ya no evoluciona con una trayectoria determinista en el espacio de parámetros, sino que tendrá definida una cierta distribución de probabilidad en ese mismo espacio. Existe una doble formulación en el estudio de estos sistemas. Una posibilidad consiste en el tratamiento de una ecuación maestra para la evolución de la probabilidad de transición. La formulación que utilizaremos, posiblemente más intuitiva, parte de ecuaciones diferenciales de tipo Langevin para las variables del sistema, en las que se distingue la acción de una fuerza determinista, que puede ser no lineal y cuya forma da cuenta del tipo de proceso que se está llevando a cabo, y un término estocástico o ruido, que modeliza las fluctuaciones. Esta ecuación recibe el nombre de Ecuación Diferencial Estocástica [SDE], y tiene la forma

I.3

$$\dot{x}(t) = f(x(t)) + g(x(t)) \xi(t) \quad (1)$$

Las funciones $f(x)$ y $\xi(t)$ son las fuerzas determinista y estocástica respectivamente. La función $g(x)$ contiene el acoplamiento entre las fluctuaciones y el sistema. La terminología usual califica al ruido de aditivo cuando g es constante; en caso contrario el ruido se dice multiplicativo. Para sistemas con varias variables y varias fuentes de ruido, la ecuación anterior se debe entender como una ecuación matricial.

En la ecuación (1) tanto $\xi(t)$ como $x(t)$ son conjuntos de variables aleatorias etiquetadas con el parámetro t , lo que recibe el nombre de Proceso Estocástico. La virtud del planteamiento de la SDE es que nos permite relacionar las estadísticas de $\xi(t)$ (que, con toda generalidad, se supondrá lo más sencilla posible) y de $x(t)$ (que representa la dinámica del sistema). Por tanto, las propiedades estadísticas del ruido definen por completo el sistema a través de la SDE. Imaginemos una colectividad de sistemas, cada uno de ellos obedeciendo la ecuación (1) con una cierta realización del ruido. La evolución de toda la colectividad nos dará la evolución de su distribución de probabilidad.

La justificación de la SDE a partir de las ecuaciones microscópicas del sistema ha sido realizada en algunos casos

particulares y bajo ciertas aproximaciones.³ Comunmente, las fluctuaciones se introducen de forma más fenomenológica, añadiendo simplemente el ruido a una ecuación determinista, y comprobando a posteriori que el modelo describe correctamente el sistema físico estudiado. La elección de la función $g(x)$ y de los parámetros del ruido depende del origen de las fluctuaciones presentes en el sistema. Estas pueden estar originadas por el gran número de grados de libertad ocultos del sistema, o bien por la naturaleza cuántica del mismo, lo que se conoce como ruido interno; su efecto es el ensanchamiento de las distribuciones de probabilidad alrededor de los estados de equilibrio, no modificando esencialmente el comportamiento del sistema (en el caso de fluctuaciones no homegéneas puede haber algún cambio en la naturaleza o en la posición de los puntos de transición^{4,5}). Su intensidad escala con una potencia inversa del tamaño del sistema y, por tanto, desaparece en el límite termodinámico. Estas fluctuaciones se modelan mediante un ruido aditivo que además, debido a la diferencia en las escalas de tiempo de las fluctuaciones frente a los tiempos de respuesta del sistema, se toma con tiempo de correlación cero (ruido blanco).

Además, puede existir una fuente adicional de fluctuaciones cuando alguno de los parámetros de control del sistema fluctúa, debido a la acción del entorno, lo cual se conoce como ruido externo. En este caso el ruido puede ser multiplicativo, su intensidad no tiene por qué ser pequeña, y

I.5

pueden existir correlaciones. Este tipo de ruido afecta drásticamente al sistema, ya que puede cambiar todo su diagrama de fases. En ciertos sistemas la presencia de fluctuaciones estabiliza nuevos estados, proceso que presenta muchas de las características de las transiciones de fase de Equilibrio, y que se ha dado en llamar transiciones inducidas por ruido.^{6,7}

Nosotros ignoraremos el problema de la justificación del modelo representado por la ecuación (1). En lugar de ello supondremos conocida la SDE para un sistema concreto, y trataremos de obtener información sobre el proceso dinámico que el sistema, gobernado por (1), está llevando a cabo.

Ecuaciones similares a (1) pueden obtenerse también para sistemas con dependencia espacial, pero el tratamiento de tales sistemas se encuentra aún en sus inicios. En este trabajo nos limitaremos a sistemas cero-dimensionales con una sola variable, pero, como veremos, su estudio abarca todavía una gran variedad de procesos, y los resultados que se obtengan podrán ser aplicados a un gran número de sistemas diferentes.

I.2 RUIDOS Y PROCESOS

La hipótesis más frecuente sobre el término estocástico que aparece en la Ec. (1) es que sigue una distribución normal, i.e. es gaussiano. En la mayoría de sistemas el ruido modela la acción de un gran número de factores aleatorios cuya suma, en virtud del teorema de límite central, se aproxima a la distribución gaussiana. No obstante, en ciertos modelos concretos se ha usado otros tipos de ruidos como el ruido blanco de Poisson, o el ruido dicotómico, que no trataremos aquí.

En cuanto a las posibles correlaciones del ruido, se suele suponer a éste descorrelacionado a tiempos distintos. Un ruido de este tipo tiene un espectro constante de frecuencias, y recibe el nombre de ruido blanco. Su función de correlación se toma como

$$\langle \xi(t) \xi(t') \rangle = 2D \delta(t-t') \quad (2)$$

donde el parámetro D representa la intensidad del ruido.

Hay que mencionar aquí que el significado de la SDE es ambiguo si el término estocástico es un ruido blanco, ya que se puede dar un número infinito de prescripciones para integrar la ecuación (1). De estas prescripciones, las únicas de interés físico son las de Ito y Stratonovich. La interpretación de Ito⁸ supone una completa independencia entre

los valores del proceso estocástico y los del ruido en el mismo instante de tiempo. La interpretación de Stratonovich⁹ tiene el interés de que resulta ser el límite de un ruido correlacionado con el tiempo de correlación tendiendo a cero, hecho relacionado con que el cálculo con una SDE de Stratonovich, a diferencia de una SDE de Ito, sigue las reglas del cálculo normal.^{10,11} En todo lo que sigue, seguiremos la interpretación de Stratonovich de las SDE con ruido blanco.

El ruido blanco es el caso límite de una fuerza estocástica que evoluciona muy rápidamente en el tiempo. Desde el punto de vista físico, esto significa que la escala de tiempo de las fluctuaciones es muy pequeña en comparación con los tiempos típicos de respuesta del sistema. Esta es una muy buena aproximación en el caso de fluctuaciones de origen interno, y puede ser un buen punto de partida en el análisis de sistemas sometidos a ruido externo.

Lo dicho anteriormente, junto con las interesantes propiedades matemáticas del ruido blanco, han hecho que éste sea el más ampliamente usado en la literatura. Un ruido blanco no tiene memoria, por lo que los procesos gobernados por él tienen la propiedad de si el estado presente del proceso es conocido, entonces cualquier información adicional sobre su historia pasada es irrelevante en la predicción de su evolución futura.^{12,13} Esta propiedad define al proceso como markoviano. La suposición de ruido blanco permite, pues,

aplicar todo el potente arsenal matemático de la teoría de los procesos de Markov, que es ampliamente conocida. En particular, su distribución de probabilidad $P(x, t)$ obedece una ecuación de Fokker-Planck de la que es posible extraer información exacta sobre su estado estacionario.¹⁴ En el caso de sistemas de varias variables, para poder obtener esa misma información son necesarias unas condiciones restrictivas adicionales conocidas como balance detallado.¹⁵

Sin embargo, el ruido blanco no puede ser más que una aproximación, más o menos buena, de un ruido real. Las fluctuaciones en un sistema tienen un tiempo de correlación que no es estrictamente cero y que, en el caso de las de origen externo, no tiene ya por qué ser pequeño. Entre los sistemas físicos que han precisado una descripción con un ruido correlacionado, podemos citar la resonancia en un campo magnético fluctuante,¹⁶ la intensidad de salida de un dye laser^{17,18} y, en general, las situaciones experimentales en las que es posible controlar la fuente de ruido.

Dedicaremos una buena parte de este trabajo a sistemas sometidos al ruido de Ornstein-Uhlenbeck, que es un ruido gaussiano con una función de correlación que decrece exponencialmente de la forma

$$\langle \xi(t) \xi(t') \rangle = \frac{D}{\tau} e^{-\frac{|t-t'|}{\tau}} \quad (3)$$

Los parámetros D y τ son la intensidad y el tiempo de correlación del ruido respectivamente. El límite $\tau \rightarrow 0$ corresponde al ruido blanco (2).

Un proceso llevado por un ruido correlacionado, llamado ruido de color en oposición al ruido blanco, no es markoviano y, en general, no es exactamente resoluble.⁷ La ecuación de evolución para la probabilidad ya no es la conocida ecuación de Fokker-Planck, sino un desarrollo en derivadas de orden infinito. Es posible recuperar la markovicidad ampliando el espacio de variables a $\{x, \xi\}$, (y, por tanto, disponiendo de una ecuación de Fokker-Planck en dos variables para la probabilidad $P(x, \xi, t)$), pero ese sistema de dos variables no cumple la condición de balance detallado.

En la última década se han publicado una serie de resultados aproximados para el problema del ruido de color. Una gran parte de ellos, que podríamos llamar aproximaciones cuasi-markovianas, obtienen ecuaciones de Fokker-Planck efectivas para la variable x a partir de desarrollos en D o en τ , de las cuales se puede obtener información por los métodos usuales de los procesos de Markov.^{19,20} Este enfoque tiene algunos problemas originados por el carácter específicamente no markoviano de las condiciones de frontera en algunos

procesos; por eso otros autores han preferido realizar desarrollos en τ directamente sobre el cálculo en la ecuación de Fokker-Planck de dos variables, en la que las condiciones de frontera pueden ser tratadas correctamente.^{21,22} Para el caso de relajación de sistemas inestables, la Teoría Cuasideterminista [QDT]²³ aprovecha la linealidad de los primeros estadios de la relajación para obtener resultados válidos para todo τ y pequeña D. También se ha atacado el límite $\tau \rightarrow \infty$,^{24,25} en el que el ruido tiene un valor constante, con el fin de obtener pistas sobre el comportamiento para τ finito. Por último, una formulación distinta del problema basada en integrales de camino,^{26,27} está empezando a dar resultados en sistemas con ruido de cualquier tiempo de correlación e intensidad pequeña.^{28,29}

I.3 CARACTERIZACION DE LA DINAMICA DEL SISTEMA

Los sistemas que han precisado una descripción en términos de una SDE han sido aquellos en los que las fluctuaciones juegan un papel fundamental en su comportamiento. En ellos, la evolución de un cierto parámetro (o conjunto de ellos), representado por la variable x , se produce desde su valor inicial hasta un cierto valor final que indica que el proceso se ha realizado.

Un conocimiento completo de la evolución del sistema (1) supondría la obtención de toda la jerarquía de distribuciones conjuntas de probabilidad $P(x,t)$, $P(x,t;x',t')$, ... para todo tiempo (sólo las dos primeras si el proceso es markoviano). Es posible, sin embargo, obtener caracterizaciones útiles del proceso dinámico representado por esa ecuación sin necesidad de obtener la evolución de las distribuciones de probabilidad. La caracterización más representativa desde el punto de vista físico es el valor de la escala de tiempo en el que la evolución tiene lugar.

La caracterización de sistemas por medio de sus tiempos característicos es, pues, sujeto de investigación tanto teórica como experimental. Podemos citar investigaciones acerca de la relajación crítica de estados de equilibrio (critical slowing down),³⁰ tiempos de formación de dominios magnéticos, gotas u otras estructuras espaciales,³¹ tiempo de

aparición de un orden macroscópico,³² tiempos de paso en sistemas físicos, químicos y biológicos,³³ dinámica de láseres^{34,35} y de cristales líquidos.³⁶

Posiblemente el tiempo característico más conocido y más ampliamente utilizado es el Tiempo Medio de Primer Paso [MFPT]. Este tiempo se define como el promedio sobre muchas realizaciones del tiempo en el que el sistema cruza por primera vez una frontera previamente establecida. Los momentos superiores del tiempo de primer paso dan, además, una idea del grado de aleatoriedad presente en dicha evolución. Este tiempo resulta ser de muy fácil medida en una simulación o en un experimento, pero en general su cálculo exacto sólo es posible en procesos markovianos.

Una definición alternativa de escala de tiempo es la del Tiempo de Relajación.^{37,38} Esta definición toma como auxiliar una función de las coordenadas del sistema cuyo promedio relaja hacia su valor estacionario, midiendo el tiempo en el que se produce esta relajación. Frente al MFPT permite también la caracterización de la dinámica de las fluctuaciones del estado estacionario. Además, su formalismo carece de muchos de los problemas matemáticos del MFPT, e incluye de forma natural el tratamiento de cualquier tipo de condiciones iniciales.

Una tercera alternativa lo constituye el inverso del valor propio más bajo del operador de evolución temporal del

I.13

sistema. Este tiempo es especialmente indicado para el cálculo numérico por el método de fracciones continuas.

I.4 TIEMPOS DE PASO EN SISTEMAS MARKOVIANOS UNIDIMENSIONALES

Nuestra intención en esta sección es establecer el método standard^{39,40} empleado en el cálculo de tiempos de paso, restringiéndonos al caso unidimensional con ruido blanco. En la sección siguiente revisaremos los métodos empleados en el caso de sistemas no markovianos.

Consideraremos el proceso dinámico gobernado por la SDE unidimensional (1), con ruido blanco. Es conocido que la evolución de la probabilidad condicional $P(x', t' | x, t)$ viene dada por la ecuación de Fokker-Planck.

$$\frac{\partial}{\partial t'} P(x', t' | x, t) = L(x') P(x', t' | x, t) \quad (4)$$

donde $L(x)$ es el operador de Fokker-Planck⁴¹

$$L(x) = -\frac{\partial}{\partial x}(f(x) + Dg(x)g'(x)) + D\frac{\partial^2}{\partial x^2}g^2(x) \quad (5)$$

Esta formulación recibe el nombre de *forward*, ya que plantea la evolución del estado final una vez fijado el estado inicial, que aparece en la ecuación de forma paramétrica. La solución estacionaria de la Ec. de Fokker-Planck es, caso de que exista,

$$P_{ss}(x') = \lim_{t \rightarrow \infty} p(x', t | x, 0) = \frac{N}{g(x')} \exp \left[\frac{1}{D} \int^{x'} dy \frac{f(y)}{g^2(y)} \right] \quad (6)$$

El objetivo al calcular el MFPT de este sistema es, como ya hemos dicho, encontrar una descripción de la dinámica de este sistema. De hecho, el conocimiento completo de la distribución de tiempos de paso supone el conocimiento completo de esa dinámica. Usualmente, se buscan los dos primeros momentos: el primero (MFPT) da la escala de tiempos del proceso, el segundo da una idea de la aleatoriedad del mismo. Este último es necesario para completar la información del MFPT, puesto que existe siempre una parte de la dinámica dominada por las fuerzas deterministas.

El cálculo de los tiempos de paso requiere una formulación *backward* del problema, en la que se fija el estado final (o frontera asociada al tiempo de paso) y se necesita la dependencia en la condición inicial. La ecuación backward es la adjunta de (4)

$$\frac{\partial}{\partial t} P(x', t' | x, t) = -L^+(x) P(x', t' | x, t) \quad (7)$$

Consideraremos que la partícula está en la posición x en el instante inicial $t=0$, y nos preguntamos por el tiempo que permanecerá en el intervalo (a, b) , que se supone contiene a x . En las posiciones límite a, b colocamos sendas barreras absorbentes. De esta forma, si la partícula se encuentra en el intervalo (a, b) en un instante dado, es seguro que todavía no ha cruzado la frontera del problema.

Definamos $G(x, t) = \text{Prob}(T \geq t)$ la probabilidad de que la partícula todavía se encuentre dentro del intervalo (a, b) en el instante t .

$$G(x, t) = \int_a^b dx' p(x', t | x, 0) \quad (8)$$

Como consecuencia, la cantidad $-\frac{\partial G(x, t)}{\partial t}$ es la densidad de probabilidad correspondiente a la distribución de tiempos de primer paso. Deduciremos la ecuación que obedece la función $G(x, t)$, de la que será posible obtener, mediante cuadraturas, el promedio de cualquier función del tiempo de primer paso. En particular, los momentos de esa distribución vienen dados por

$$T_n(x) = -\int_0^\infty t^n \frac{\partial}{\partial t} G(x, t) dt = n \int_0^\infty t^{n-1} G(x, t) dt \quad (9)$$

Como el sistema es homogéneo en el tiempo, se cumple que $p(x', t | x, 0) = p(x', 0 | x, -t)$, y la Ec. backward (7) se puede escribir de la forma siguiente

$$\frac{\partial}{\partial t} p(x', t | x, 0) = L^+(x) p(x', t | x, 0) \quad (10)$$

con las condiciones de contorno dadas por la condición inicial en x y por las barreras absorbentes en a y b

$$\begin{aligned} p(x', 0 | x, 0) &= \delta(x - x') \\ p(x', t | a, 0) &= p(x', t | b, 0) = 0 \end{aligned} \tag{11}$$

de forma que $G(x, t)$ cumple la ecuación

$$\begin{aligned} \frac{\partial}{\partial t} G(x, t) &= L^+(x) G(x, t) \\ G(x, 0) &= \begin{cases} 1 & x \in (a, b) \\ 0 & x \notin (a, b) \end{cases} \\ G(a, t) &= G(b, t) = 0 \end{aligned} \tag{12}$$

Multiplicando esta última ecuación por nt^{n-1} , e integrando sobre la variable t , se obtiene la ecuación que cumplen los momentos $T_n(x)$ (donde definimos $T_0 \equiv 1$)⁴²

$$-n T_{n-1}(x) = L^+(x) T_n(x) \tag{13}$$

con la condición de contorno

$$T_n(a) = T_n(b) = 0 \tag{14}$$

La varianza de la distribución de tiempos de paso $(\Delta T)^2 = T_2 - T^2$ obedece una ecuación con la misma estructura. Tomando la Ec. (13) para $n=1$ y $n=2$, se obtiene

$$L^+(x) (\Delta T(x))^2 = -2D g^2(x) (T'(x))^2 \tag{15}$$

Por tanto, la varianza y los momentos se pueden ir obteniendo por integraciones sucesivas.

En el caso de que una de las fronteras corresponda a una

barrera reflectante, la condición de contorno es ligeramente diferente. Para concretar, supongamos que la coordenada a es una barrera reflectante. Entonces la condición de contorno en a debe ser modificada a

$$\frac{\partial}{\partial x} G(x, t) \Big|_{x=a} = 0 \quad (16)$$

es decir,

$$T'_n(a) = 0 \quad (17)$$

$$T_n(b) = 0$$

Estas últimas condiciones de frontera son las que aparecen en un gran número de casos de interés, y son las utilizadas en los sistemas estudiados en este trabajo.

La integración de las ecuaciones (13) ($n=1$) y (15), con las condiciones de contorno (17), da como resultado

$$T(x) = \int_x^b \frac{dx_1}{Dg^2(x_1) P_{ss}(x_1)} \int_a^{x_1} dx_2 P_{ss}(x_2) \quad (18)$$

para el MFPT, y para su varianza

$$(\Delta T(x))^2 = \frac{4}{D^2} \int_x^b \frac{dx_1}{g^2(x_1) P_{ss}(x_1)} \int_a^{x_1} \frac{dx_2}{g^2(x_2) P_{ss}(x_2)} \quad (19)$$

$$\times \int_a^{x_2} dx_3 P_{ss}(x_3) \int_a^{x_3} dx_4 P_{ss}(x_4)$$

Hemos de señalar aquí que el problema del tiempo de

primer paso por una frontera se ha podido expresar como una condición de contorno absorbente. Cualquier proceso continuo debe tocar una frontera para poder cruzarla, lo que provoca que la distribución de tiempos de primer paso venga dada por una condición de contorno. Esto es debido a la naturaleza continua del proceso. Sin embargo, la naturaleza concreta de la condición de contorno es una consecuencia directa de que el ruido sea blanco.⁴³

I.5 TIEMPOS DE PASO EN SISTEMAS CON RUIDO DE COLOR

El ruido de color gaussiano más sencillo es el proceso de Ornstein-Uhlenbeck,⁴⁴ el cual se puede generar a partir de una SDE con un ruido blanco auxiliar $\eta(t)$:⁴⁵

$$\xi(t) = -\frac{1}{\tau} \xi(t) + \frac{1}{\tau} \eta(t) \quad (20)$$

La función de correlación de un ruido de este tipo es (3). Cuando $\xi(t)$ actúa en la SDE (1), el sistema formado por las dos variables $\{x, \xi\}$ es markoviano, y su evolución, dada por la pareja de ecuaciones (1), (20), obedece la ecuación de Fokker-Planck

$$\frac{\partial}{\partial t'} P(x', \xi', t' | x, \xi, t) = L(x', \xi') P(x', \xi', t' | x, \xi, t) \quad (21)$$

con

$$L(x, \xi) = -\frac{\partial}{\partial x} (f(x) + g(x) \xi) + \frac{1}{\tau} \frac{\partial}{\partial \xi} \xi + \frac{D}{\tau^2} \frac{\partial^2}{\partial \xi^2} \quad (22)$$

Ya se ha mencionado anteriormente que este sistema no cumple las condiciones de balance detallado, lo que impide que se pueda obtener en general, por ejemplo, información exacta sobre su estado estacionario. Tampoco se conoce ninguna relación exacta entre la dinámica dada por (21), (22) y el problema del MFPT.

Dado que la dificultad proviene de tratar con un sistema

en dos variables, una posible solución es encontrar la ecuación dinámica que obedece la variable x , i.e. la ecuación de evolución para $P(x', t' | x, t)$. Esta ecuación puede obtenerse de muchas maneras, incluyendo la integración de la ecuación de Fokker-Planck (21), (22) sobre la variable ruido. La expresión resultante es, en general, no local, y su conexión con el MFPT es obscura. En particular, éste ya no puede ser expresado como un problema de condiciones de contorno.

La mayoría de las aproximaciones realizadas sobre este sistema tratan de representar la evolución de $P(x', t' | x, t)$ mediante una ecuación de Fokker-Planck efectiva que tenga en cuenta de forma aproximada los efectos de la correlación del ruido. Para ello pueden usarse diversas técnicas, pero siempre se toma como muy pequeño alguno de los parámetros del ruido, D o τ . La ventaja de esta formulación es, disponiendo de una Ec. de Fokker-Planck para una variable, es posible aplicar las técnicas de la sección anterior para obtener el estado estacionario y su conexión con el MFPT.

El método standard¹⁹ de atacar este problema parte de la Ecuación de Liouville estocástica⁴⁶, en la que se toma un promedio sobre realizaciones, con el resultado

$$\begin{aligned} \frac{\partial}{\partial t'} P(x', t' | x, t) &= -\frac{\partial}{\partial x'} f(x') P(x', t' | x, t) \\ &- \frac{\partial}{\partial x'} g(x') \langle \xi(t) \delta(X(t) - x) \rangle \end{aligned} \quad (23)$$

donde la trayectoria $X(t)$ es un funcional del ruido $\xi(t)$ y

$$P(x', t' | x, t) = \langle \delta(X(t) - x') \rangle_{X(0)=x} \quad (24)$$

Es posible utilizar la gaussianidad del ruido mediante el Teorema de Novikov,⁴⁷ resultando la (todavía) exacta ecuación de evolución

$$\begin{aligned} \frac{\partial}{\partial t'} P(x', t' | x, t) &= -\frac{\partial}{\partial x'} f(x') P(x', t' | x, t) - \frac{\partial}{\partial x'} g(x') \frac{\partial}{\partial x'} \\ &\times \int_t^{t'} ds \frac{D}{\tau} e^{-\frac{|t'-s|}{\tau}} \left\langle \frac{\delta X(t')}{\delta \xi(s)} \Big|_{X(t)=x'} \delta(X(t) - x') \right\rangle \end{aligned} \quad (25)$$

Todo el problema se reduce a encontrar una expresión aproximada tratable (en la que no aparezca explícitamente el ruido) de la función respuesta, definida como la derivada funcional $\frac{\delta X(t')}{\delta \xi(t)}$. De esta forma, integrando la Ec. (25) se

llega a una expresión formalmente idéntica a las Ecs. (4), (5), pero donde el operador de evolución tiene un coeficiente de difusión local que depende de τ

$$L(x) = -\frac{\partial}{\partial x} (f(x) + D_\tau(x) g(x) g'(x)) + \frac{\partial^2}{\partial x^2} D_\tau(x) g^2(x) \quad (26)$$

De esta forma, siguiendo el mismo procedimiento que en caso de ruido blanco, se llega a la expresión para el MFPT⁴⁸

$$T(x) = \int_x^b \frac{dx_1}{D_\tau(x_1) g^2(x_1) P_{ss}(x_1)} \int_a^{x_1} dx_2 P_{ss}(x_2) \quad (27)$$

con

$$P_{ss}(x) = \frac{N}{D_\tau(x) g(x)} \exp \left[\int_x^\infty dy \frac{f(y)}{D_\tau(y) g^2(y)} \right] \quad (28)$$

Se han desarrollado diversos métodos para encontrar expresiones de la difusión efectiva $D_\tau(x)$. Aproximando a primer orden en τ el desarrollo correspondiente a la Ec. (25) se obtiene la llamada *small τ approximation*, dada por

$$D_\tau(x) = D \left(1 + \tau g(x) \left(\frac{f(x)}{g(x)} \right)' \right) \quad (29)$$

Otra expresión, válida a primer orden en D y conservando los términos de todos los órdenes en τ , es la serie correspondiente a la llamada *Best Fokker-Plank Equation*, representada simbólicamente como

$$D_\tau(x) = D \frac{f(x)}{g(x)} \left(1 + \tau f(x) \frac{d}{dx} \right)^{-1} \frac{g(x)}{f(x)} \quad (30)$$

Uno de los inconvenientes de este tipo de aproximaciones es la aparición de fronteras no naturales en el problema, debido a la posible presencia de cambios de signo en la difusión efectiva $D_\tau(x)$ y, por tanto, de zonas no físicas de probabilidad negativa. Es posible evitar esto utilizando resumaciones de términos de órdenes más altos en τ . Las

aproximaciones que se obtienen mediante estos métodos coinciden en el término lineal, y su dominio de validez en el cálculo del MFPT se limita siempre a valores pequeños de τ . En este trabajo, utilizaremos estos resultados como una aproximación de primer orden en τ , con el fin de obtener de forma consistente correcciones a primer orden en τ en el MFPT.

La formulación mediante una ecuación de Fokker-Planck efectiva supone implícitamente que las condiciones de contorno son las mismas que las del mismo sistema con ruido blanco, lo cual sólo es cierto bajo ciertas condiciones. Este es un punto al que volveremos varias veces a lo largo de este trabajo.

Las condiciones de contorno pueden introducidas de forma correcta en la Ec. de Fokker-Planck en dos variables (21), aunque la conexión, incluso aproximada, con el MFPT puede resultar problemática. Esto se ha podido llevar a cabo en algunos casos particulares.^{21,22} Una forma de hacerlo, diferente de la explicada, consiste en formular el problema del MFPT considerando el estado estacionario correspondiente al caso de partículas inyectadas a un ritmo constante y que, evolucionando de acuerdo con Ec. (21), son aniquiladas por la barrera absorbente.^{49,21}

Recientemente se han desarrollado unas aproximaciones diferentes al problema del MFPT con ruido de color, basadas en formulaciones de integrales de camino.²⁶⁻²⁹ En este formalismo,

la trayectoria se obtiene minimizando un cierto funcional de la misma, llamado acción. La aplicación al paso entre los dos pozos de un sistema biestable da, para D pequeña, un MFPT de la forma

$$T = K(\tau) e^{S(\tau)/D} \quad (31)$$

donde $S(\tau)$ es el valor de la acción mínima, y $K(\tau)$ da cuenta de las fluctuaciones alrededor de la trayectoria de acción mínima. Esta trayectoria se obtiene numéricamente. Por el momento se han podido obtener, en el límite $D \rightarrow 0$, valores del término exponencial de la Ec. (31) para el potencial de Ginzburg-Landau,^{27,29} y del MFPT para un sistema biestable formado por partes lineales.²⁸

La Teoría QDT^{23,50} proporciona una aproximación alternativa al MFPT correspondiente a la relajación de estados inestables. Esta teoría sustituye la dinámica estocástica de la Ec. (1) por una dinámica determinista con una condición inicial aleatoria. Consideraremos la SDE correspondiente a un sistema inestable lineal

$$\dot{x} = \alpha x + \xi(t) \quad (32)$$

Esta ecuación gobierna los primeros estadios de la relajación de los estados inestables, en los que el ruido desencadena el proceso de relajación. La solución de la Ec. (31), con la condición inicial $x(0)=0$, es

$$x(t) = h(t) e^{\alpha t} \quad (33)$$

donde

$$h(t) = \int_0^t dt' e^{\alpha t'} \xi(t') \quad (34)$$

Para tiempos $t \ll \alpha^{-1}$, τ , se puede reemplazar $h(t)$ por $h(\infty)$, que es un número gaussiano de media cero y varianza

$$\langle h^2(\infty) \rangle = \frac{D}{\alpha(1+\alpha\tau)} \quad (35)$$

De esta forma, la dinámica lejos de el punto inestable es determinista, quedando el efecto de las fluctuaciones en una condición inicial. El Tiempo de Paso correspondiente a la llegada a una distancia R del punto inicial viene dado, para intensidades pequeñas de ruido, por

$$T = \frac{1}{2\alpha} \ln \left(\frac{\alpha R^2}{2D} (1+\alpha\tau) \right) - \frac{1}{2} (\gamma + 2 \ln 2) \quad (36)$$

I.6 SIMULACION

La simulación numérica de los sistemas estudiados es una potente herramienta auxiliar a la hora de elaborar modelos y comprobar la validez de las aproximaciones efectuadas. En el caso de la integración de una SDE, el método de simulación es diferente del de una ecuación diferencial ordinaria. Lo que se hace es obtener trayectorias particulares a partir de realizaciones diferentes del ruido, sobre las que se realizan los promedios estadísticos correspondientes. Cada una de las realizaciones corresponde a una secuencia distinta de números aleatorios, generados con la estadística apropiada mediante las técnicas usuales de los métodos de Monte Carlo.

Los algoritmos empleados en la simulación de la SDE (1) son standard, y están descritos en la Ref. 19. Describiremos a continuación las expresiones más importantes de la simulación para ruido blanco y ruido de color.

Consideremos en primer lugar la SDE (1) con el ruido blanco gaussiano de correlación (2). La trayectoria se calcula mediante una discretización en el tiempo, con un *step* Δ . Integrando (1) de t a $t+\Delta$, se obtiene el valor de $q(t+\Delta)$ a partir $q(t)$:

$$\begin{aligned} x_{t+\Delta} = & x_t + f(x_t) \Delta + g(x_t) X_1(t) \\ & + \frac{1}{2} g(x_t) g'(x_t) X_1^2(t) + O(\Delta^{3/2}) \end{aligned} \quad (37)$$

donde $X_1(t)$ es un número gaussiano de media nula y varianza

$$\langle X_1^2(t) \rangle = 2D\Delta \quad (38)$$

En el caso de tener ruido de color de Ornstein-Uhlenbeck, hay que integrar simultáneamente las dos ecuaciones (1), (20). Un procedimiento similar al utilizado para ruido blanco da como resultado para la evolución de la pareja de variables $\{x, \xi\}$

$$\begin{aligned} x_{t+\Delta} = & x_t + f(x_t) \Delta + g(x_t) \xi_t \Delta + \frac{1}{2} g'(x_t) g(x_t) \xi_t^2 \Delta^2 \\ & + \frac{1}{2} f'(x_t) f(x_t) \Delta^2 + \frac{1}{2} f'(x_t) g(x_t) \xi_t \Delta^2 \\ & + \frac{1}{2} g'(x_t) f(x_t) \xi_t \Delta^2 - \frac{1}{2} \tau^{-1} g(x_t) \xi_t \Delta^2 \\ & + \tau^{-1} g(x_t) X_2(t) + O(\Delta^{5/2}) \end{aligned} \quad (39)$$

$$\xi_{t+\Delta} = \xi_t - \frac{1}{\tau} \xi_t \Delta + \frac{1}{\tau} X_1(t) + O(\Delta^{3/2}) \quad (40)$$

donde $X_2(t)$ es un número gaussiano de media nula y varianza

$$\langle X_2^2(t) \rangle = \frac{2}{3} D \Delta^3 \quad (41)$$

Además, $X_1(t)$ y $X_2(t)$ no son independientes, sino que se cumple

que

$$\langle X_1(t) X_2(t) \rangle = D\Delta^2 \quad (42)$$

I.7 ESQUEMA DEL TRABAJO

El presente trabajo se centra en el problema de las escalas de tiempo de ciertos tipos de procesos bastante generales. En particular, utilizaremos el formalismo del MFPT en los siguientes sistemas: paso a través de una barrera en un potencial biestable, paso a través de una inestabilidad marginal, y relajación de un sistema determinista bajo la acción de un ruido multiplicativo.

Se ha dividido la exposición en tres partes principales, redactadas en inglés, pues corresponden a trabajos de investigación publicados en ese idioma. Cada una de las secciones es autoconsistente, de forma que incluye las conclusiones correspondientes y su bibliografía. A continuación vamos a comentar los aspectos más relevantes de los mismos.

I.7.a Cap. II: First Passage Time for a bistable potential driven by colored noise.

El Capítulo II es el más extenso, y corresponde al problema del MFPT de un sistema biestable sometido a ruido de color.

El paso de sistemas a través de una barrera de potencial

llevados por fluctuaciones de origen externo ha sido objeto estos últimos años de estudio por parte de numerosos grupos, dando lugar a una serie de resultados parciales y a veces contradictorios, mayormente para el caso $\tau > 0$. El sistema en cuestión obedece la SDE

$$\dot{x} = x - x^3 + \xi(t) \quad (43)$$

El potencial asociado $\phi(x) = -\frac{1}{2}x^2 + \frac{1}{4}x^4$ presenta dos mínimos en $x=1$ y $x=-1$ y un máximo en $x=0$. Cualquier otro potencial biestable llevaría a los mismos resultados, salvo contribuciones no muy relevantes, debido a la universalidad del proceso dinámico. La situación inicial corresponde al ruido en su estado estacionario, y el sistema situado en el pozo $x=-1$. El sistema, bajo la acción del ruido, acaba por cruzar la barrera y alcanza el otro pozo.

Dos MFPT distintos se definen en este sistema, y son calculados por los diferentes grupos: el correspondiente al paso por la coordenada $x=0$, que denominamos T_{top} , y el correspondiente al paso por la coordenada $x=1$, denominado T_{bot} . Los resultados existentes son cálculos asintóticos en alguno de los límites $D \rightarrow 0$ o $\tau \rightarrow \infty$. Ambos límites se caracterizan por un MFPT exponencialmente grande y, por tanto, fuera de las posibilidades de una simulación analógica o digital.

Nuestro objetivo es clarificar el campo de los procesos

biestables, determinando los dominios de validez de las diferentes teorías, y estableciendo la forma en la que debían interpretarse las aproximaciones. Para ello se ha realizado un exhaustivo conjunto de simulaciones del sistema de estudio, y se ha llevado a cabo un análisis teórico de las situaciones no explicadas satisfactoriamente por los resultados disponibles.

En la Sec. II.1,⁵¹ se realiza una simulación digital del sistema biestable bajo la acción de ruido de color, estudiando la dependencia del MFPT en los parámetros del ruido. Para ruido blanco, el resultado teórico de Kramers⁵², resultado asintótico para D pequeña producto de una aproximación *steepest descent*, presenta grandes discrepancias con los valores del MFPT procedentes de la simulación y del cálculo numérico exacto para los valores accesibles de D . Resulta así claro el origen de parte de la confusión acerca de la corrección de los distintos cálculos en el caso de τ pequeña. Siendo estos cálculos resultado del mismo tipo de aproximación asintótica, la forma de poder comparar con las simulaciones sin que la dependencia en τ quede enmascarada por los errores sistemáticos ocasionados por el valor finito de D , es fijarse en la cantidad $T(\tau)/T(\tau=0)$.

El siguiente problema es el relativo a las diferencias entre los distintos MFPT definidos en este sistema. Siendo T_{top} y T_{bot} representativos de la escala de tiempos en la que se produce el paso de uno a otro pozo, es fácil ver que éstos no

atracción del segundo pozo si $\tau > 0$, y por eso T_{top} se aproxima a T_{bot} a medida que aumenta la correlación del ruido.

Así, las teorías que calculan T_{top} en la aproximación cuasi-markoviana de una difusión efectiva para la variable x , en realidad obtienen resultados que se corresponden con T_{sep} , o con $\frac{1}{2}T_{bot}$, como se muestra en la comparación con la simulación. Sólo el cálculo de Doering²¹, realizado en el espacio $\{x, \xi\}$, obtiene la dependencia en $\tau^{1/2}$ observada en la simulación. Por otro lado, respecto al resto de resultados, todas las teorías concuerdan con la simulación para pequeños valores de τ , pero para valores más grandes, donde aparecen las diferencias entre las distintas teorías, ninguna de ellas concuerda especialmente mejor que las demás.

Esto nos lleva a considerar el caso del límite $\tau \rightarrow \infty$. En este límite, la teoría del potencial fluctuante de Tsironis y Grigolini [TG]²⁴ predice la dependencia asintótica del MFPT como una exponencial en $\frac{2}{27} \frac{\tau}{D}$, dependencia no observada en los

rangos de parámetros accesibles mediante simulación o cálculo numérico. Otros cálculos obtienen esta misma dependencia. El análisis de TG está basado en el carácter constante del ruido cuando τ tiende a infinito, de forma que identifican el MFPT con el tiempo necesario para que el ruido alcance el valor crítico mínimo necesario para que se produzca la transición. Para τ finito, sin embargo, el ruido efectúa una relajación (o

pérdida de memoria de su condición inicial, si se prefiere, dictada por su función de correlación) que dura un tiempo del orden de τ , que puede no ser suficiente para que el sistema alcance el segundo pozo. Así pues, el sistema necesita realmente un valor mínimo del ruido más grande que el predicho por TG, dando lugar a un drástico aumento del MFPT. Un trabajo previo,⁵³ recogido en la Sec. II.2, establece una cota inferior para el ruido crítico imponiendo la condición de que el tiempo de transición determinista (con ruido constante) sea menor que τ . Aquí atacamos el cálculo de una corrección al MFPT con τ grande pero finito refinando el cálculo de TG. El argumento utiliza el hecho de que, para τ grande y D pequeña, el ruido relaja de forma determinista siguiendo una ley exponencial conocida. Un análisis lineal del sistema cuando pasa por el punto más alto de la barrera, $x=0$, permite calcular el diferente efecto del ruido (relajando exponencialmente) sobre la transición del sistema según cuál sea su valor inicial y su tiempo de correlación τ . Esto permite establecer una relación entre los valores críticos del ruido para $\tau \rightarrow \infty$ y τ finito. A partir de ello obtenemos una ley de escala que resulta ser el resultado más prometedor obtenido para el MFPT de un sistema biestable con un ruido con tiempo de correlación grande. Según esta ley, el MFPT es τ veces una función del parámetro de escala $\frac{\tau}{D} \left(1 + \frac{1}{\tau}\right)^2$.

Por último, la Sec. II.1 revisa el problema de la

comparación de las escalas de tiempo del sistema biestable con los resultados numéricos del valor inverso del autovalor más bajo de la Ec. de Fokker-Planck bidimensional del sistema (4). Tal cálculo coincide en realidad con T_{sep} o con $\frac{1}{2}T_{bot}$, y sólo para D pequeña, aunque en la literatura se le ha relacionado con frecuencia con T_{top} . Como comentario adicional podríamos decir que T_{sep} y T_{bot} son escalas de tiempo físicamente más relevantes y relacionadas con el proceso de paso de uno a otro dominio de atracción, mientras que la T_{top} encierra información más matemática que física sobre la especial condición de frontera contenida en su definición.

Las secciones II.2⁵³ y II.3⁵⁴ están dedicadas a partes del análisis efectuado sobre el caso del límite τ grande. La Sec. II.2 contiene la ya mencionada explicación del fallo de la teoría de TG para dar valores del MFPT con τ finito. La Sec. II.3 apunta la posibilidad de que el resultado de una dependencia exponencial con un factor 2/27, predicho por TG y por el resto de teorías disponibles, sea incorrecto en un factor 4/3, salvo quizás para valores de τ extraordinariamente grandes, inaccesibles por completo a cualquier experimento o simulación. En efecto, la evidencia de los resultados numéricos disponibles en la literatura, así como una extrapolación de la ley de escala obtenida y confirmada en la Sec. II.1, indican que el coeficiente tiene un valor próximo a 32/81. En esta sección se da una explicación de esta modificación, basada en el análisis de las simulaciones

efectuadas por Mannella y Palleschi⁵⁵. Estos autores comprobaron el aumento del valor crítico del ruido al disminuir τ predicho en Ref. 53, observando que los valores del ruido cuando se produce la transición siguen una distribución cuyo máximo se desplaza de la forma prevista y cuya anchura aumenta al disminuir τ , proponiendo una modificación del resultado TG contemplando la existencia de tal distribución. Nuestro análisis muestra que la anchura finita de esta distribución, aún tendiendo a cero en el límite $\tau \rightarrow \infty$, produce unos efectos exponencialmente grandes en el MFPT, que se traducen en un cambio en el coeficiente de la exponencial tal y como aparece en las simulaciones.

En la Sec. II.4⁵⁶ se hacen dos últimas consideraciones sobre el problema del sistema biestable. La primera de ellas hace referencia a la forma en la que T_{top} se hace igual a T_{bot} cuando τ se hace infinito. Partiendo de las leyes conocidas para τ pequeña, y suponiendo un decaimiento exponencial a 1 del cociente entre las dos cantidades, obtenemos una ley que es confirmada por los datos de la simulación. La segunda de las consideraciones es la existencia de una única escala temporal, que caracterice la evolución del sistema a tiempos largos, incluso para valores grandes de τ . La condición de la existencia de esa única escala temporal es que el autovalor más bajo del operador de evolución (la ecuación de Fokker-Planck bidimensional) esté aislado. Se ve que eso ocurre si el cociente entre el MFPT y su desviación standard

es la unidad, condición que cumplen los resultados de la simulación para todo τ .

I.6.b First Passage Times for a marginal state driven by colored noise

El Capítulo III⁵⁷ está dedicado al cálculo del MFPT en sistemas que presentan inestabilidades de tipo no lineal, llamados marginales, cuando el ruido que actúa es de color. La SDE de estos sistemas tiene una forma típica

$$\dot{x} = \beta + ax^n + \xi(t) \quad (44)$$

con $n > 1$. Cuando $\beta = 0$, el punto $x=0$ es el punto marginal.

El cálculo concreto se ha realizado para un potencial cúbico, i.e. $n=2$, potencial que ya ha sido analizado en el caso de ruido blanco.^{58,59} Aquí obtenemos el primer orden en τ del MFPT y de su varianza, correspondiente al proceso de paso desde una coordenada inicial $x=-\infty$ hasta una final $x=\infty$.

En un modelo de este tipo el ruido realmente sólo actúa en las proximidades del punto marginal, siendo toda la evolución lejos de él resultado de la acción del potencial determinista. Por ello, todos los sistemas que cerca del punto marginal admitan un desarrollo similar a (44), responderán en realidad a la misma física, encontrándose sus diferencias

contenidas en la parte determinista de su evolución (y por tanto, esas diferencias serán fáciles de calcular). Como ejemplo de sistema real con un punto marginal similar encontramos el modelo de Bonifacio-Lugiato para la intensidad de un láser.⁶⁰ En este modelo, la coordenada x se corresponde con la intensidad de luz emitida, y el encendido del láser se efectúa cambiando el valor del parámetro de control β . La correspondencia es total entre los dos modelos, una vez corregida la parte determinista de los resultados.

Es posible extender el resultado (a primer orden en τ) del MFPT del sistema marginal ($\beta=0$) a valores grandes del tiempo de correlación del ruido. Un cálculo dimensional nos dice cómo depende de los parámetros del potencial y del ruido la extensión de la zona alrededor del punto marginal donde la dinámica está dominada por el ruido. Dentro de tal zona, el movimiento del sistema es prácticamente una difusión libre. Suponiendo inicialmente el sistema en $x=0$, es posible calcular exactamente la evolución de la anchura de la distribución de probabilidad $P(x,t)$. Identificando el MFPT como proporcional al tiempo de salida de la zona marginal, e identificando este tiempo con el tiempo necesario para que la distribución de probabilidad alcance una anchura del tamaño de esa zona, se obtiene una ecuación que da el MFPT, y en donde los únicos parámetros son T_0 y T_1 , los órdenes cero y primero del MFPT que han sido calculados por los métodos conocidos. Un cálculo similar es aplicado también al sistema inestable lineal ($n=1$,

$\beta=0$), resultando equivalente a la QDT para D pequeña, pero con buenos resultados para D grande.

1.6.c Stochastic Dynamics of the Chlorite-iodide reaction.

En el Capítulo IV⁶¹ se presenta el caso de un sistema químico en el que existe una fuerte irreproducibilidad experimental en los tiempos de reacción. El mecanismo de reacción se modeliza mediante una ecuación cinética para la variación de la concentración de uno de los productos de reacción, ecuación que, al contrario de los sistemas estudiados en las secciones anteriores, da una evolución determinista sin necesidad de la presencia de fluctuaciones. El tiempo de reacción se corresponde en este formalismo con el MFPT para que la variable que representa esa concentración alcance un cierto valor prefijado.⁶² El elemento de aleatoriedad es atribuido a inhomogeneidades locales amplificadas por la no linearidad del mecanismo de reacción. Estas inhomogeneidades producen que el valor efectivo de la constante de reacción fluctúe, lo que se traduce en las ecuaciones en la presencia de un ruido multiplicativo. Como veremos, el hecho de que el ruido sea multiplicativo explica la fuerte irreproducibilidad del proceso, representada por la varianza de los tiempos de reacción, magnitud que se puede comparar con los experimentos.

El modelo de tal reacción es el siguiente

$$\dot{x} = k_a(\alpha - x)(\beta - 4x) + k_b \frac{x(\alpha - x)}{(\beta - 4x)} + \frac{x(\alpha - x)}{(\beta - 4x)} \xi(t) \quad (45)$$

donde ξ es un ruido blanco de intensidad D. La magnitud experimental que se correlaciona con D es el inverso del stirring o ritmo al que se produce la mezcla de los ingredientes. Con esta formulación se logra predecir los valores medios y las varianzas de los tiempos de reacción.

I.7 CONCLUSIONES, RESULTADOS ORIGINALES Y PERSPECTIVAS

I.7.a Conclusiones

Entre las conclusiones de este trabajo, hay que distinguir entre las más generales, referidas a la problemática de los Tiempos de Paso, y una serie de conclusiones específicamente relacionadas con cada uno de los sistemas concretos que se han estudiado.

Entre las conclusiones de índole general, mencionaremos en primer lugar que las técnicas del MFPT han mostrado ser desde hace tiempo extraordinariamente útiles en la descripción de la dinámica transitoria de sistemas sometidos a fluctuaciones, y por ello han sido ampliamente utilizadas. No obstante, existen serios problemas en la descripción, para ciertos rangos de parámetros, del MFPT incluso en los sistemas más sencillos.

Hemos visto que en cada tipo de inestabilidad las fluctuaciones actúan de la misma forma y, por tanto, encontramos unos conjuntos o clases de sistemas que presentan la misma dinámica. Un proceso complicado puede ser analizado en términos de cada una de sus partes, que responderá a leyes específicas. Por ello es importante extraer la máxima información posible de los casos más sencillos, ya que puede servir para conocer mejor los procesos reales. En este trabajo

hemos estudiado un amplio espectro de procesos de una variable, cubriendo los procesos más significativos con ruido aditivo y resolviendo un problema experimental concreto en el que aparece un ruido multiplicativo.

El problema correspondiente a sistemas sometidos a la acción de ruido blanco o con tiempo de correlación pequeño se considera resuelto, si bien aún puede quedar la tarea de establecer en cada caso los modelos apropiados y relacionar los resultados con las magnitudes experimentales.

En el caso de ruidos con grandes tiempos de correlación la fundamentación teórica no se encuentra totalmente desarrollada, y falta todavía el establecimiento de métodos sistemáticos de cálculo. En este estado de cosas, las leyes obtenidas mediante razonamientos físicos cobran un especial valor, puesto que proporcionan resultados numéricos fuera del rango de parámetros accesibles por las técnicas usuales, y dan una interpretación de la física involucrada en el proceso estudiado.

En cuanto a las conclusiones más específicas sobre cada uno de los sistemas estudiados en este trabajo, nos remitimos a las especificadas en cada una de las secciones del mismo. No obstante, enumeraremos las más significativas.

Respecto al MFPT del proceso de paso en un sistema

biestable (Cap. II):

- Las fórmulas de Kramers para ruido blanco y sus correcciones de Larson y Kostin son resultados asintóticos, y no pueden ser usadas para decidir la validez de simulaciones digitales o numéricas.

- T_{bot} y T_{top} son magnitudes que contienen una información física de naturaleza distinta. Las simulaciones indican una aproximación exponencial entre ambos valores al aumentar τ .

- La situación de pequeña τ para T_{bot} es explicada satisfactoriamente por las teorías disponibles. Sin embargo no es posible concluir cuál de ellas da mejor la dependencia en D que aparece en las simulaciones para τ grande. Por otro lado, las simulaciones de T_{top} para τ pequeña confirman la contribución $\tau^{1/2}$ encontrada por Doering *et al.*²¹

- El caso τ grande está explicado sólo cualitativamente por las teorías; quedan todavía grandes diferencias cuantitativas con los resultados de las simulaciones. La teoría de Tsironis y Grigolini,²⁴ corregida para tener en cuenta el cambio con τ de la distribución del ruido en la transición, aparece como el modelo más correcto de la dinámica en este régimen.

- La escala de tiempo asociada al autovalor dominante de la ecuación de Fokker-Planck debe ser identificada con T_{bot} para D pequeña. T_{bot} aparece como el tiempo físicamente más relevante de este proceso.

Respecto al proceso de paso a través de una inestabilidad

marginal (Cap.III):

- Las predicciones a primer orden en τ para el MFPT y la variaza obtenidas con la aproximación cuasimarkoviana describen correctamente los resultados de la simulación para pequeños valores de τ . La razón estriba en tener alejadas de la inestabilidad tanto la posición inicial (que ha evitado tener en cuenta el desacoplamiento inicial posición-ruido) como las fronteras del problema y la posición final (que ha permitido el cálculo en la variable x con una difusión efectiva, sin tener que utilizar el sistema en dos variables).

- La dependencia de la dinámica en un único parámetro de escala ha sido confirmada para todos los valores de τ simulados tanto para el sistema modelo como para otro sistema con el mismo desarrollo en el punto marginal. Por tanto, la idea de que el ruido sólo afecta en la zona marginal es físicamente correcta.

- Es posible utilizar las ideas anteriores para obtener una extensión del cálculo del MFPT a valores grandes del tiempo de correlación. Además, la aplicación de un razonamiento similar al caso de la relajación de un sistema inestable lineal proporciona resultados válidos a intensidades grandes del ruido.

c) Modelo de la reacción Clorito-Ioduro mediante una SDE con ruido multiplicativo (Cap. IV).

- La aleatoriedad observada experimentalmente en los tiempos de reacción de este sistema ha sido explicada mediante

una SDE con ruido multiplicativo. El modelo utilizado es cerodimensional, y las inhomogeneidades espaciales han sido modelizadas mediante fluctuaciones en la constante de reacción.

- Los valores de la intensidad del ruido D se correlacionan con el inverso del *stirring*, lo que confirma el origen de la aleatoriedad de la reacción en las inhomogeneidades espaciales, así como la corrección del modelo cinético empleado en el cálculo.

- El modelo da una dependencia correcta del MFPT y de su varianza en la intensidad del ruido y en el parámetro de la reacción β' . Así mismo, predice la presencia de un máximo de la magnitud relativa $\Delta T/T$ en función de β' .

- Las técnicas de MFPT en el marco del empleo de SDE's aparecen como un método prometedor en el análisis teórico de la irreproducibilidad de este tipo de sistemas.

I.7.b Resultados Originales

Hemos separado las distintas contribuciones originales de este trabajo según los capítulos del mismo

- i) MFPT en un Sistema Biestable (Cap. II): Sobre este sistema, las contribuciones originales de este trabajo han sido:

- Se ha realizado una exhaustiva serie de simulaciones del sistema biestable, obteniendo resultados para T_{top} y T_{bot}

para un gran rango de variación de los parámetros del ruido.

- Se ha analizado las teorías existentes para los MFPT definidos en este sistema, comparándolas con los resultados de las simulaciones y estableciendo el dominio de aplicabilidad de cada una de ellas.

- Se ha contribuido al entendimiento de la dinámica para τ grande, obteniendo la causa de la discrepancia de la teoría de TG con los resultados de la simulación para los valores accesibles de τ .

- Se ha modificado dicha teoría, corrigiéndola para dar cuenta de la situación de τ finita, obteniendo una ley de escala para el MFPT válida en el régimen de τ media-grande.

- Así mismo, se ha obtenido la evidencia de unos efectos de τ finita exponencialmente grandes en el MFPT, que son explicados satisfactoriamente dentro del mismo marco teórico.

- Se ha obtenido una relación entre T_{bot} y T_{top} , bajo la hipótesis de una dependencia exponencial.

ii) MFPT de un sistema marginal.

- Se ha obtenido la primera contribución en τ de los primeros momentos del Tiempo de Primer Paso para el modelo marginal (Ec. (2.3) del Cap. III) tanto para el caso $\beta=0$ (marginal puro) como para $\beta \neq 0$.

- Se ha aplicado estos resultados para la predicción del comportamiento de un sistema distinto, correspondiente al modelo de Bonifacio-Lugiato de Biestabilidad Óptica.

- Se ha desarrollado la extensión de los resultados de

los MFPT de inestabilidades lineales y marginales a valores grandes del tiempo de correlación. En el caso lineal, el resultado incluye la aproximación QDT, pero no está limitado a intensidades pequeñas del ruido.

- Se ha desarrollado la simulación numérica de los sistemas estudiados, con el fin de confirmar las predicciones teóricas.

iii) Dinámica estocástica de la reacción Clorito-Ioduro.

- Se ha establecido el modelo dinámico de la reacción Clorito-Ioduro, mediante una SDE en la que el término estocástico da cuenta de las inhomogeneidades espaciales.

- Se ha calculado a primer orden en D el MFPT y su varianza correspondientes a ese modelo.

- Se ha establecido la correspondencia entre el experimento y el modelo, determinando la relación entre las respectivas escalas de tiempo, y correlacionando la intensidad del ruido con el inverso del *stirring* experimental.

- Se ha utilizado los resultados analíticos y de simulación del MFPT y de la varianza del modelo para comparar con las magnitudes medidas experimentalmente, encontrando un buen acuerdo. Se ha encontrado así mismo el comportamiento cualitativo correcto de la magnitud relativa $\Delta T/T$.

I.7.c Perspectivas

- Queda abierta la cuestión de la fundamentación del cálculo del MFPT para cualquier tiempo de correlación del ruido. En particular, sería interesante obtener, por métodos más rigurosos, la información que, en ese régimen, se ha obtenido por argumentos físicos. Para el sistema biestable, posiblemente el sistema que ha generado más controversia en este campo, ha quedado abierta una vía con la formulación del MFPT en integrales de camino que, por el momento, sólo ha dado una información parcial del comportamiento asintótico del MFPT para D pequeña.²⁷⁻²⁹

- Sobre los sistemas marginales, queda por estudiar la validez de las predicciones realizadas para valores grandes de τ en sistemas con potenciales marginales de grado más alto.

- En un nivel más general, la aplicación de estas técnicas a otros sistemas, tanto de la Física como de la Química o de la Biología, pueden proporcionar información valiosa de la dinámica de los mismos.

- Dentro de este contexto, resulta inevitable plantearse a largo plazo el problema de los Tiempos de Paso en sistemas con dependencia espacial, para los que se tiene muy pocos resultados analíticos. Este es un problema de extraordinario interés, puesto que toca campos tan actuales como el crecimiento de interfaces, la descomposición espinodal, etc, y significaría un gran progreso la obtención de resultados correspondientes a las escalas de tiempos de este tipo de procesos.

Referencias

1. P. Glansdorff, I. Prigogine, *Thermodinamic Theory of Structure, Stability and Fluctuations*. Wiley, New York 1971.
2. G. Nicolis, I. Prigogine, *Self-Organization in Nonequilibrium Systems. From Dissipative Structure to Order Through Fluctuations*. Wiley, New York 1977
3. R. Zwanzig, Phys. Rev. 124, 983 (1961).
4. R. Brout, *Phase Transitions*. Benjamin, New York 1965.
5. A.Z. Patashniskii, V.I. Pokrovskii, *Fluctuation Theory of Phase Transitions*, Int. Ser. in Natural Philosophy, Vol. 98. Pergamon, New York 1979.
6. H. Haken, *Synergetics. An Introduction*. Springer Ser. Synergetics, Vol. 1, Springer, Berlin 1977.
7. W. Horsthemke, R. Lefever, *Noise-Induced Transitions*. Springer Ser. Synergetics, Vol. 15, Springer, Berlin 1984.
8. K. Ito, Nagoya Math. J. 6, 35 (1950)
9. R.L. Stratonovich, SIAM J. Control 4, 362 (1966)
10. E. Wong y M. Zakai, Ann. Math. Stat. 36, 1560 (1965).
11. G. Blankenship y G.C. Papanicolaou, SIAM J. Appl. Math. 34, 437 (1978)
12. R.L. Stratonovich, *Topics in the Theory of Random Noise*, Gordon and Breach (New York, 1963)
13. L. Arnold, *Stochastic Differential Equations: Theory and Applications*, Wiley, New York 1974.
14. H. Risken, *The Fokker-Planck Equation*, Springer Ser. Synergetics, Vol. 18, Springer-Verlag, Berlin, 1984.
15. R. Graham y H. Haken, Z. Phys. 243, 289 (1971);
 R. Graham y H. Haken, Z. Phys. 245, 141 (1971);
 R. Graham, en *Stochastic Nonlinear Systems in Physics, Chemistry, and Biology*, Springer Ser. Synergetics, Vol. 8. Springer (Berlin 1981).
16. R. Kubo, J. Math. Phys. 4, 174 (1963).
17. S.W. Dixit y P.S. Sahni, Phys. Rev. Lett. 50, 1273 (1983).

18. A. Hernández-Machado, M. San Miguel y S. Katz, Phys. Rev. A 31, 2362 (1985).
19. J.M. Sancho, M. San Miguel, S.L. Katz y J.D. Gunton, Phys. Rev. A 26, 1589 (1982).
20. K. Lindenberg y B.J. West, Physica A 119, 485 (1983).
J.M. Sancho y F. Sagués, Physica A 132, 489 (1985).
R.F. Fox, Phys. Rev. A 34, 4525 (1986).
P. Hänggi, T.J. Mroczkowski, F. Moss y P.V.E. McClintock, Phys. Rev. A 32, 695 (1985).
P. Grigolini, Phys. Lett. A 119, 157 (1986).
21. C.R. Doering, P.S. Hagan y C.D. Levermore, Phys. Rev. Lett. 59, 2129 (1987)
22. M.M. Klosek-Dygas, B.J. Matkowsky y Z. Schuss, Phys. Rev. A 38, 2605 (1988)
23. F. De Pasquale y P. Tombesi, Phys. Lett. A 25, 7 (1979).
F. De Pasquale, J.M. Sancho, M. San Miguel y P. Tartaglia, Phys. Rev. Lett. 56, 2473 (1986).
24. G. Tsironis y P. Grigolini, Phys. Rev. Lett. 61, 7 (1988).
G. Tsironis y P. Grigolini, Phys. Rev. A 38, 3749 (1988)
25. P. Hänggi, P. Jung y F. Marchesoni, J. Stat. Phys 54, 1367 (1989).
26. P. Colet, H.S. Wio y M. San Miguel, Phys. Rev. A 39, 6094 (1989).
H.S. Wio, P. Colet, M. San Miguel, L. Pesquera y M.A. Rodríguez, Phys. Rev. A 40, 7312 (1989).
M. San Miguel, P. Colet, H.S. Wio, L. Pesquera y M.A. Rodríguez, en *Noise and Chaos in Nonlinear Dynamical Systems*, Ed. F. Moss, Cambridge Univ. Press.
27. A.J. McKane, H.C. Luckock y A.J. Bray, Phys. Rev. A 41, 644 (1990)
A.J. Bray, A.J. McKane y T.J. Newman Phys. Rev. A 41, 657 (1990)
28. J.F. Luciani y A.D. Verga, Europhys. Lett. 4, 255 (1987).
J.F. Luciani y A.D. Verga, J. Stat. Phys. 50, 567 (1988).
29. A.J. Bray y A.J. McKane, Phys. Rev. Lett 62, 493 (1989).
30. P.C. Hohenberg y B.I. Halperin, Rev. Mod. Phys 49, 435 (1977).
31. J.D. Gunton, M. San Miguel y P. Sahni, en *Phase Transitions and Critical Phenomena* Vol. 8, Eds. C. Domb y J. Lebowitz, Academic Press.

32. M. Suzuki, en *Order and Fluctuations in Equilibrium and Nonequilibrium Statistical Mechanics*, Eds. G. Nicolis, G. Gewel y J.W. Turner, Wiley (1980)
33. P. Hänggi, J. Stat. Phys 42, 105 (1986).
34. P. Lett y L. Mandel, J. Opt. Soc. of America B 2, 1615 (1985).
35. R. Roy, A.W. Yu y S. Zhu, Phys. Rev. Lett. 55, 2794 (1985).
36. S. Kay, S. Wakabayashi y M. Ymanasaki, Phys. Rev. A 33, 2612 (1986).
37. J. Casademunt, R. Mannella, P.V.E. McClintock, F.E. Moss y J.M. Sancho, Phys. Rev. A 35, 5183 (1987).
38. J. Casademunt, J.I. Jiménez-Aquino y J.M. Sancho, Phys. Rev. A 40, 5905 (1989).
J. Casademunt, J.I. Jiménez-Aquino, J.M. Sancho, C.J. Lambert, R. Mannella, P. Martano, P.V.E. McClintock y N.G. Stocks, Phys. Rev. A 40, 5915 (1989).
39. R.L. Stratonovich, *Topics in the Theory of Random Noise* Vol. 2, Gordon and Breach (New York, 1967)
40. C.W. Gardiner, *Handbook of Stochastic Methods*, Springer Ser. Synergetics, Vol. 13, Springer, Berlin 1985.
41. M.C. Wang y G.E. Uhlenbeck, Rev. Mod. Phys. 17, 323 (1945).
42. L. Pontryagin, A. Andronov y A. Vitt, Zh. Eksp. Theor. Fiz. 3, 165-80 (1933).
43. K. Lindenberg, B.J. West y J. Masoliver, en *Noise in Nonlinear Dynamical Systems*, Vol. 1, Ed. F. Moss y P.V.E. McClintock, Cambridge Univ. Press (Cambridge, 1989).
44. El proceso de Ornstein-Uhlenbeck es el único proceso estocástico markoviano y con una distribución gaussiana, según establece el Teorema de Doob: J.L. Doob, Ann. Math. 43, 351 (1942). Ver también la Sec. 4.3 de la Ref. 7
45. G.E. Uhlenbeck y L.S. Ornstein, Phys. Rev. 36, 823 (1930).
46. R. Kubo, J. Math. Phys. 4, 174 (1963).
47. E.A. Novikov, Zh. Eksp. Teor. Fiz. 47, 1919 (1964).
48. J. Masoliver, B.J. West y K. Lindenberg, Phys. Rev. A 35, 3086 (1987).
49. R. Landauer y J.A. Swanson, Phys. Rev. 121, 1668 (1961).

50. J.M. Sancho y M. San Miguel, en *Noise in Nonlinear Dynamical Systems*, Eds. Frank Moss y P.V.E. McClintock, Cambridge Univ. Press (Cambridge, 1989).
51. L. Ramírez-Piscina, J.M. Sancho, F.J. de la Rubia, K. Lindenberg y G.P. Tsironis, Phys. Rev. 40, 2120 (1989).
52. H.A. Kramers, Physica 7, 284 (1940)
53. F.J. de la Rubia, E. Peacock-López, G.P. Tsironis, K. Lindenberg, L. Ramírez-Piscina y J.M. Sancho, Phys. Rev. A 38, 3827 (1988)
54. K. Lindenberg, L. Ramírez-Piscina, J.M. Sancho y F.J. de la Rubia, Phys. Rev. A 40, 4157 (1989)
55. R. Mannella y V. Palleschi, Phys. Rev. A 39, 3751 (1989)
56. L. Ramírez de la Piscina, J.M. Sancho, K. Lindenberg y F.J. de la Rubia, *Escape over a Potential Barrier driven by Colored noise*, en *Noise in Physical Systems*, Ed. A. Ambrózy, Budapest (1990)
57. L. Ramírez-Piscina y J.M. Sancho. Enviado para su publicación.
58. P. Colet, M. San Miguel, J. Casademunt y J.M. Sancho, Phys. Rev. A 39, 149 (1989)
59. D. Sigeti, Dissertation, University of Texas at Austin (1988)
D. Sigeti and W. Horsthemke, J. Stat. Phys 54, 1217 (1989)
60. L.A. Lugiato, *Progress in Optics XXI*, ed. E. Wolf (North-Holland, Amsterdam, 1984).
R. Bonifacio y L.A. Lugiato, Phys. Rev. A. 18, 1129 (1978).
61. F. Sagués, L. Ramírez-Piscina y J.M. Sancho, J. Chem. Phys. 92, 4786 (1990).
62. F. Sagués y J.M. Sancho, J. Chem. Phys. 89, 3793 (1988)

**II. FIRST PASSAGE TIME FOR A BISTABLE POTENTIAL
DRIVEN BY COLORED NOISE**

II.1

II.1 GENERAL REMARKS

1. Introduction

A number of (sometimes conflicting) views have recently dominated the literature on bistable processes driven by external noise. Most of the conflicts arise in the context of the effects of external noise that is colored, e.g. whose correlations decay exponentially with a correlation time $\tau > 0$. Various theoretical approaches have been developed in the small- τ^{1-7} and in the large- τ^{7-10} limits, and some of the predictions emerging from these theories have been tested against analog simulations,² numerical computations,^{11,12} and a few numerical (digital) simulations.^{1,13,14}

In order to attain a better understanding of the relations among these various theories and the accuracy of their predictions, we have carried out extensive numerical simulations of the Langevin equations that serve as the model from which all these theories depart. By covering extensive ranges of parameter values (in particular, of the correlation time τ of the noise), we are able to arrive at some definitive conclusions that should help to sort out some of the present uncertainties in the field. It should be remarked that the main contribution of this paper lies not in the accuracy of the computer simulations (which is comparable to that of other recent simulations¹³) but in the insight and better understanding of the present theories acquired through the data.

As our system we shall consider the generic and widely studied bistable system

$$\dot{q}(t) = q(t) - q^3(t) + \mu(t) \quad (1.1)$$

where $\mu(t)$ is the noise driving the system, which we shall assume to be Gaussian throughout this analysis. In the absence of the noise, the system has fixed points at $q = \pm 1$ (stable) and at $q = 0$ (unstable). If $\mu(t)$ represents white noise, then its correlation function is

$$\langle \mu(t)\mu(t') \rangle = 2D \delta(t-t') \quad (1.2)$$

If the noise is Gaussian colored, then

$$\langle \mu(t)\mu(t') \rangle = \frac{D}{\tau} e^{-|t-t'|/\tau} \quad (1.3)$$

The colored noise can itself be generated from a white noise process $\mu_w(t)$ via the dynamical equation

$$\dot{\mu}(t) = -\frac{1}{\tau}\mu(t) + \frac{1}{\tau}\mu_w(t) \quad (1.4)$$

Herein we consider two quantities most frequently discussed in the literature: the mean first passage time (MFPT) for the system starting from one well of the bistable potential, e.g.

II.2

at $q = -1$, to reach $q = 0$ (T_{top}) or to cross the barrier and reach the other potential well, e.g. at $q = 1$ (T_{bot}). A third time of interest that we consider but that we have not simulated is the MFPT to reach the separatrix between the wells (T_{sep}).

Considerable discussion has recently centered on the appropriate (meaningful) endpoints to use in MFPT calculations since the fixed points in the absence of the noise are instantaneously shifted by the (colored) noise, and especially since $q = 0$ is not the separatrix between the two potential wells in the presence of (colored) noise. Thus, whereas it is generally agreed upon that T_{bot} does represent a transition time from one well to the other (even in the face of shifting minima), T_{top} is only an accurate measure of this transition when the noise is white and D is small, and T_{sep} is only an accurate measure of T_{bot} when D is small. These remarks notwithstanding (and we shall return to this issue later), we will use these two quantities to assess the validity of various theories because they have been so prominent in the literature. Quite aside from the physical content of these measures, they can of course still be used to compare analytic theories with simulations.

For white noise the MFPT can be expressed exactly as a double integral^{3,15} that can then be evaluated by numerical procedures. When a steepest descent approximation is applied to these integrals, one obtains analytic estimates ("Kramers times"¹⁶) for T_{top}^K and T_{bot}^K :

$$T_{top}^K = \frac{\pi}{\sqrt{2}} e^{1/4D} \quad (1.5)$$

and

$$T_{bot}^K = \pi\sqrt{2} e^{1/4D} \quad (1.6)$$

These results, valid only in the "high-barrier" asymptotic limit $D \rightarrow 0$, reflect the fact that upon reaching the top of the barrier half of the trajectories immediately go on to the new well while the other half return to the original well. For finite D Larson and Kostin¹⁷ have calculated the first correction to these results. This correction reads

$$T^{LK} = \left(1 + \frac{3}{2}D\right) T^K \quad (1.7)$$

There exist no exact analytic results (or even analytic results in the form of integral expressions) when the noise driving the system is colored. A number of approximate theories have been developed, all of them dealing with the limiting cases of either very short or very long correlation time of the noise. The small- τ theories arrive at expressions similar to (1.5) and (1.6) with corrections that contain a τ -dependence. The long- τ theories arrive at

II.3

expressions that are quite different from the white noise results. In the first (small- τ) group the following expressions have appeared in the literature:

$$T_{top}(\tau) = \frac{\pi}{\sqrt{2}} \left(\frac{1+2\tau}{1-\tau} \right)^{\frac{1}{2}} e^{1/4D} , \quad (1.8)$$

$$T_{top}(\tau) = \frac{\pi}{\sqrt{2}} e^{\frac{1}{4D} + \frac{3}{2}\tau} , \quad (1.9)$$

$$T_{sep}(\tau) = \frac{\pi}{\sqrt{2}} \frac{(1-2\tau+\tau^2)^{\frac{1}{2}}}{(1+4\tau+4\tau^2)^{\frac{1}{2}}} \frac{\left(1+3\tau+\frac{5}{2}\tau^2\right)}{\left(1-\frac{3}{2}\tau+\frac{5}{8}\tau^2\right)} \\ \times \exp \left[\frac{1}{D} \left(\frac{1}{4} + \frac{\tau^2}{8} - \frac{3\tau^4}{10} \right) \right] , \quad (1.10)$$

$$T_{top}(\tau) = \frac{\pi}{\sqrt{2}} \left[1 - \sqrt{\frac{2}{\pi}} \zeta(\frac{1}{2}) \sqrt{\tau} + \frac{3}{2}\tau \right] e^{1/4D} . \quad (1.11)$$

Equation (1.8) was derived by Hänggi, Marchesoni and Grigolini;^{1,5} Eq. (1.9) was obtained by Masoliver, West and Lindenberg;³ Eq. (1.10) is the MFPT to the separatrix derived by Klosek, Matkowsky and Schuss;⁶ Eq. (1.11) (with $\zeta(\frac{1}{2}) = -1.460354\dots$) is due to Doering, Hagan and Levermore.⁴

An approximation for T_{bot} valid for small D but for arbitrary correlation times τ was proposed by Luciani and Verga.⁷ Their "interpolation formula" (Eq. (66) of Reference 7), applied to our system, is

$$T_{top}(\tau) = \pi\sqrt{2} (1+3\tau)^{\frac{1}{2}} \exp \left[\frac{1}{4D} \frac{1 + \frac{27}{16}\tau + \frac{1}{2}\tau^2}{1 + \frac{27}{16}\tau} \right] . \quad (1.12)$$

For very large τ the following approximations have been published:

$$T(\tau) = \left[\frac{\pi}{\sqrt{2}} + \left(\frac{27}{2}\pi D \tau \right)^{\frac{1}{2}} e^{\frac{2\tau}{27D}} \right] e^{1/4D} , \quad (1.13)$$

$$T(\tau) = [27\pi D (\tau + \frac{1}{2})]^{\frac{1}{2}} \exp \left(\frac{2\tau}{27D} + \frac{1}{9D} \right) . \quad (1.14)$$

Equation (1.13) was obtained by Tsironis and Grigolini⁸ and is designed to bridge the $\tau \rightarrow 0$ and $\tau \rightarrow \infty$ results. Equation (1.14) is due to Hänggi, Jung and Marchesoni.⁹

II.4

It should be noted that the small- τ expressions (1.8) and (1.9) are to be interpreted not as representing T_{top} but rather $T_{bot}/2$. These two quantities are only equal for white noise and in the weak noise limit, where $q = 0$ is actually the separatrix between the two wells and where the trajectories reaching this value immediately proceed to one well (half) or the other (the other half). The theory of Doering et al.⁴ incorporates finite- τ subtleties that arise from the fact that $q = 0$ is no longer the separatrix and results in the $\sqrt{\tau}$ contribution evident in (1.11). It has been argued¹⁸ (and agreed to by Doering et al.¹⁹) that a more physical characterization of the transition process is the time to reach the actual separatrix (or the other well), and in this latter calculation [cf. (1.10)] there appear no $\sqrt{\tau}$ contributions.

All the small- τ theories with the exception of Eq. (1.11) thus predict a leading behavior of the form

$$\frac{T_{bot}(\tau)}{T_{bot}(0)} \approx 1 + \frac{3}{2}\tau \quad (1.15)$$

whereas Doering et al.⁴ predict the leading behavior

$$\frac{T_{top}(\tau)}{T_{top}(0)} = 1 - \sqrt{\frac{2}{\pi}} \zeta(1/2) \sqrt{\tau} + \frac{3}{2}\tau , \quad (1.16)$$

thus exhibiting the $\sqrt{\tau}$ correction mentioned above.

The large- τ theories [Eqs. (1.13) and (1.14)] and the interpolation formula (1.12) all have the same leading exponential dependence $2t/27D$, which is exact in the limit $\tau \rightarrow \infty$. The theories differ from one another in their predictions of the behavior at large but finite τ .

2. Numerical Algorithms

The numerical integration of Eq. (1.1) with Gaussian noise $\mu(t)$ of correlation properties (1.2) or (1.3) has been carried out following the procedure detailed in Reference 20. We have simulated a number of trajectories (typically 500 or 1000) for each choice of parameter values, each driven by a different realization of the noise.

For the case of white noise, the discrete version of Eq. (1.1) is

$$q(t+h) = q(t) + [q(t) - q^3(t) + X(t)] h \quad (2.1)$$

where $X(t)$ is a random number chosen from a Gaussian distribution of mean zero and variance $\sqrt{2D/h}$. We have not retained terms of higher order in the integration step h because their effects are negligible if h is chosen to be sufficiently small. For each realization of the sequence $X(t)$ we compute the time that it takes the process $q(t)$ starting from $q = -1$ to first

II.5

arrive at $q = 0$ and to first arrive at $q = 1$.

If the noise driving Eq. (1.1) is colored then we must discretize the coupled set (1.1) and (1.4):

$$q(t+h) = q(t) + [q(t) - q^3(t) + \mu(t)] h , \quad (2.2)$$

$$\mu(t+h) = \mu(t) + [X(t) - \mu(t)] \frac{h}{\tau} , \quad (2.3)$$

where once again we have neglected higher order contributions in h . Initially the value of q is -1 and the process $\mu(t)$ has a stationary Gaussian distribution. Again, for every trajectory we compute the time for the system to first reach the values $q = 0$ and $q = 1$.

In order to test the accuracy of our simulations we have in a few cases carried out a much more accurate simulation for comparison. This latter procedure, requiring much more computing time, uses a different random number generator, a smaller integration step, an improved algorithm for the integration of the equations,²¹ and a greater number of trajectories (5000). The results from this more accurate simulation confirm the numbers that we report below within our estimated errors.

A different algorithm for the numerical simulation of colored noise has been reported recently by Fox et al.²² This new algorithm uses an integral version of Eq. (1.4):

$$\mu(t+h) = \mu(t)e^{-h/\tau} + g(t) , \quad (2.4)$$

where $g(t)$ is a Gaussian number of zero mean and variance $[D(1-\exp(-h/\tau))/\tau]^{1/2}$. Since Eq. (2.4) is exact even for long step sizes, we could in principle save computing time. The actual situation for a MFPT simulation, however, is not so optimistic, as is shown in Reference 23. The boundary conditions that appear in a MFPT simulation cause a strong dependence of the result on the step size. Therefore, the step has to be sufficiently small and there is no difference between the two methods. This is clearly seen in Fig. 1, where the two algorithms are tested in the MFPT simulation for the *noise* variable to reach a prefixed value. We see that the smallness of the needed step size makes the difference between the two methods irrelevant.

II.6

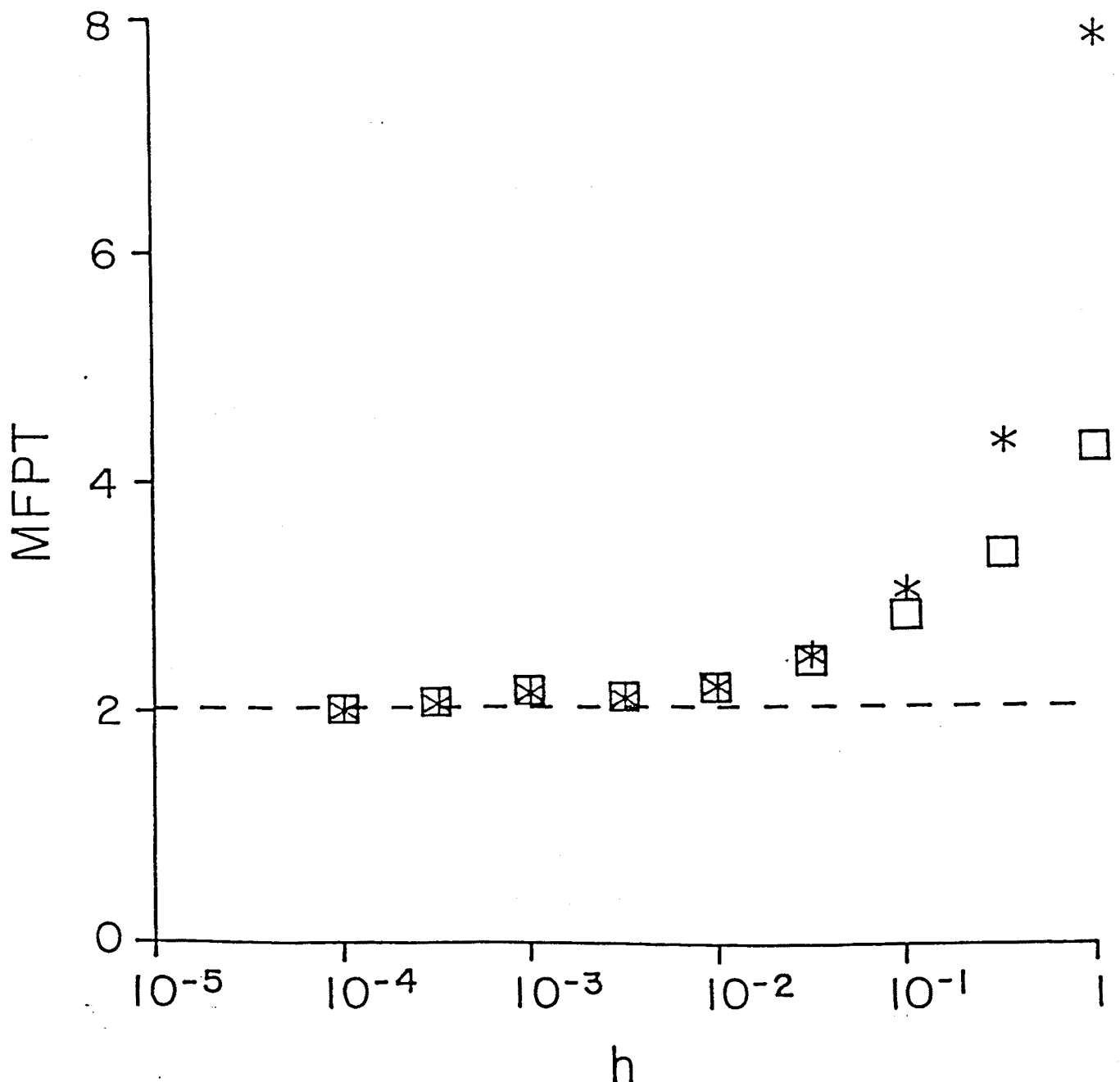


Fig. 1 MFPT results for Eq. (1.4) versus the integration step h . The noise variable $\mu(t)$ starts from $\mu = 0$ and reaches the boundary at $\mu = 0.31$. The parameters $D = 0.1$, $\tau = 1$ lead to the numerical result $T = 2.026$. Asterisks: algorithm of Fox et al.;²² squares: algorithm of Eq. (2.3).²⁰ The CPU time is nearly the same for both points of each pair.

3. Results

3.1. White Noise

We begin by studying the process (1.1) driven by white noise. The purpose is to test the theoretical approximations and the digital simulation in the limit in which it is possible to obtain precise numerical results from exact quadratures. In particular, we want to test the reliability of our MFPT simulation and the domain of validity of Eqs. (1.5) and (1.6).

In Fig. 2 we show the relation T_{bot}/T_{bot}^K , using as T_{bot} both the exact numerical integral and the simulation results. There are clearly important corrections to the Kramers time. In the range $0.1 \leq D \leq 0.2$, i.e. for relatively small values of D , the errors in the Kramers time exceed 25%. Kramers' time formula requires noise intensities smaller than 0.05 for the error to be smaller than 10%. Unfortunately, the calculation time grows exponentially with decreasing D for small D in a MFPT simulation, and it is not practical to simulate noises of intensities smaller than 0.07. The correction (1.7) of Larson and Kostin¹⁷ improves the theoretical prediction substantially for intensities smaller than 0.2.

The assumption $T_{bot}/T_{top} = 2$ is asymptotically valid in the limit $D \rightarrow 0$. In Fig. 3 we see that the departure from this assumption for intermediate D is quite significant. The value of T_{bot}/T_{top} is 2.15 for $D = 0.1$ and reaches 2.7 for $D = 1$.

These remarks serve to stress the fact that Eqs. (1.5) and (1.6) fail to describe accurately the properties of the MFPT for finite D . The disagreements are substantial even for the smallest D that can be implemented reasonably in a digital simulation or, which is perhaps more important, in analog experiments.²

Finally, the simulation of the white noise case has been useful to test the MFPT algorithm. In Figs. 2 and 3 we see that the results of our simulation fit the exact theoretical curves reasonably well.

3.2. Colored Noise: Small τ

Since all the theories for small τ [Eqs. (1.8)-(1.12)] converge to Eqs. (1.5), (1.6) in the limit $\tau \rightarrow 0$, the failure of these latter equations for finite D described in the previous section presents a new problem. If we were to compare directly the results of the small- τ theories with the ones obtained from simulations, the effects of the correlation time τ , which we are interested in, may be masked by errors introduced by small- D approximations. The way to avoid this problem is to analyze the ratio $T(\tau)/T(0)$ instead of $T(\tau)$. In this way, the errors arising from the steepest descent calculation are expected to be reduced.

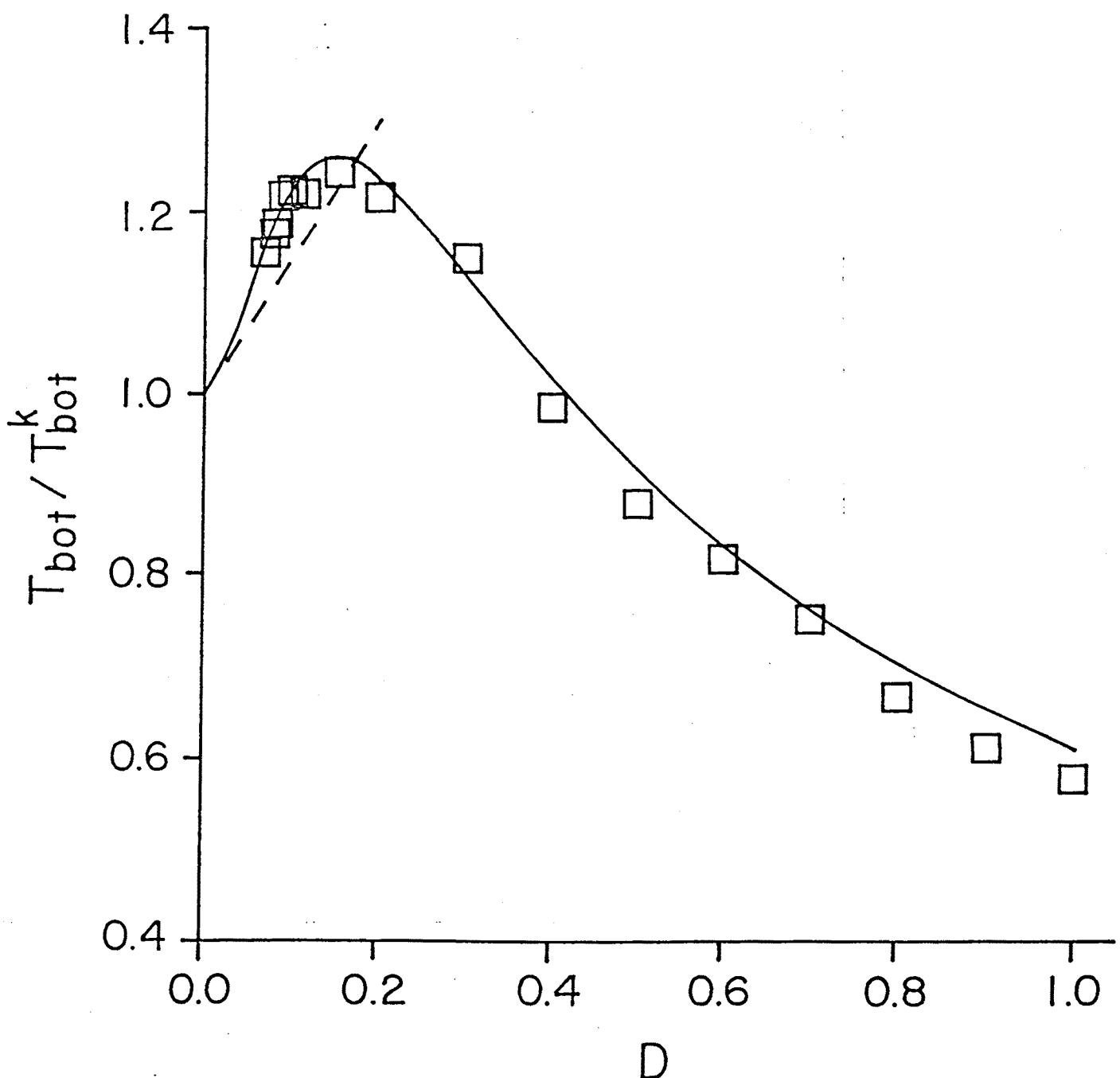


Fig. 2 T_{bot} / T_{bot}^K vs. D for the white noise case. Squares: simulation; solid line: exact result; dashed line: Larson and Kostin correction (1.7).

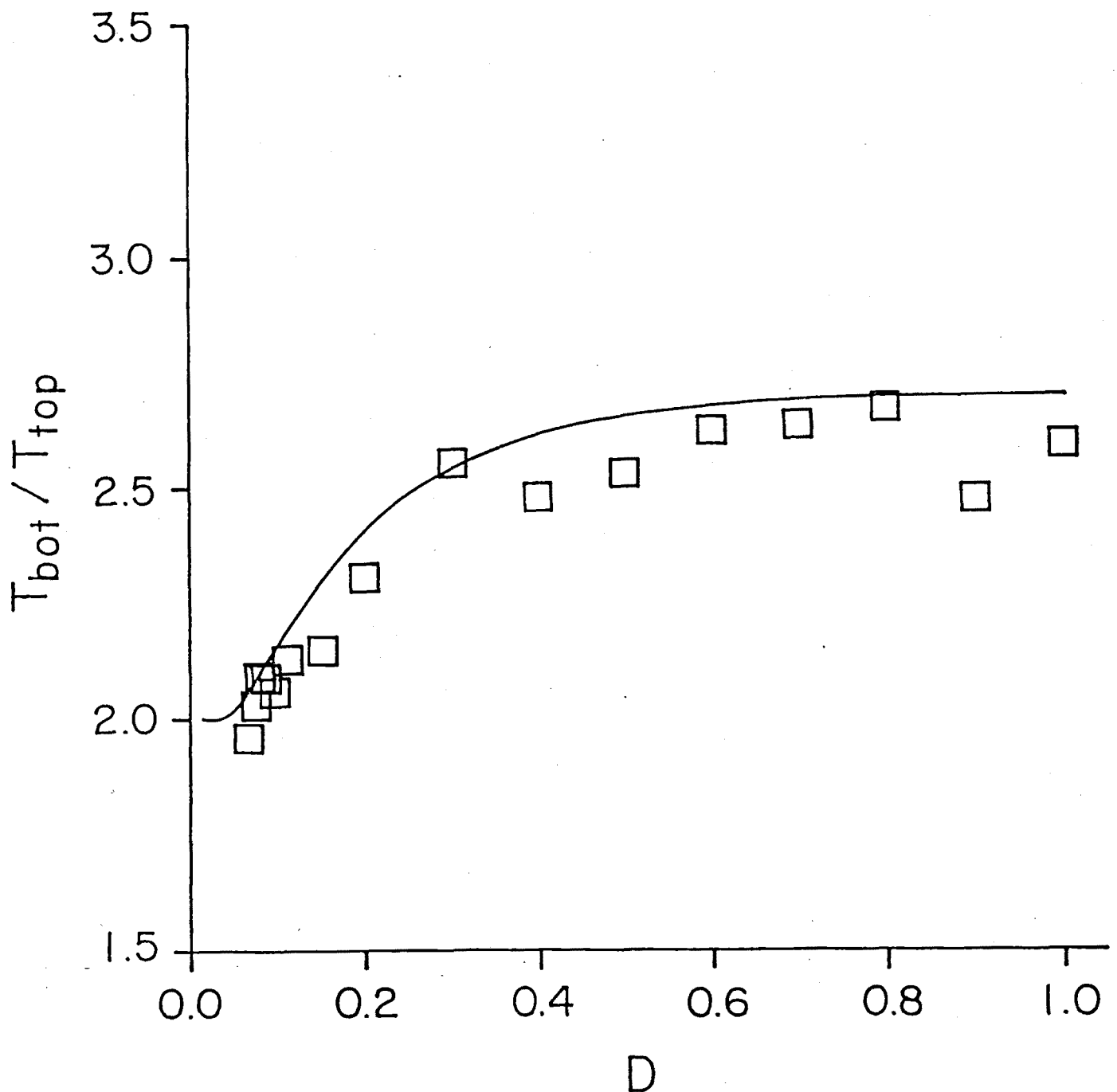


Fig. 3 T_{bot} / T_{top} vs. D for the white noise case. Squares: simulation; solid line: exact result.

The first point we wish to stress via the simulation results is the very different behavior of $T_{top}(\tau)$ and $T_{bot}(\tau)$. The comparison of the two MFPTs is plotted in Fig. 4 for the three intensities D considered. We see that T_{bot}/T_{top} has a value near 2 for $\tau \rightarrow 0$, but this ratio decreases very rapidly with τ , reaching the value 1 for moderately colored noises. This departure is of course related to the departure of the separatrix from $q = 0$ with increasing τ and reflects the fact that the actual separatrix has already been crossed when $q = 0$ is reached. Any assumption of a simple proportionality between $T_{bot}(\tau)$ and $T_{top}(\tau)$ is thus seen to fail for colored noise even for small values of τ .

The results of different theories are usually given by expressions for T_{top} or T_{sep} such as Eqs. (1.8)-(1.11) whose white noise limit is (1.4). For the correct interpretation of the results for T_{top} one must consider two possibilities: a) The theory gives the correct behavior for T_{top} . In that case the theory does not directly address the behavior of T_{bot} . b) The theory gives the correct behavior for T_{bot} , i.e. one must interpret the result as $T_{bot} = 2T_{top}$, T_{top} then being a function with no simple connection to the actual MFPT to reach $q = 0$. This explains the existence of two different leading behaviors in τ among the theories for small τ .

The values of T_{bot} obtained from our simulations show a slope for $T_{bot}(\tau)/T_{bot}(0)$ of $3/2$ for very small values of τ . This is the prediction of Eqs. (1.10) and (1.12) and also of (1.8) and (1.9) if these latter two are interpreted as representing $T_{bot}/2$ (the interpretation we adopt henceforth). The results are seen in Fig. 5, where we have plotted Eq. (1.9) as representative of the $T_{bot} = 2T_{top}$ theories. All the theories fit the simulation data quite well for small τ . For larger τ the differences between the theories become apparent, but none of them seems to fit the simulations much better than the others. We have also plotted Eqs. (1.10) (using $T_{sep}(\tau)/T_{sep}(0)$ in this case) and (1.12) because these theories predict a D -dependent slope for $T(\tau)/T(0)$. The variation of the slope is predicted by both equations, but the actual value is underestimated by Eq. (1.12) and is overestimated by Eq. (1.10).

The plot of $T_{top}(\tau)/T_{top}(0)$ in Fig. 6 shows a distinctive small- τ curvature that is correctly predicted by Eq. (1.11) and not by the other theories. The special boundary conditions that have to be imposed, and that only the theory of Doering et al.⁴ considers, give the new term proportional to $\sqrt{\tau}$ that leads to this curvature.

3.3. Colored Noise: Large τ

The large correlation time expressions (1.13) and (1.14) predict a MFPT that grows exponentially with $2\tau/27D$ in the limit $\tau \rightarrow \infty$. It is not possible to deal with very large

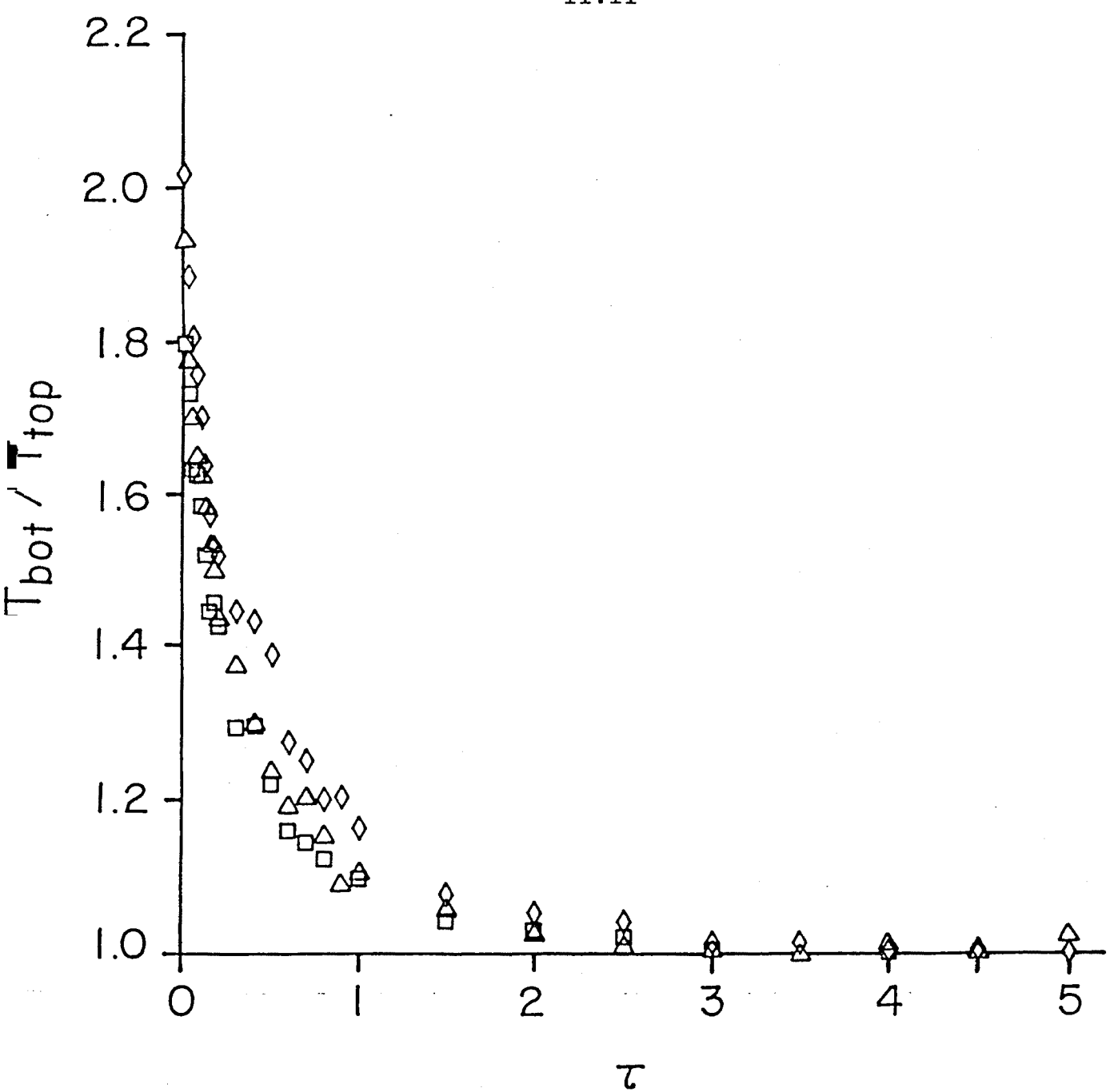


Fig. 4 Simulation results for T_{bot}/T_{top} vs. τ . Squares: $D = 0.083$; triangles: $D = 0.114$; rhombuses: $D = 0.153$.

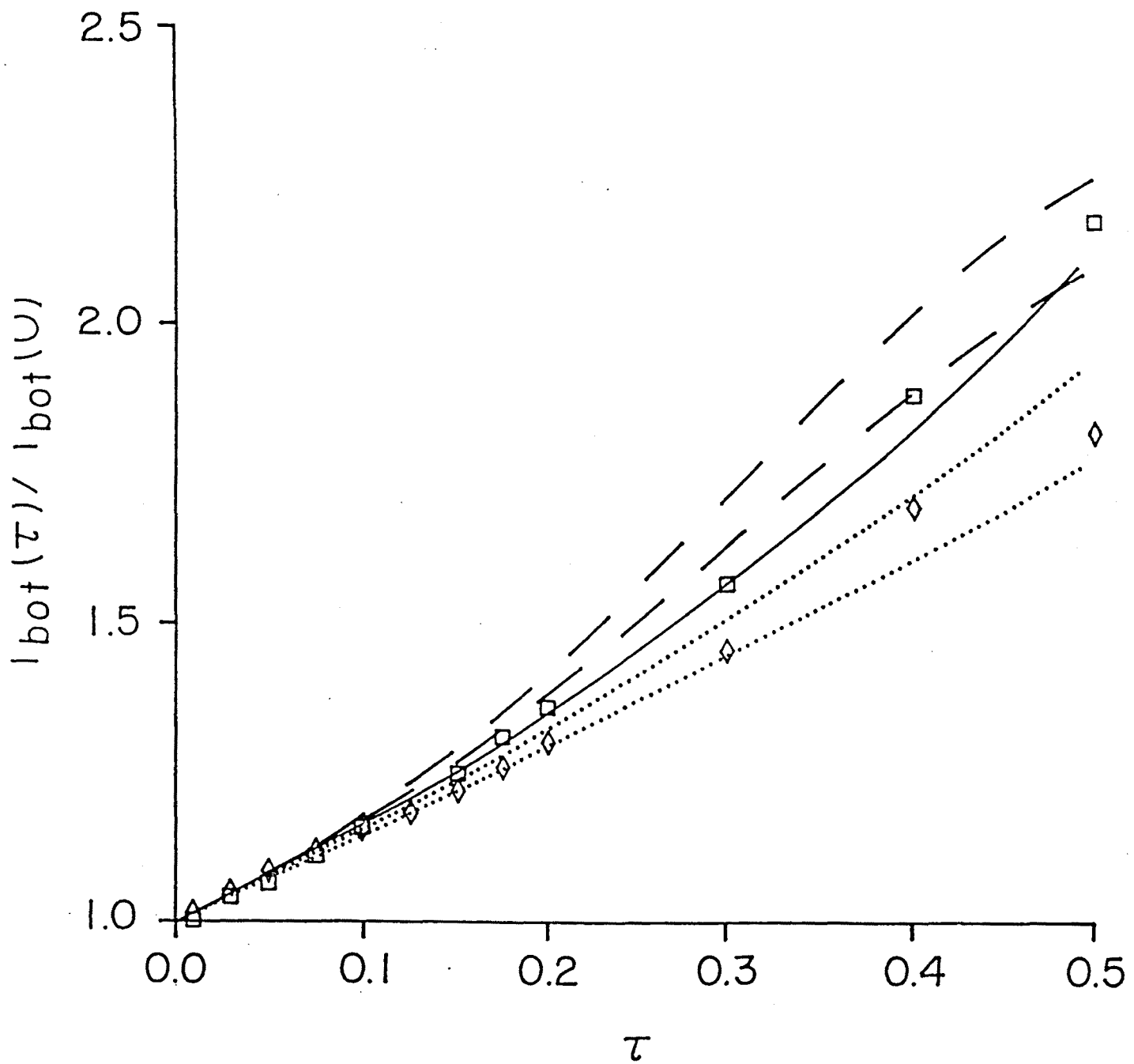


Fig. 5 $T_{bot}(\tau)/T_{bot}(0)$ vs. τ . Squares: $D = 0.083$; rhombuses: $D = 0.153$; solid line: Eq. (1.9); dashed line: Eq. (1.10); dotted line: Eq. (1.12).

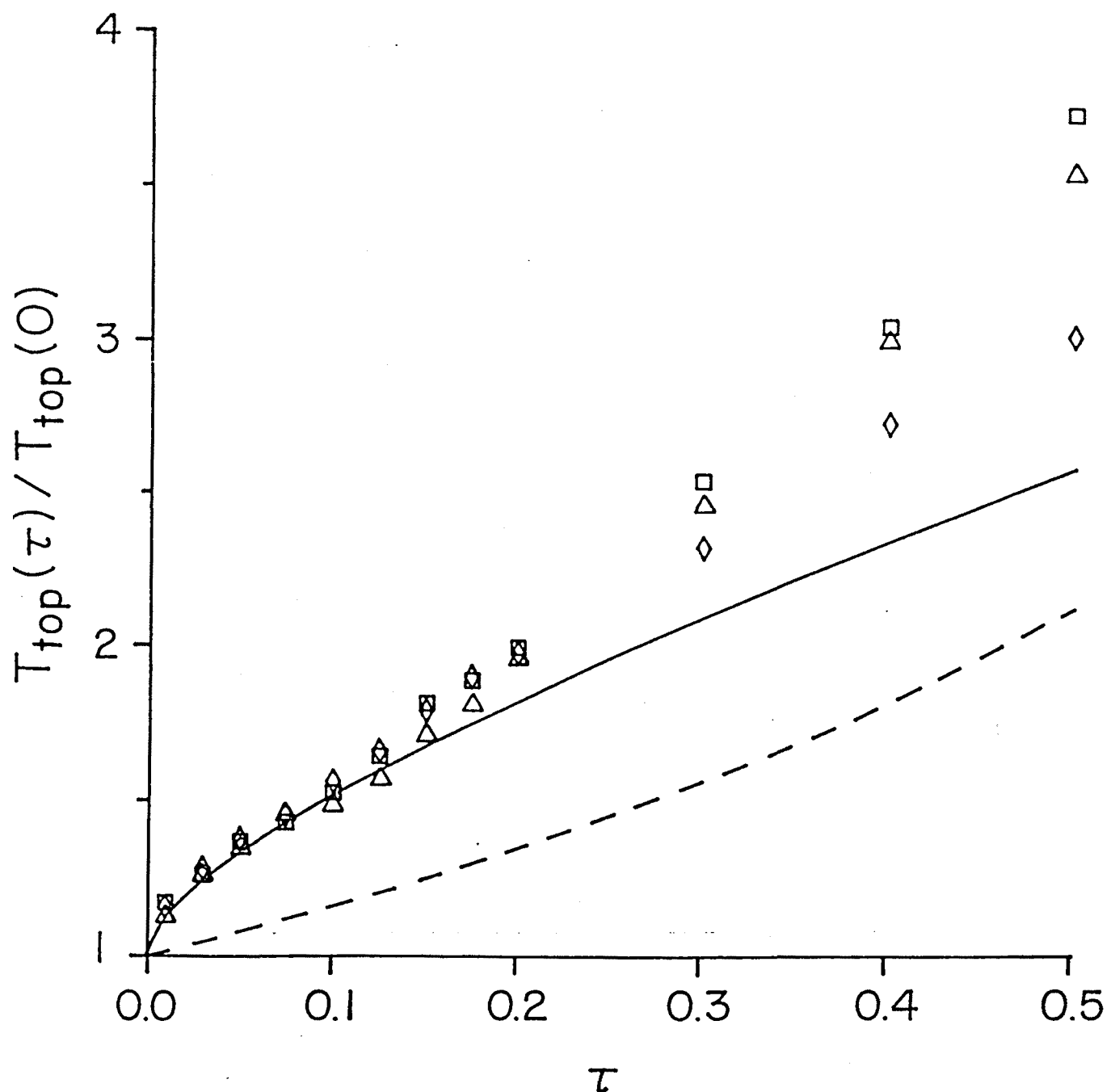


Fig. 6 $T_{top}(\tau)/T_{top}(0)$ vs. τ . Squares: $D = 0.083$; triangles: $D = 0.114$; rhombuses: $D = 0.153$; solid line: Eq. (1.11); dashed line: Eq. (1.9).

values of τ in a MFPT simulation because the calculation time grows as its own result, i.e. exponentially. In the present simulation, with D near 0.1, the values of τ used, though perhaps not asymptotically large, give values of τ/D larger than 40, which is sufficiently large to allow comparison of the diverse large- τ theories.

This comparison is shown in Fig. 7, where we plot $T_{bot}(\tau)$ on a logarithmic scale. The plot of $T_{top}(\tau)$ is indistinguishable from that of $T_{bot}(\tau)$ for τ larger than 1.5. It follows from Fig. 7 that all the theories try to have the correct exponential behavior, but the precise values predicted for the MFPT are clearly wrong (in some cases with deviations of orders of magnitude).

These results seem to indicate that the discrepancies between the theories and the numerical results lie in the prefactors and not in the exponential dependence on τ .¹⁴ In the following, instead of trying to calculate that prefactor, we use approximate arguments to obtain a scaling law that fits the numerical results reasonably well and gives a possible dependence of the MFPT on the noise parameters τ and D .

For large values of the correlation time, the change in the noise is so slow that the analysis of the system (1.1), (1.4) can be done from a semideterministic point of view. The dashed line in Fig. 8 represents the separatrix $\mu_{sep}(q)$ between the initial conditions that drive the system to each well. The deterministic evolution ($D = 0$) of the two variables q, μ is shown in the figure for two values of τ .

If τ is very large, the evolution of the noisy system from a given initial condition is very similar to the deterministic evolution, and therefore the MFPT to reach the second well is related to the mean time taken by the system to reach the separatrix. In Fig. 8 a sample trajectory of the system is shown. Once the system has crossed this curve, it has a finite probability (parameter-independent to leading order) of actually reaching the second well. Therefore, the MFPT in which we are interested is likely to be proportional to the mean time to reach the separatrix. The dependence of the separatrix-crossing position on the parameters of the problem should then give the dependence of the MFPT on these parameters.

This kind of reasoning is followed in References 8 and 9 to obtain Eqs. (1.13) and (1.14). In the case of Eq. (1.14), the actual separatrix is replaced by the straight line $q = -1/\sqrt{3}$ (vertical dotted line in Fig. 8). In the case of Eq. (1.13) the noise is considered as constant, and the actual separatrix is replaced by a critical value $\mu_c = 2/3\sqrt{3}$ (horizontal dotted line in the same figure).

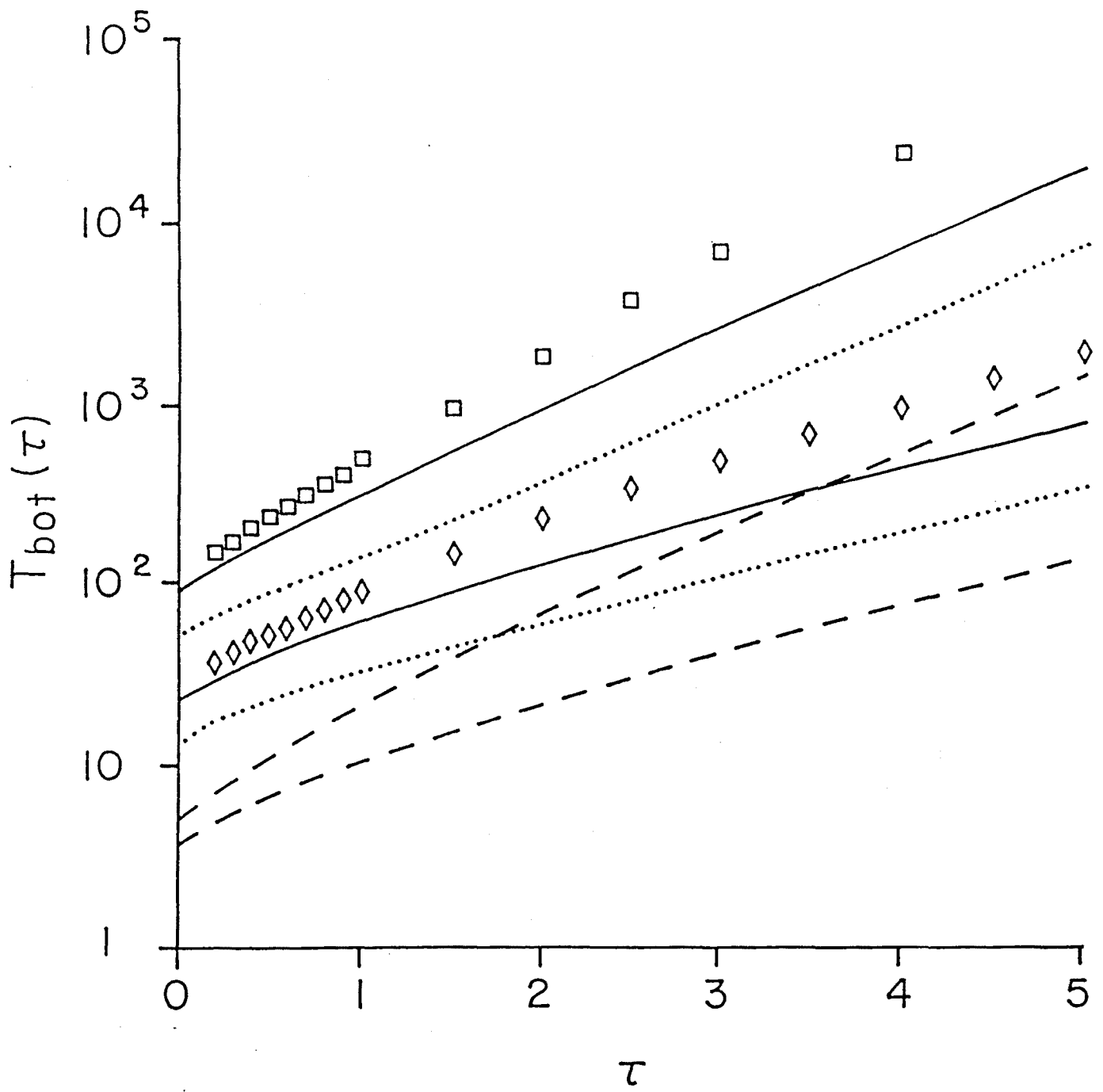


Fig. 7 $T_{bot}(\tau)$ vs. τ . Squares: $D = 0.083$; rhombuses: $D = 0.153$; solid lines: Eq. (1.12); dashed lines: Eq. (1.14); dotted lines: Eq. (1.13).

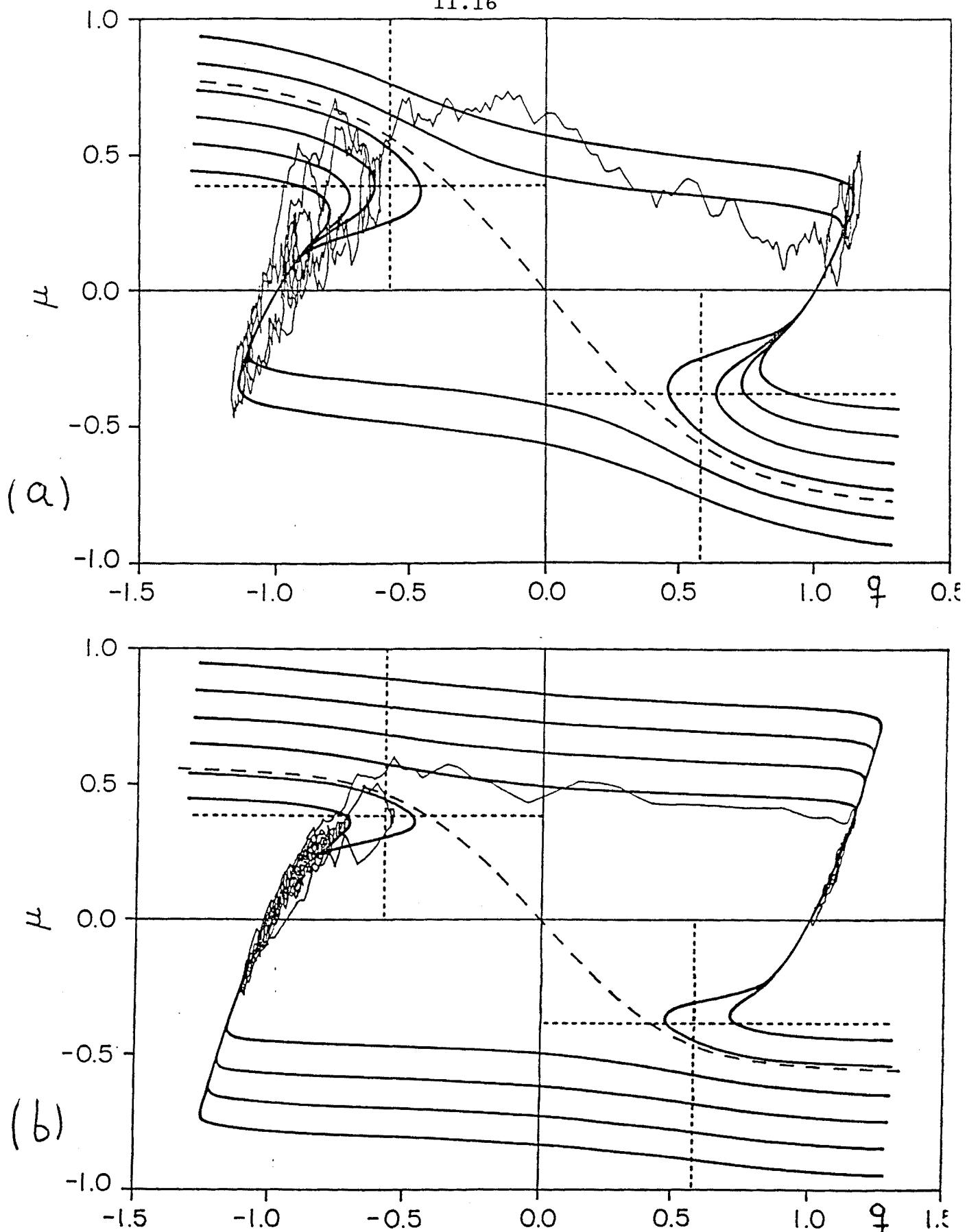


Fig. 8 Trajectories for the two variables q, μ . Solid thick lines: deterministic trajectories ($D = 0$); solid thin line: stochastic trajectory ($D = 0.5$); dashed line: actual separatrix; dotted lines: $q = \pm 1/\sqrt{3}$ and $\mu = \pm 2/3\sqrt{3}$ used as effective separatrices in the theories leading to Eqs. (1.14) and (1.13) respectively. (a) $\tau = 5$. (b) $\tau = 15$.

The extension of the Tsironis-Grigolini (TG) calculation⁸ to large but finite correlation times is discussed in Reference 10, where it is argued that a system with the "noise" equal to the (constant) critical value μ_c requires an infinite time to cross the inflection point $= -1/\sqrt{3}$; it is furthermore shown that the system must typically reach values of the noise much larger than μ_c to complete the transfer from one well to the other. This larger value $> \mu_c$ of the noise must depend on τ , and its lower bound μ_τ is calculated under the condition that the deterministic time to go to the other well be smaller than the correlation time τ of the noise. This lower bound for the critical value of the noise gives a correction in the exponent of order $1/\tau^2$ to the TG result.

We shall here obtain the (approximate) τ -dependence of μ . We start from the TG calculation.⁸ In this model one must wait a time T to let the noise reach the critical value μ_c (note that if μ were constant then μ_c would be the separatrix). This time is calculated by standard procedures:¹⁵

$$T(\mu_c) = \frac{\tau^2}{D} \int_0^{\mu_c} dy \int_{-\infty}^y dz \exp \left[-\frac{\tau}{2D}(z^2 - y^2) \right] . \quad (3.1)$$

After some manipulation, this equation yields

$$\begin{aligned} T(\mu_c) &= \tau\sqrt{\pi} \left(1 + \operatorname{erf} \left[\left(\frac{\tau}{2D} \right)^{1/2} \mu_c \right] \right) e^{\frac{\tau}{2D}\mu_c^2} F \left[\left(\frac{\tau}{2D} \right)^{1/2} \mu_c \right] \\ &\quad - 2\tau \int_0^{(\frac{\tau}{2D})^{1/2}\mu_c} dy F(y) \end{aligned} \quad (3.2)$$

where $\operatorname{erf}(x)$ is the error function and $F(x)$ is the Dawson Integral.²⁴ For large τ , the asymptotic behavior of Eq. (3.2) is

$$T(\mu_c) = \frac{\sqrt{2\pi D \tau}}{\mu_c} e^{\frac{\tau}{2D}\mu_c^2} \quad (3.3)$$

which is the TG result.⁸ In view of Eqs. (3.2) and (3.3), the MFPT in the TG model is τ times a function of $\tau\mu_c^2/D$.

Let us go one step further and neglect only the white stochastic driving force in (1.4) but retain the dissipative time dependence of μ . The variable μ then experiences exponential relaxation. Retaining this feature yields behavior closer to the true evolution of the two-dimensional system. With this deterministic but time-varying- μ approximation, the slope of

the separatrix at $q = 0$ is a simple function of τ as a consequence of the exponential relaxation of the "noise" variable:⁹

$$\frac{d\mu_{sep}}{dq} \Big|_{q=0} = - \left(1 + \frac{1}{\tau} \right) . \quad (3.4)$$

Therefore, near $q = 0$ the position of the separatrix is given by

$$\mu_{sep}(q, \tau) = \left(1 + \frac{1}{\tau} \right) \mu_{sep}(q, \infty) . \quad (3.5)$$

Although this relation is only valid close to $q = 0$, we assume the same dependence for the entire separatrix.

These arguments can be reasonably retained even in the presence of the white noise in (1.4) if τ is sufficiently large that if at a given time the system is above the separatrix, it has enough time to evolve towards the other well before the noise $\mu(t)$ departs appreciably from its deterministic exponential relaxation. Then, generalizing the ideas of References 8 and 10, we take for the MFPT calculation the approximate τ -dependent critical value

$$\mu(\tau) = \left(1 + \frac{1}{\tau} \right) \mu(\infty) = \left(1 + \frac{1}{\tau} \right) \mu_c \quad (3.6)$$

which is consistent with the lower bound found in Reference 10. As a consequence, the dependence of the MFPT on the noise parameters is

$$\frac{T}{\tau} = f \left[\frac{\tau}{D} \left(1 + \frac{1}{\tau} \right)^2 \right] . \quad (3.7)$$

This scaling law is tested in Fig. 9, where we have plotted the simulation points for τ above 0.9. For τ smaller than this value the points deviate from the behavior predicted by Eq. (3.7), as can be expected from the singularity in (3.6) at $\tau = 0$. In light of this figure, the predicted scaling is convincingly confirmed. The result (3.7) calls for more theoretical work.

4. The Eigenvalues of the Fokker-Planck Equation

A method frequently used to estimate the MFPT without carrying out digital or analog simulations is the numerical solution of the eigenvalue problem for the two-dimensional Fokker-Planck equation corresponding to the system (1.1), (1.4) (e.g. by using a matrix continued-fraction expansion).^{11,12} The MFPT to reach the barrier is calculated as the inverse of the first non-vanishing eigenvalue λ_1 :

$$T = \lambda_1^{-1} . \quad (4.1)$$

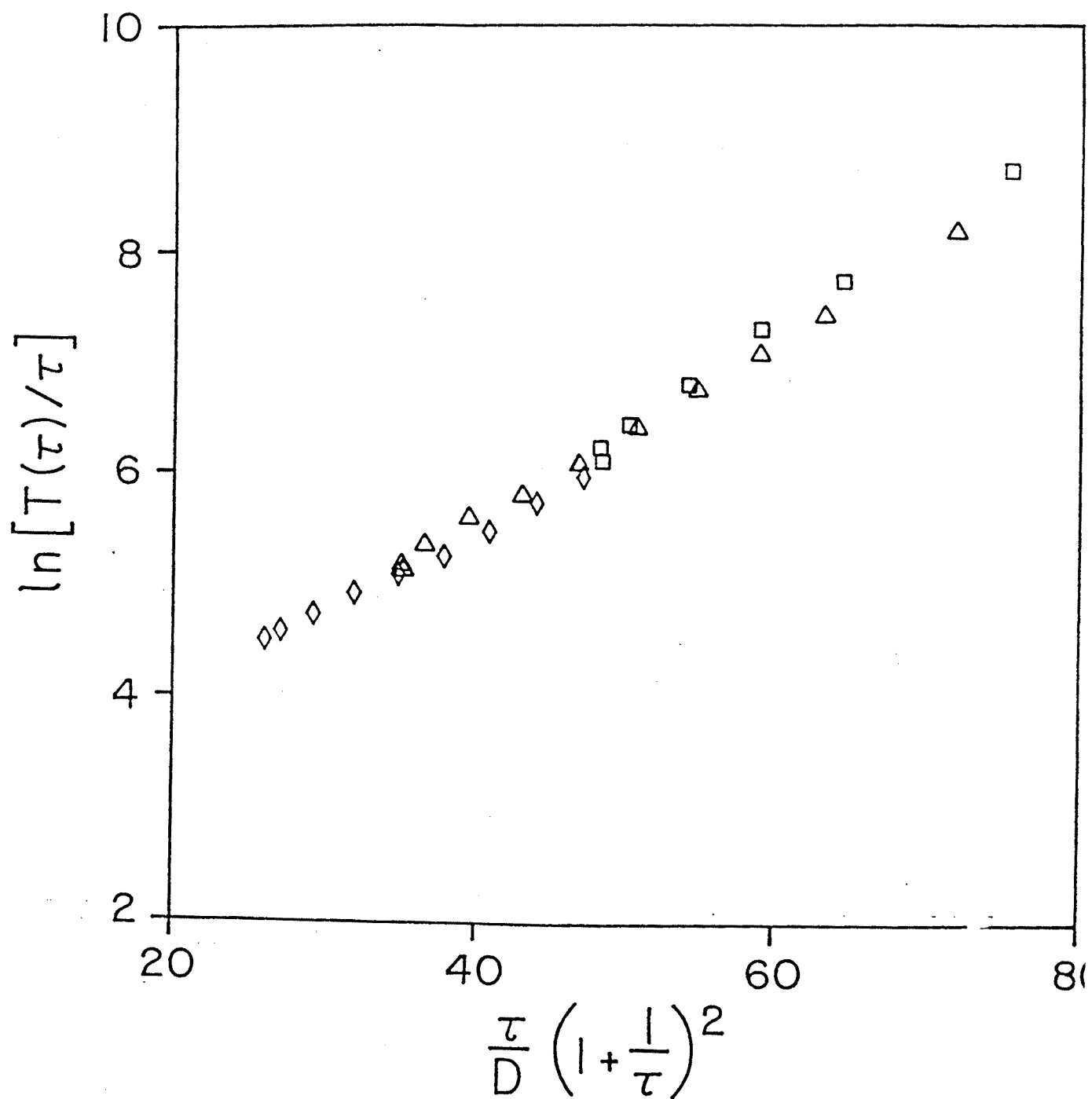


Fig. 9 $T(\tau)/\tau$ vs. $(\tau/D)(1 + 1/\tau)^2$ for $\tau \geq 0.9$. Squares: $D = 0.083$; triangles: $D = 0.114$;

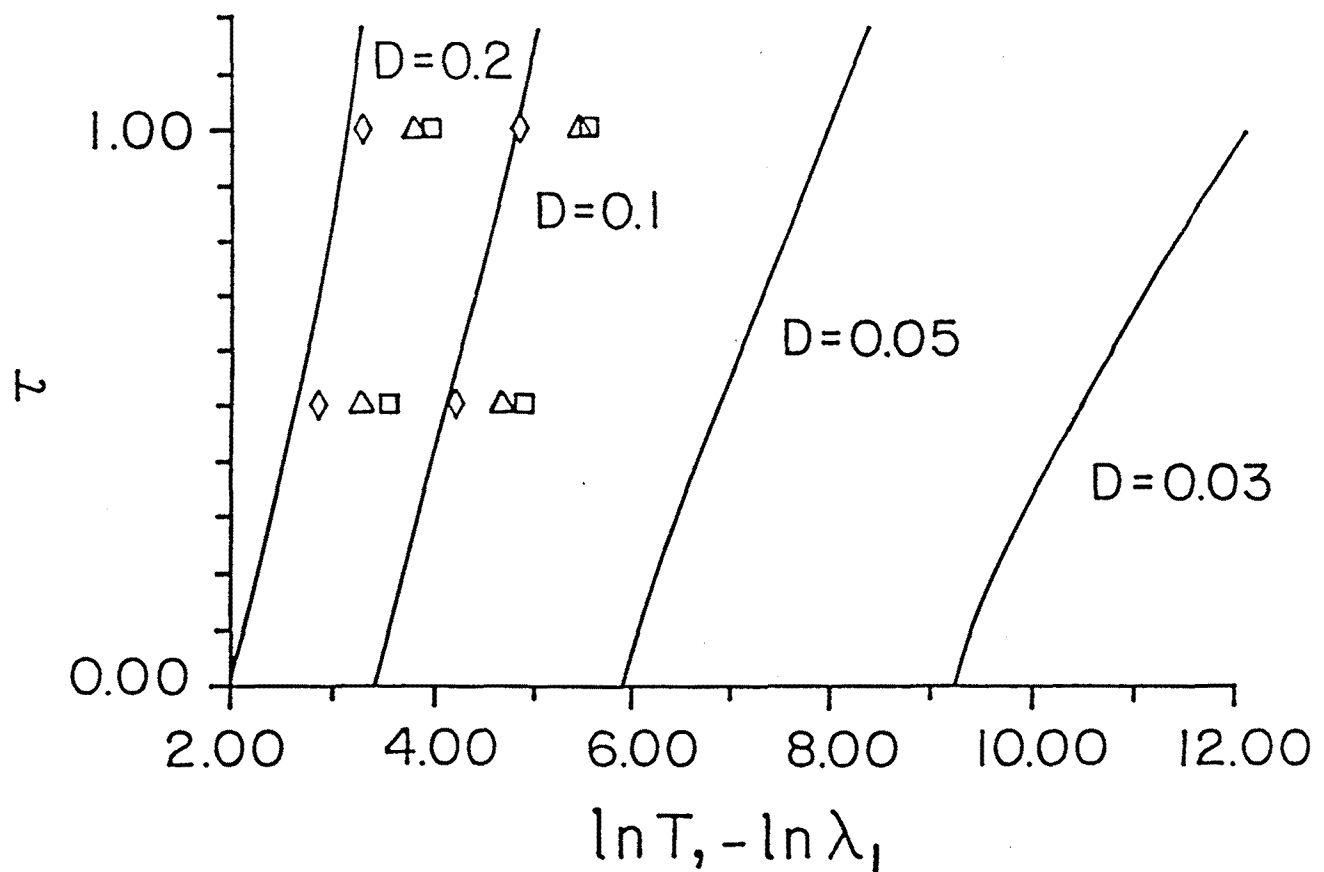


Fig. 10 $\ln \lambda_1^{-1}$ and $\ln T$ vs. τ . Solid lines: numerical results from Reference 9. Symbols: simulation results for $D = 0.2$ and $D = 0.1$. Squares: T_{bot} ; triangles: T_{top} ; rhombuses: $T_{bot}/2$.

However, the connection between the MFPT and the eigenvalue λ_1 in a system with various attractors such as ours is only clear under certain conditions.²⁵ First, one must be in the weak noise limit. Second, the probability of turning back to the first attractor (the first well) without reaching the second one, once the system has crossed the boundary condition of the MFPT, must be small. This second condition clearly does not hold for the boundary condition at $q = 0$ because the probability of turning back once the system reaches the top of the barrier is not necessarily small (it is equal to 1/2 for white noise). However, this condition holds for the boundary at $q = 1$ because the crossing of this boundary means that the second well has been reached.

The eigenvalue λ_1 is therefore in general related to the MFPT T_{bot} and not to T_{top} . This conclusion is tested in Fig. 10, where T_{top} and T_{bot} are compared with the numerical eigenvalue results of Reference 12. It can be seen there that the inverse of the eigenvalue λ_1 coincides for small D with half of the MFPT T_{bot} and not with T_{top} . Thus, the precise relation (4.1) reads

$$T_{bot} = 2\lambda_1^{-1} \quad (4.2)$$

and one should bear in mind that even this relation is only valid for small D .

5. Conclusions

The main conclusions of this paper can be summarized as follows:

a) Kramers' formulas (1.5) and (1.6) and their correction (1.7) by Larson and Kostin are asymptotic results. In the experimentally accessible range of variables further corrections to these results become important. Hence these formulas cannot be used to conclude the validity of numerical or digital simulations.

b) T_{bot} and T_{top} are neither equivalent nor are they in general related in a simple universal way; they contain different physical information. Therefore one of these quantities can not in general be used to deduce the behavior of the other. T_{bot} is the more physically relevant time and is rather insensitive to the precise location of the initial and final values so long as they are both deep within their respective wells.

c) At present only the small- τ case ($\tau < 0.3$) is explained satisfactorily by the theories. All existing small- τ theories for T_{bot} and T_{sep} yield an initial slope of $3/2$, which is clearly the behavior also observed in numerical simulations. The differences between (1.8), (1.10) (in both of which the $3\tau/2$ arises from the prefactor) and (1.9) (where it arises in the exponent) are not apparent in the range $\tau < 0.2$. Therefore all the theories are equivalent from a

practical point of view in this range. It is not possible to conclude which theory leads to the most accurate D -dependence that becomes evident in the larger- τ simulations ($0.2 < \tau < 1$).

d) Simulations of T_{top} for small τ clearly confirm the $\sqrt{\tau}$ contribution found by Doering et al. in (1.11).

e) The large- τ case is explained only qualitatively by current theories; there remain large quantitative differences between the theories and the results of numerical simulations. For very large values of τ the fluctuating potential picture of Tsironis and Grigolini ⁸ yields the correct asymptotic exponential dependence on $2\tau/27D$ in the MFPT. Corrections to the asymptotic exponent can be obtained by a simple extension of the fluctuating potential idea, cf. Eqs. (3.6) and (3.7). Nevertheless there are serious quantitative disagreements with the simulations that arise from prefactor contributions that have not been properly captured.

f) The dominant eigenvalue of the two-variables (q, μ) Fokker-Planck equation should be identified with T_{bot} through Eq. (4.2) for small D . ¹⁹

References

1. P. Hänggi, F. Marchesoni and P. Grigolini, *Z. Phys. B* **56**, 333 (1984).
2. P. Hänggi, T.J. Mroczkowski, F. Moss and P.V.E. McClintock, *Phys. Rev. A* **32**, 695 (1985).
3. J. Masoliver, B.J. West and K. Lindenberg, *Phys. Rev. A* **35**, 3086 (1987).
4. C.R. Doering, P.S. Hagan and C.D. Levermore, *Phys. Rev. Lett.* **59**, 2129 (1987).
5. R.F. Fox, *Phys. Rev. A* **37**, 911 (1988).
6. M.M. Klosek-Dygas, B.J. Matkowsky and Z. Schuss, *Phys. Rev. A* **38**, 2605 (1988).
7. J.F. Luciani and A.D. Verga, *J. Stat. Phys.* **50**, 567 (1988).
8. G.P. Tsironis and P. Grigolini, *Phys. Rev. Lett.* **61**, 9 (1988); G.P. Tsironis and P. Grigolini, *Phys. Rev. A* **38**, 3749 (1988).
9. P. Hänggi, P. Jung and F. Marchesoni, to appear in *J. Stat. Phys.* (1989).
10. F.J. de la Rubia, E. Peacock-López, G.P. Tsironis, K. Lindenberg, L. Ramirez-Piscina and J.M. Sancho, *Phys. Rev. A* **38**, 3827 (1988).
11. P. Jung and H. Risken, *Z. Phys. B* **61**, 367 (1985).
12. P. Jung and P. Hänggi, *Phys. Rev. Lett.* **61**, 11 (1988).
13. R. Mannella and V. Palleschi, *Phys. Lett. A* **129**, 317 (1988).
14. R. Mannella and V. Palleschi, unpublished.
15. C.W. Gardiner, *Handbook of Stochastic Methods* (Springer-Verlag, Berlin, 1983).
16. H.A. Kramers, *Physica* **7**, 284 (1940).
17. R.S. Larson and M.D. Kostin, *J. Chem. Phys.* **69**, 4821 (1978).
18. P. Hänggi, P. Jung and P. Talkner, *Phys. Rev. Lett.* **60**, 2804 (1988).
19. C.R. Doering, R.J. Bagley, P.S. Hagan and C.D. Levermore, *Phys. Rev. Lett.* **60**, 2805 (1988).
20. J.M. Sancho, M. San Miguel, S.L. Katz and J.D. Gunton, *Phys. Rev. A* **26**, 1589 (1982).
21. W. Rumelin, *SIAM J. Numer. Anal.* **19**, 604 (1982).
22. R.F. Fox, I.R. Gatland, R. Roy and G. Vemuri, *Phys. Rev. A* **38**, 5938 (1988).
23. W. Strittmatter, unpublished (1988).
24. M. Abramowitz and I. A. Stegun, *Handbook of Mathematical Functions* (Dover, New York, 1965).
25. P. Talkner, *Z. Phys. B* **68**, 201 (1987).

II.2 A LOWER BOUND FOR THE CRITICAL NOISE OF THE FLUCTUATING POTENTIAL APPROXIMATION

Recently Tsironis and Grigolini (TG) ^{1,2} presented a new theory for the mean first passage time from one metastable state to another of a bistable process driven by colored noise. Their theory is expected to be valid when the correlation time τ of the noise is extremely long ($\tau \rightarrow \infty$). TG specifically considered the system

$$\dot{x} = \alpha x - \beta x^3 + \xi(t) \quad (1)$$

wherein the fluctuations $\xi(t)$ are Gaussian and exponentially correlated:

$$\langle \xi(t)\xi(t') \rangle = \frac{D}{\tau} e^{-|t-t'|\tau} . \quad (2)$$

Let us briefly restate the TG argument in a way convenient for our purposes. One can associate with the process (1) an instantaneous "potential"

$$V(x) = -\alpha \frac{x^2}{2} + \beta \frac{x^4}{4} - \xi x . \quad (3)$$

The number of extrema of this potential depends on the value of ξ . If $|\xi| < \xi_c \equiv (4\alpha^3/27\beta)^{1/2}$ then $V(x)$ has three extrema, a maximum corresponding to an unstable state and two minima corresponding to stable states. When $|\xi| = \xi_c$, two of these extrema merge into a single marginally stable state. If $|\xi| > \xi_c$ then there is only a single extremum (a minimum). These three cases are illustrated in Fig. 1.

For large τ ($\tau \rightarrow \infty$) TG argue that passage from one metastable state to the other occurs when the metastable state in which the process finds itself disappears. Thus, if the process is in the left-hand well ($x < 0$) then the first passage to the right-hand well ($x > 0$) occurs when $\xi(t)$ first reaches the value ξ_c . To calculate this passage time, one notes that the fluctuations $\xi(t)$ constitute an Ornstein-Uhlenbeck process whose evolution can be described by the Langevin equation

$$\dot{\xi} = -\frac{1}{\tau}\xi + \frac{1}{\tau}f(t) \quad (4)$$

where $f(t)$ is Gaussian delta-correlated noise:

$$\langle f(t)f(t') \rangle = 2D \delta(t-t') . \quad (5)$$

The mean time for $\xi(t)$ to first reach ξ_c is obtained using standard methods ³ and for $\xi_c\tau/D \gg 1$ is found to be

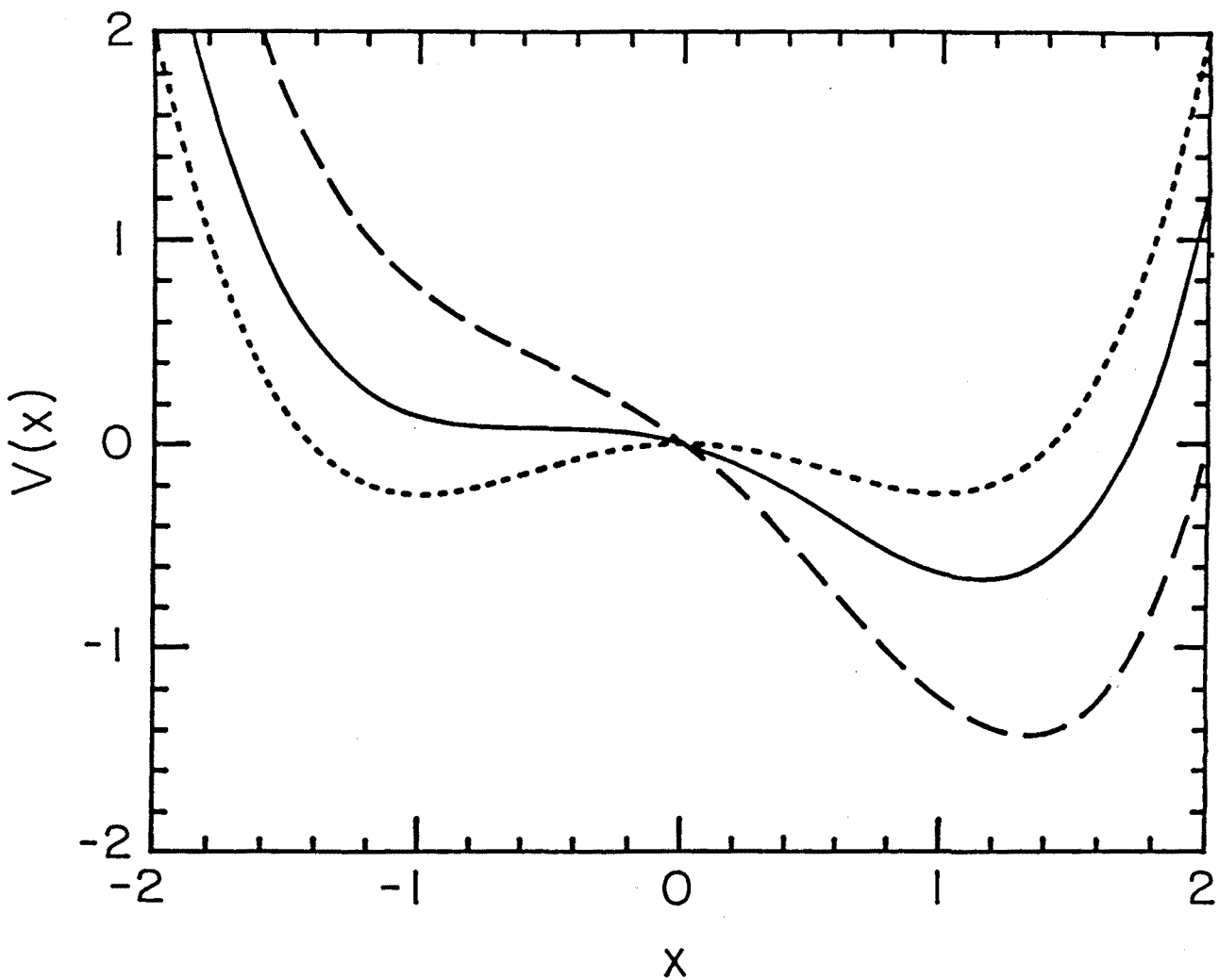


Figure 1 The "potential" of Eq. (3) with $\alpha = \beta = 1$ for three values of ξ . Dashed curve: $\xi > \xi_c$; solid curve: $\xi = \xi_c$; dotted curve: $\xi < \xi_c$.

$$T = \frac{(2\pi D \tau)^{\frac{1}{2}}}{\xi_c} \exp\left(\frac{\xi_c^2}{2D}\tau\right). \quad (6)$$

TG subsequently proposed a bridging formula involving (6) and the $\tau \rightarrow 0$ result to represent the mean first passage time for all τ :

$$T = \exp\left(\frac{V_0}{D}\right) \left[\frac{\pi}{\alpha\sqrt{2}} + \frac{(2\pi D \tau)^{\frac{1}{2}}}{\xi_c} \exp\left(\frac{\xi_c^2}{2D}\tau\right) \right] \quad (7)$$

where $V_0 = \alpha^2/4\beta$. According to TG, Eq. (7) then is the mean first passage time for x to make a transition from one metastable state to the other. The exponential prefactor $\exp(\frac{V_0}{D})$ is not derived within the fluctuating potential argument but it has been justified on other grounds in Reference 2. Our purpose here is to discuss the coefficient of τ in the second exponential factor in (7) and not this prefactor. In particular, according to Eq. (7) a plot of $\ln T$ vs. τ should yield for large τ essentially a straight line of slope $\xi_c^2/2D$ (deviations from a straight line predicted by the theory are small but visible as τ decreases).

Using a continued fraction method to calculate an eigenvalue closely related to T , Risken *et al.* have shown that for large but finite τ ($\tau < 3$) the slope of $\ln T$ vs. τ is greater than $\xi_c^2/2D$ by a substantial D -dependent amount (approximately 20% for $D = 0.2$).⁶ Our own (unpublished) numerical simulations of Eq. (1) confirm this result.⁷ Herein we provide an explanation for this behavior in the context of the TG model and we give a lower bound for the slope of $\ln T$ vs. τ .

Figure 2 shows a typical (single) trajectory of x and ξ for two values of τ , one large but finite ($\tau = 5$) and one extremely large ($\tau = 50$). In each of these trajectories the transition from one metastable state to the other is clearly visible and takes place when ξ reaches a value considerably greater than ξ_c . In fact, the noise crosses the value ξ_c several times without effect on x .

The reason for this behavior can clearly be seen upon examination of the "potential" curves in Fig. 1. When $\xi = \xi_c$ the potential near the marginally stable state is extremely flat and it takes the process a very long (∞) time T_r to "roll" down to the

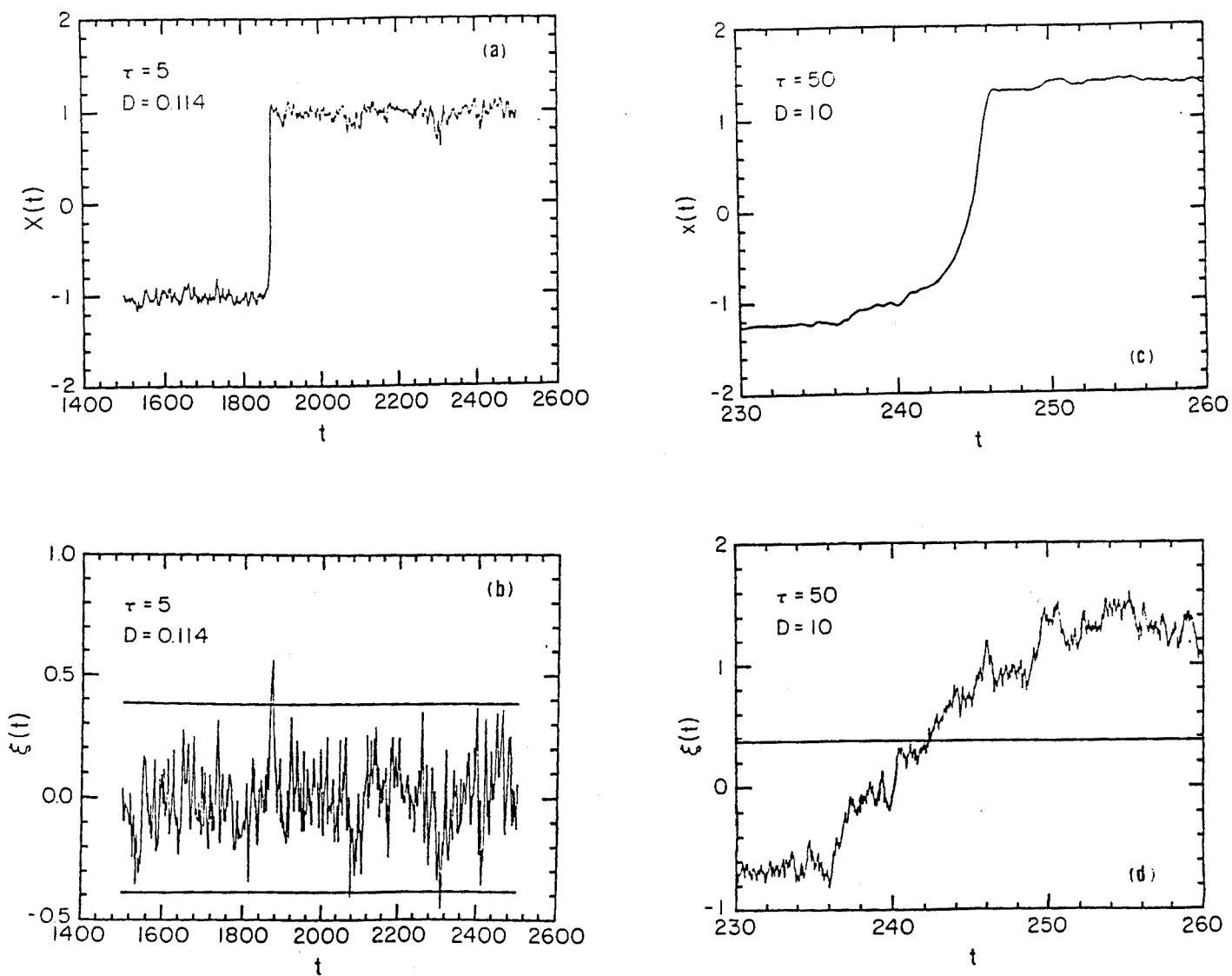


Figure 2 Typical trajectories generated by Eqs. (1) and (4) with $\alpha = \beta = 1$. In Figs. 2a and 2b $\tau = 5$ and $D = 0.114$. In Figs. 2c and 2d $\tau = 50$ and $D = 10$.

minimum of the potential. In fact, during this long time the noise (which is only correlated over a time τ) will change and the previously marginally stable state may eventually become metastable again. We suggest that a successful transition requires that the passage be complete before the noise changes its value, i.e. that

$$T_r \leq \tau . \quad (8)$$

For this condition to be satisfied, ξ must exceed a τ -dependent value $\xi_\tau^0 > \xi_c$ given below, a value that increases with decreasing τ .

To estimate the τ -dependence of ξ_τ^0 , we note that the (deterministic) time for the process to go from a point x_1 to a point x_2 for a fixed ξ (cf. Fig. 3) is given by

$$T_r = \int_{x_1}^{x_2} \frac{dx}{\alpha x - \beta x^3 + \xi} , \quad (9)$$

and it is this time that enters the inequality (8). For the upper limit we choose a value representative of "arrival at the right-hand well", e.g. $x_2 = 0$. For the lower limit we choose $x_2 = -(\alpha/3\beta)^{1/2}$, the position of the marginally stable state when $\xi = \xi_c$. Small changes in these choices do not materially affect our estimate of ξ_τ^0 for large τ .

We thus propose the following formula for the mean first passage time when τ is large but finite:

$$T = \exp \left[\frac{V_0}{D} \right] \left[\frac{\pi}{\alpha \sqrt{2}} + \frac{(2\pi D \tau)^{1/2}}{\xi_\tau} \exp \left(\frac{\xi_\tau^2}{2D} \tau \right) \right] . \quad (10)$$

where

$$\xi_\tau \geq \xi_\tau^0 \quad (11)$$

and ξ_τ^0 is found from the equality

$$\int_{-1/\sqrt{3}}^0 \frac{dx}{\alpha x - \beta x^3 + \xi_\tau^0} = \tau . \quad (12)$$

Figure 3 shows ξ_τ^0 vs. τ obtained from Eq. (12). Clearly, for the values of τ considered in most available simulations and numerical calculations ($\tau < 5$) the noise indeed has to be considerably larger than ξ_c for passage from one metastable state to another to occur. An analytic expression for this curve can be obtained from the integral (12), which we have performed for large τ :

$$\xi_\tau^0 = \xi_c + \frac{\pi^2}{4\sqrt{3}} \frac{1}{\tau^2} + O(\tau^{-3}\ln\tau) \quad (13)$$

where we have set $\alpha = \beta = 1$.

Let us consider the specific trajectories shown in Fig. 2 in light of these predictions. One should be aware that single trajectories may behave quite differently from the behavior envisioned when one talks about average results. Thus, it could even happen (although it does not in the trajectories shown here) that a transition occurs when the instantaneous value of the noise is actually smaller than ξ_c . It should also be noted that even a very large value of ξ may not lead to a transition if that value is not retained for a sufficiently long time: after all, the correlation time τ is again only an average. The trajectory for $\tau = 50$ shows a transition when $\xi = 0.48$, i.e. a value above ξ_c . Note that in this particular trajectory an even larger value of ξ attained earlier did not lead to a transition because it was not retained for a sufficiently long time. Our lower-bound estimate indicates that for such a large $\tau = 50$ the value of the noise required for a successful transition is, on the average, greater than $\xi_{50}^0 = 0.3855$. The $\tau = 5$ trajectory shown in Fig. 2 requires a ξ of 0.57 before the transition occurs. Our lower bound indicates that the value of ξ for a successful transition must, on the average, be greater than 0.4419, again consistent with this result. Numerical simulations⁷ yield $T = 8575$ for $D = 0.114$; this value is obtained from Eq. (10) with $\xi_\tau = 0.5024$ (that the particular realization shown in Fig. 2 requires a larger value of ξ is of course not inconsistent with this result).

In summary, we have provided an explanation for the deviations of numerical simulations and eigenvalue calculations from the large- τ results of Tsironis and Grigolini. We have provided a quantitative lower bound for the mean first passage time when the correlation time of the noise is large but finite. We note that the TG theory

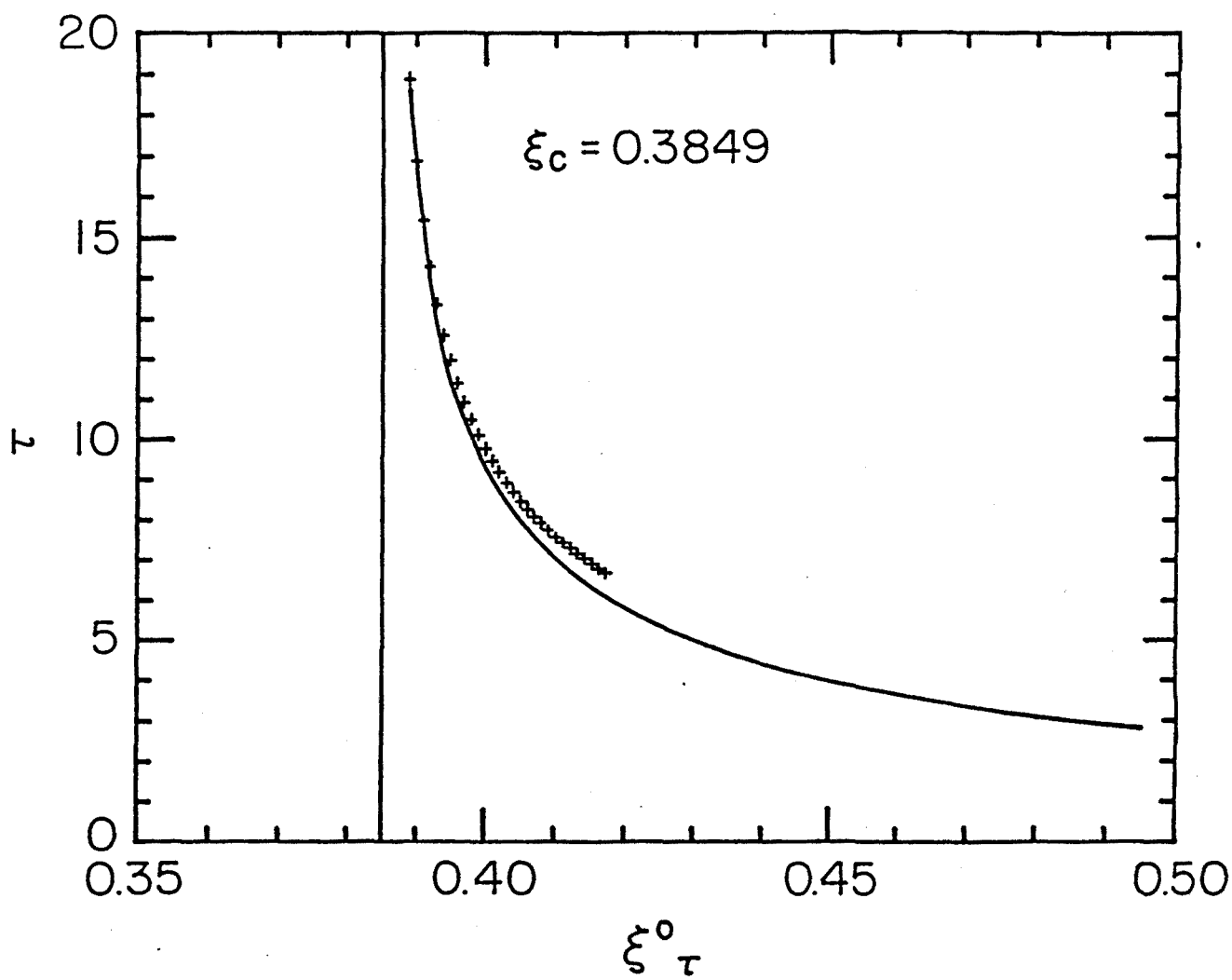


Figure 3 Numerical solution of Eq. (12) (solid line) and analytic large- τ estimate as given in Eq. (13) (+). The vertical line indicates the critical value ξ_c .

on which our analysis is based and our arguments to improve it are not related in any way to existing effective Fokker-Planck theories.

References

1. G. Tsironis and P. Grigolini, Phys. Rev. Lett. **61**, 7 (1988).
2. G. Tsironis and P. Grigolini, to appear in Phys. Rev. A.
3. K. Lindenberg and V. Seshadri, J. Chem. Phys. **71**, 4075 (1979).
4. J. F. Luciani and A. D. Verga, J. Stat. Phys. **50**, 567 (1988).
5. P. Jung and P. Hänggi, Phys. Rev. Lett. **61**, 11 (1988); P. Hänggi, P. Jung and F. Marchesoni, to appear in J. Stat. Phys.
6. Th. Leiber, F. Marchesoni and H. Risken, Phys. Rev. Lett. **59**, 1381 (1987); *ibid.* **60**, 659 (1988); G. P. Tsironis, Phys. Rev. Lett., to be published; Th. Leiber, F. Marchesoni and H. Risken, Phys. Rev. Lett., to be published.
7. L. Ramirez-Piscina, F. J. de la Rubia, E. Peacock-López, G. P. Tsiorinis, K. Lindenberg and J. M. Sancho, unpublished

II.3 HIGHLY COLORED NOISE

A number of theoretical approaches have recently been used to obtain the mean first-passage time from one well to the other of a bistable system driven by highly colored noise.¹⁻⁶ The generic system of interest evolves according to the dynamical equation

$$\dot{X}(t) = aX - bX^3 + f(t) \quad (1)$$

and the noise $f(t)$ is assumed to be zero-centered and Gaussian with exponential correlations

$$\langle f(t)f(t') \rangle = \frac{D}{\tau} e^{-|t-t'|/\tau}. \quad (2)$$

D is the noise intensity and τ its correlation time. The "potential"

$$V(X) = \frac{b}{4}X^4 - \frac{a}{2}X^2 \quad (3)$$

implicit in Eq. (1) has two minima separated by a barrier of height $V_0 = a^2/4b$. The noise $f(t)$ is said to be highly colored when τ/D is large compared to the deterministic quantity V_0^{-1} :

$$\tau V_0/D \gg 1. \quad (4)$$

A number of methods have been used to calculate the mean first passage time T from one well of the potential (3) to the other.⁷ Although these methods are all approximate and different from one another, there seems to be universal agreement as to the dominant features of the result in the "large- t " limit $\tau \rightarrow \infty$. In this limit [cf. Eq. (4)] all the large- τ theories lead to¹⁻⁷

$$\lim_{\tau \rightarrow \infty} T = \left(\frac{27\pi D \tau}{8V_0} \right)^{1/4} \exp \left(\frac{8}{27} \frac{V_0 \tau}{D} \right). \quad (5)$$

Furthermore, there also seems to be universal agreement that the asymptotic result is achieved very slowly and requires extremely large values of the exponent.^{2-5,8}

The approximations that lead to Eq. (5) are typically not systematic expansions in any parameter; consequently, there exists considerable disagreement and uncertainty as to the corrections to this result with decreasing τ , both in the prefactor and in the exponent. It should be stressed that these differences notwithstanding, all the corrections consist of (small) additions to the exponent $8V_0\tau/27D$ (and less importantly and not of particular interest here, small additions to the $\tau^{1/4}$ prefactor). We have also recently developed an argument that leads to such a correction.⁶ Our argument is based on the approach of Tsironis and Grigolini,² who obtain (5) by assuming that a transition from one well to the other occurs when the noise $f(t)$ reaches the critical value $\mu_c \equiv (16V_0/27)^{1/4}$ at which the "effective potential"

$$V_{eff}(X, f) = V(X) - Xf \quad (6)$$

first ceases to be bistable. We note that this argument is valid only when $\tau \rightarrow \infty$, whence $f(t)$ is essentially constant and μ_c marks the separatrix between the two wells of $V_{eff}(X, f)$. With decreasing τ one must consider the variation of $f(t)$ with time, and $f(t)$ must in general reach a value greater than μ_c for a successful transition to occur.^{4,6} We do not repeat the detailed argument here,⁶ but simply state our result, which replaces Eq. (5) with

$$T = \frac{(2\pi D \tau)^{1/2}}{\mu(\tau)} \exp\left(-\frac{\mu^2(\tau)}{2D}\tau\right). \quad (7)$$

Equation (5) corresponds to the choice $\mu(\tau) = \mu_c$ while we obtain

$$\mu(\tau) = \mu_c(1 + 1/\tau) = (4/27)^{1/2}(1 + 1/\tau). \quad (8)$$

In (8) and frequently henceforth we have set $a = b = 1$, so that $V_0 = 1/4$.

In reference 6 we have plotted our simulation results⁹ for the mean first passage time in the form $\ln(T/\tau)$ vs. $(\tau/D)(1 + 1/\tau)^2$. Our simulations were carried out for three different values of D in the range $5 < (\tau V_0/D)(1 + 1/\tau)^2 < 20$, and all our points fall close to the same line on this plot, thus confirming the functional dependence on $\mu(\tau)\tau/D$ predicted in the exponent of (7) (see Fig. 1).

Having confirmed the expected functional dependence in the exponent, our next question (and the central question of this communication) is to investigate the value of the slope $8V_0/27 = 2/27$ predicted in Eqs. (5) and (7) and in all other large- τ theories as well. To explore this question we sought the best fit of our simulations for the parameters α and β arbitrarily introduced as follows:

$$T = \alpha \left(\frac{27\pi D \tau}{2\beta} \right)^{1/2} \frac{1}{(1 + 1/\tau)} \exp\left[-\frac{2}{27}\beta \frac{\tau}{D}(1 + \frac{1}{\tau})^2\right]. \quad (9)$$

Equation (7) with (8) corresponds to the choice $\alpha = \beta = 1$. We find the best agreement between simulations and (9) to occur for the choices $\alpha = 6.17$ and $\beta = 1.29 \approx 4/3$. In Fig. 1 we have plotted our simulation results for $\ln(T/\tau)$ for three values of D as a function of $(\tau/D)(1 + 1/\tau)^2$ (as we did in reference 6). The results fall on a straight line of slope $2\beta/27 \approx 8/81$, indicated as a solid line. On the same graph (arbitrarily starting at the same point on the abscissa simply to highlight the different slopes) we show the dotted line whose slope is $2/27$, representing the large- τ theoretical predictions.

Note that the difference in the slopes between the theoretical predictions and the numerical simulations reported in Fig. 1 represents a change in the *coefficient* of the *leading term* in

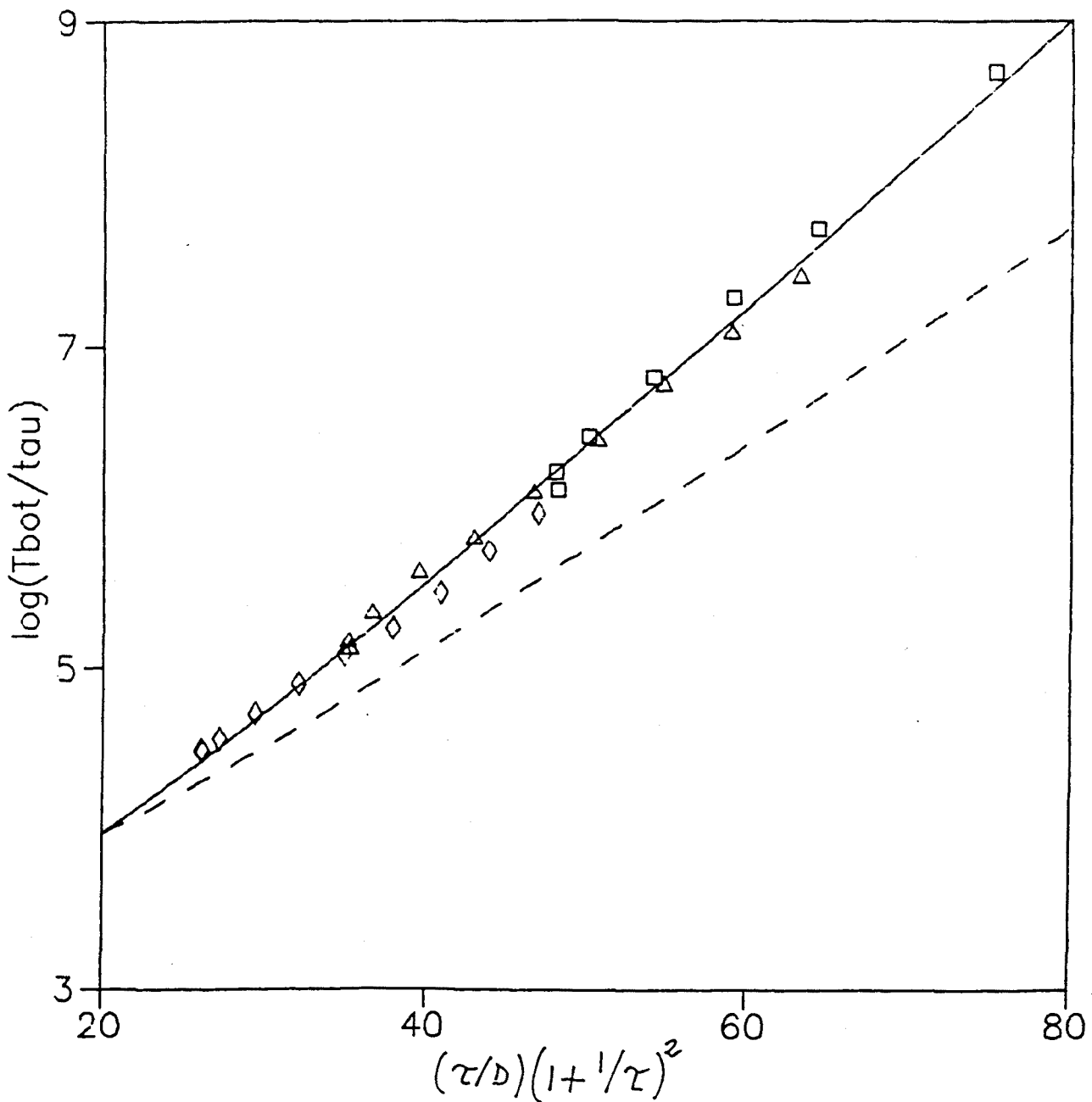


Fig. 1 $\ln(T/\tau)$ vs. $(\tau/D)(1 + 1/\tau)^2$ for $\tau \geq 0.9$. The symbols denote numerical simulation results with $D = 0.083$ (squares), $D = 0.114$ (triangles) and $D = 0.153$ (rhombuses). Solid line: $(2\beta\tau)/27D(1 + 1/\tau)^2$ with $\beta = 1.29 \approx 4/3$. Dashed line: same function with $\beta = 1$.

the exponent of T , a coefficient about which no question has been raised heretofore. In view of this unexpected behavior, we returned to some of the existing (far from plentiful) numerical data to be found in the literature and found confirmation of the behavior reported here. Fox⁸ reports two large- τ simulations in the range $1 < \tau < 10$ for $D = 0.1$ and $D = 0.2$. These values correspond to $\tau V_0/D$ within the same range of values as we have considered. For $D = 0.1$ Fox obtains a slope of 1.0 from his simulations whereas the large- τ theories would have predicted $8V_0/27D = 0.74$. For $D = 0.2$ Fox's simulations give a slope of 0.5 instead of the predicted value 0.37. Note that the ratios 0.5/0.37 and 1.0/0.74 are indeed approximately 4/3. The numerical results of Jung and Hänggi^{10,11} for the lowest eigenvalue λ of the two-dimensional Fokker-Planck operator are restricted to the range $\tau V_0/D \leq 2.5$ and therefore may not be in the regime appropriate for our large- τ analysis. Nevertheless we observe that in this case the slope of $\ln(\lambda^{-1}/\tau)$ vs. $(\tau V_0/D)(1 + 1/\tau)^2$ exceeds 8/27 by an amount not inconsistent with our value of β .

We thus conclude that the existing numerical evidence points to a dependence of T on τ which is exponentially larger than that predicted by the large- τ theories. It may of course be possible that the predicted large- τ are recovered (i.e. that β in Eq. (9) $\rightarrow 1$) if $\tau V_0/D$ greatly exceeds the values presently accessible to numerical computation. On the other hand, we note that the exponent in Eq. (9) achieves values of $O(10)$ in the available results. The explanation of the observed results, we believe, can be found in the numerical studies of Mannella and Palleschi⁵ and their analysis of the results. To describe their analysis, we first note that the large- τ theories are all based on the notion that the process first reaches a particular curve in (x, f) phase space in time T , and that the further passage of the process from that curve to the other well occurs deterministically in essentially zero time. The agreed-upon curve that must be reached is the (τ -dependent) separatrix between the wells. Since the separatrix can not be specified analytically for large τ , approximations are made; different theories specify this curve in different ways. In spite of these differences, all the theories lead to the same exponential coefficient for T in the large- τ limit.

The detailed analysis of individual trajectories by Mannella and Palleschi⁵ reveals the problem with this viewpoint: in reality there is considerable dynamics in the region of the separatrix, as shown in Figs. 2 and 3. These figures show that once a trajectory reaches the region in (x, f) -space from which the theories assume immediate passage to the other well, the actual trajectory spends a considerable time crossing and recrossing this region before moving on. This "residence time" contributes exponentially to the mean first passage time.

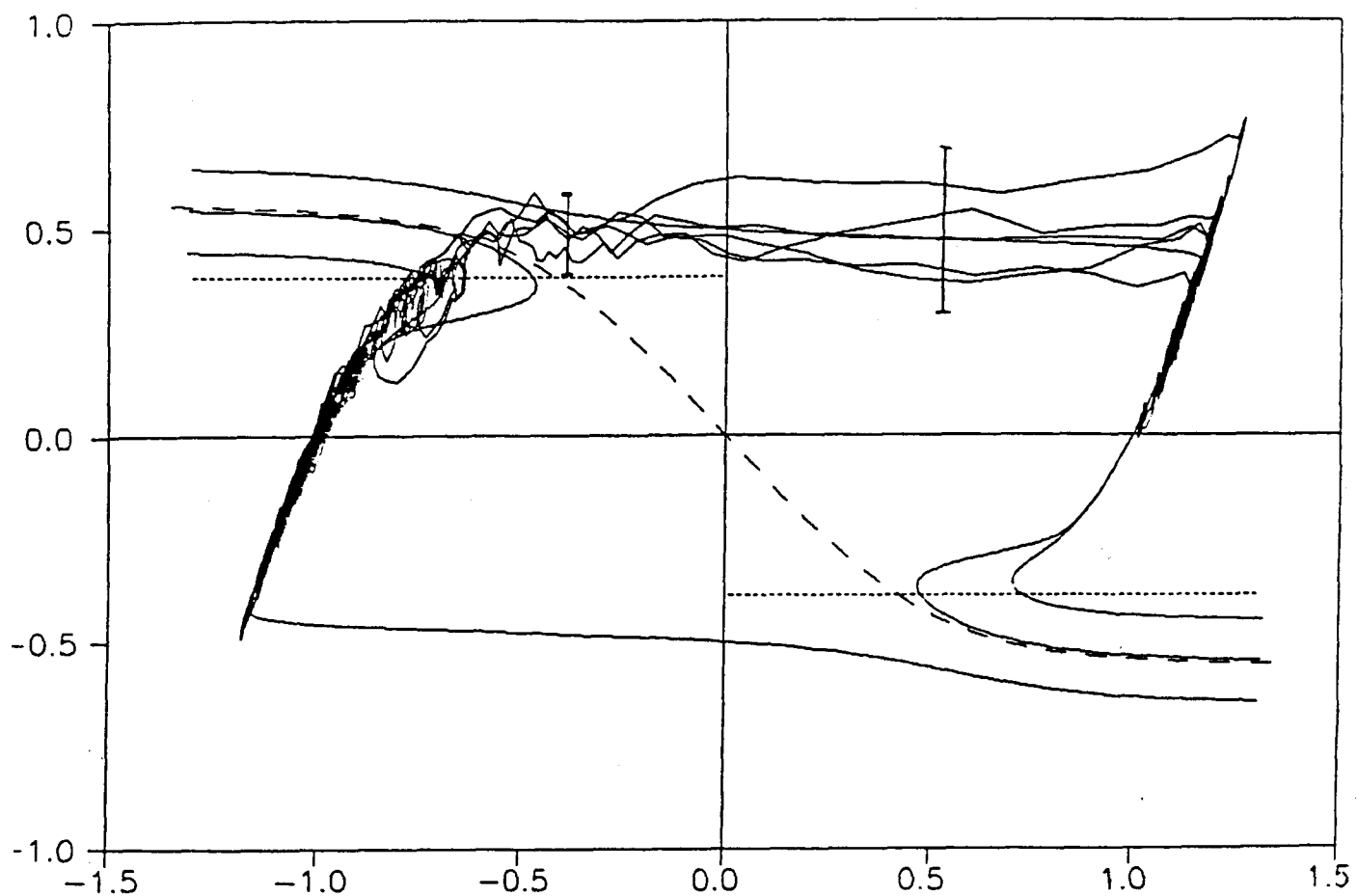


Fig. 2 A number of trajectories in phase space for $D = 0.5$ and $\tau = 15$. Note the dynamics in the region of the separatrix. The first vertical bar indicates the distribution of values of $f(t)$ in the vicinity of the separatrix. The second vertical bar is twice as long as the first and indicates that even in the process of crossing, the trajectories spread to encompass the full width of the distribution of $f(t)$.

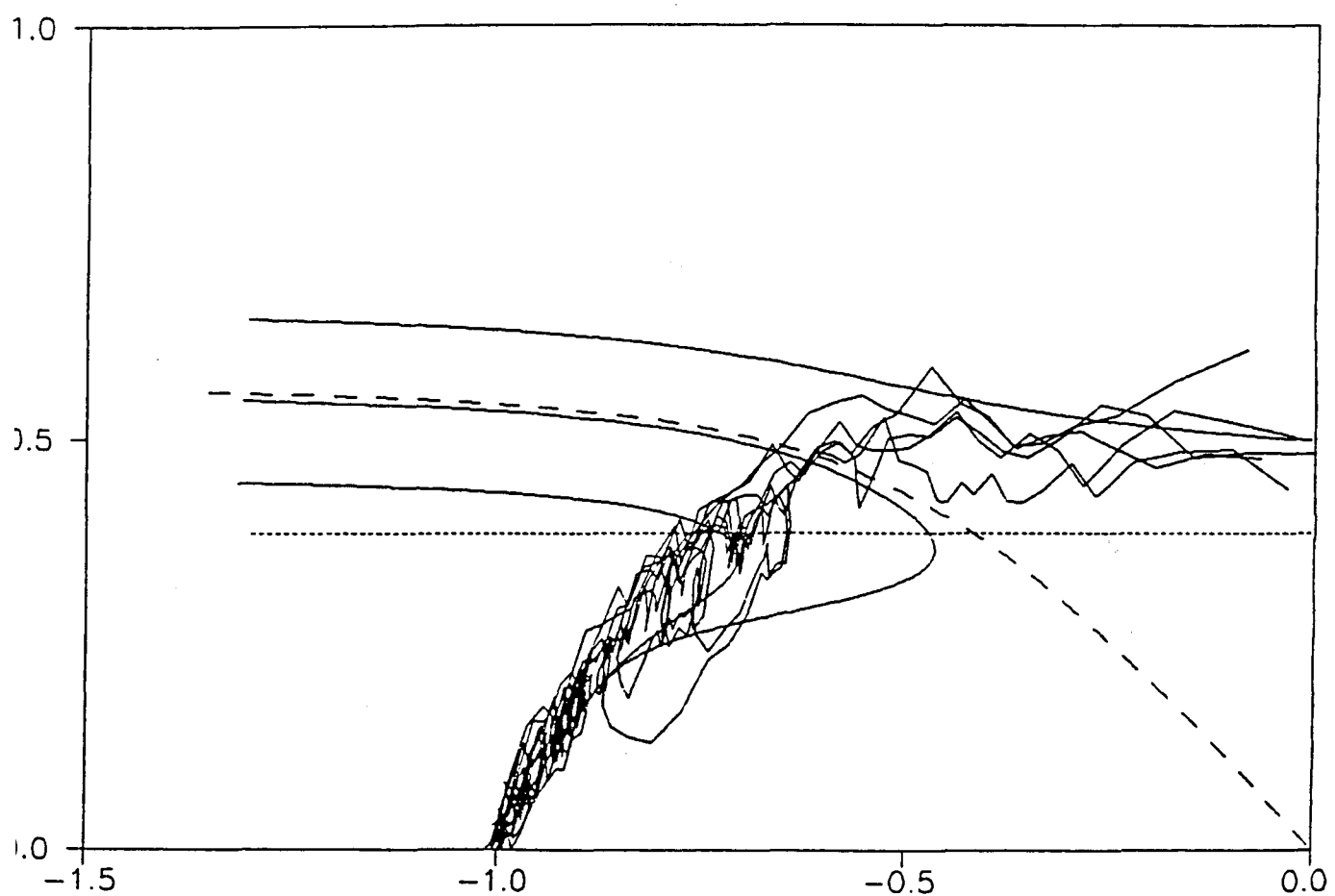


Fig. 3 Expanded view of Fig. 2 in the region of the separatrix. We have also indicated the distribution $P(\mu)$ on the figure.

To estimate the effect of the residence time of the process in the region of the separatrix we follow the reasoning of Mannella and Palleschi and write the mean first passage time \bar{T} as

$$\bar{T} = \int d\mu T(\mu) P(\mu) . \quad (10)$$

Here $T(\mu)$ is the mean first passage time for $f(t)$ to first reach the value μ and is given by^{6,12}

$$\begin{aligned} T(\mu) &= \tau\sqrt{\pi} \left[1 + \operatorname{erf} \left[(\tau/2D)^{1/2}\mu \right] \right] e^{\frac{\tau}{2D}\mu^2} F \left((\tau/2D)^{1/2}\mu \right) \\ &\quad - 2\tau \int_0^{(\tau/2D)^{1/2}\mu} dy F(y) \\ &= \frac{(2\pi D \tau)^{1/2}}{\mu} e^{\mu^2\tau/2D} \end{aligned} \quad (11)$$

[cf. Eq. (7)], where $\operatorname{erf}(x)$ is the error function and $F(x)$ is the Dawson Integral.¹³ The second expression follows from the first when a steepest descent analysis is carried out for large $\mu^2\tau/D$. The long- τ theories identify (11) with the transition time from one well to the other, each theory with a particular choice of μ . $P(\mu)$ in (10) is the probability density for a crossing to the other well to actually occur when $f(t)$ reaches the interval $(\mu, \mu + d\mu)$, and the bar in \bar{T} indicates the average over this distribution. Mannella and Palleschi find the distribution $P(\mu)$ from their simulations. They observe that it is centered at a value that decreases towards μ_c with increasing τ , that it has a width that also decreases with increasing τ , and that it falls off more rapidly than a Gaussian in the wings of the distribution. Their simulations do not reveal whether $P(\mu)$ eventually (i.e. with increasing τ) becomes a delta function at μ_c or whether it retains a finite width. Only if the former occurs would \bar{T} eventually reach the value (5) with the exponential slope 8/27.

No one has yet developed a theory that leads to an analytic prediction of the distribution $P(\mu)$. We may nevertheless deduce its qualitative effects via phenomenological arguments. For this purpose we choose $P(\mu)$ to be a Gaussian centered at μ_c and of width σ . Since the stochasticity manifest in $P(\mu)$ must of course arise from the random nature of $f(t)$, the width σ must be a function of the parameters of $f(t)$. It thus seems reasonable to write $\sigma = cD/\tau$ where c is an unknown coefficient whose value we expect to be of $O(1)$. This admittedly *ad hoc* choice for the width is consistent with the numerical results of Mannella and Palleschi and causes $P(\mu)$ to have the observed narrowing tendency as τ increases. Thus we write

$$P(\mu) = (2\pi c D / \tau)^{-1/2} e^{-(\mu - \mu_c)^2 c D / \tau} \quad (12)$$

(we require that $c < 1$; otherwise (10) leads to unphysical results and the distribution (12) must be modified to have a sharper cutoff as observed in the simulations). The integral (10) with (11) and (12) can be evaluated approximately using a steepest descents procedure to yield for the mean first passage time

$$\begin{aligned}\bar{T} &= \frac{(2\pi D \tau)^{1/2}}{\mu(\tau)} (1 - c)^{1/2} \exp \left[-\frac{\mu(\tau)}{2D(1 - c)} \right] \\ &= \left[\frac{27\pi D \tau}{8V_o (1 + i/\tau)^2} (1 - c) \right]^{1/2} \exp \left[-\frac{8V_o (1 + i/\tau)^2}{27D(1 - c)} \tau \right].\end{aligned}\quad (13)$$

The effect of the residence time reflected in $P(\mu)$ is thus to increase the slope in the exponent from $8/27$ to $8/27(1 - c)$. The choice $c = 1/4$ (which corresponds to $P(\mu)$ having half the width of the Gaussian distribution for $f(t)$ itself) leads to a slope of $8/27 \times 4/3 = 32/81$, consistent with our numerical simulations.

In conclusion, we have argued that the finite residence time in the region of the separatrix and the resultant distribution of first passage times leads to exponentially large effects in the mean first passage time for a bistable system driven by highly correlated noise. In all the large- τ simulations carried out to date the exponential correction of the theoretical mean first passage time is approximately $4/3$. Whether the existing large- τ theories correctly predict results for values of τ well beyond those presently accessible remains an open question.

References

1. J. F. Luciani and A. D. Verga, *Europhys. Lett.* **4**, 255 (1987); *J. Stat. Phys.* **50**, 567 (1988).
2. G. P. Tsironis and P. Grigolini, *Phys. Rev. Lett.* **61**, 7 (1988); *Phys. Rev. A* **38**, 3749 (1988).
3. P. Hänggi, P. Jung and F. Marchesoni, *J. Stat. Phys.* **54**, 1367 (1989).
4. F. J. de la Rubia, E. Peacock-López, G. P. Tsironis, K. Lindenberg, L. Ramirez-Piscina and J. M. Sancho, *Phys. Rev. A* **38**, 3827 (1988).
5. R. Mannella and V. Palleschi, *Phys. Rev. A* **39**, 3751 (1989).
6. L. Ramirez-Piscina, J. M. Sancho, F. J. de la Rubia, K. Lindenberg and G. P. Tsironis, *Phys. Rev. A* (in press).
7. For a review see K. Lindenberg and B. J. West, in *Reviews of Solid State Science* (World Scientific, Singapore, 1989), in press.
8. R. F. Fox, to appear in the proceedings of the conference on *Noise and Chaos in Non-linear Dynamical Systems*, Torino, Italy, 1989, eds. F. Moss, F. Lugiatto and P. V. E. McClintock (Cambridge University Press, Cambridge, 1989).
9. J. M. Sancho, M. San Miguel, S. L. Katz and J. D. Gunton, *Phys. Rev. A* **26**, 1589 (1982).
10. P. Jung and P. Hänggi, *Phys. Rev. Lett.* **61**, 11 (1988).
11. G. P. Tsironis, K. Lindenberg, E. Peacock-López and B. J. West, *Phys. Rev. Lett.* (comment on reference 10), in press.
12. C. W. Gardiner, *Handbook of Stochastic Methods* (Springer-Verlag, Berlin, 1983).
13. M. A. Abramowitz and I. A. Stegun, *Handbook of Mathematical Functions* (Dover, New York, 1965).

II.4 NEW ASPECTS OF THE BISTABLE SYSTEM

The problem of evaluating the Mean First Passage Time of a system with two wells under the influence of colored noise has received a great deal of attention in the past few years (see Ref. 1 for a review and references therein). A number of different theories and techniques (some of them conflictive) have recently appeared in the literature. Most of the conflicts arise on the different interpretations of the numerical or analogical available data.

In order to attain a better understanding of the relations among these various theories and the accuracy of their predictions, we have carried out extensive numerical simulations of the Langevin equations that serve as the model from which all these theories depart [2,3]. By covering extensive ranges of parameter values (in particular the correlation time τ of the noise), we were able to arrive at some definitive conclusions that should help to clarify some of the present uncertainties in the field.

As our system, we shall consider the generic and widely studied bistable model

$$\dot{q}(t) = q(t) - q^3(t) + \mu(t) \quad (1)$$

where $\mu(t)$ is the noise driving the system, which we shall assume to be Gaussian throughout this paper. In the absence of noise, the system has three fixed points, two stable at $q = \pm 1$ and one unstable at $q = 0$. The correlation function of the colored noise is taken as

$$\langle \mu(t)\mu(t') \rangle = \frac{D}{\tau} e^{-|t-t'|/\tau} \quad (2)$$

where D is the intensity and τ the correlation time. When the correlation time τ is zero, the correlation function becomes a delta, which corresponds to the white noise case.

The analysis of the digital simulation have established some points which gave a better understanding of the present theories and that have clarified the apparent conflicts between them. It is now clear [2] that Kramers's approximation for the white noise limit ($\tau = 0$) should be taken with care due to the important errors introduced for finite intensity. In this sense the relevant quantity to compare the different predictions for the dependence on τ (calculated following Kramers's approximation) is the quotient between the mean first passage times corresponding to $\tau \neq 0$ and $\tau = 0$. This procedure compensates the systematic finite-D errors introduced in the steepest descent calculation. The importance of the boundaries has also been confirmed mainly when the final point is not in the well but at the top of the potential, and the role of the separatrix is now well understood [2]. The behavior of the MFPT for small values of τ (up to 0.2) is explained correctly, but for intermediate τ (from 0.2 to 1) it is impossible to conclude which theory leads to a better τ -dependence due to the uncertainties of the digital simulation and the asymptotic character of the theoretical predictions.

For very large values of τ ($\tau \gg 1$) the fluctuating potential picture of Tsironis and Grigolini [4] leads to a qualitatively correct asymptotic exponential dependence in $2\tau/27D$ in the MFPT, but a very recent analysis of this situation [3] shows that this exponential dependence should be modified by a factor near to 4/3.

In this communication we have explored two new aspects of this problem not discussed in our previous works [2,3]. The first one is the way in which T_{top} (MFPT corresponding to the system starting from the well at $q=-1$ and reaching the top at $q=0$) approaches T_{bot} (from $q=-1$ to the other well at $q=1$) when τ grows. For white noise and very small D, Kramers's theory predicts $T_{\text{bot}}=2T_{\text{top}}$. For highly colored noise we have found in our digital simulations that T_{bot} becomes equal to T_{top} . The qualitative explanation is clear. When $\tau=0$ the separatrix is placed at $q=0$, and when the particle is there it has the same probability to reach the other well than to turn back to the first well. However, when τ is larger, the separatrix moves near the starting point, and if the particle reaches $q=0$ (now in the attraction region of the second well), the probability of reaching first the second well is larger, and the mean time (T_{bot}) is closer to T_{top} . In Fig. 1 we see that $T_{\text{bot}}/T_{\text{top}}$ as a function of τ decays exponentially. To date there is only a partial explanation of this behavior. It is known that the dependence of these two quantities to order τ is

$$T_{\text{bot}}(\tau) = T_{\text{bot}}(0)\left(1 + \frac{3}{2}\tau\right) \quad (3)$$

$$T_{\text{top}}(\tau) = T_{\text{top}}(0)\left(1 + \alpha\sqrt{\tau} + \frac{3}{2}\tau\right) \quad (4)$$

with $\alpha=1.16519\dots$, [5]. To the same order in τ , and assuming $T_{\text{bot}}(0)=2T_{\text{top}}(0)$ (which is asymptotically valid for small D) the ratio $T_{\text{bot}}/T_{\text{top}}$ is

$$\frac{T_{\text{bot}}(\tau)}{T_{\text{top}}(\tau)} = 2 - 2\alpha\sqrt{\tau} + 2\alpha^2\tau \quad (5)$$

We have interpreted this result as the first terms of an exponential decay

$$\frac{T_{\text{bot}}(\tau)}{T_{\text{top}}(\tau)} - 1 = \exp(-2\alpha\sqrt{\tau}) \quad (6)$$

As we see in Fig. 1 the agreement is very good, mainly for very small values of D, as one can expect from the theoretical analysis.

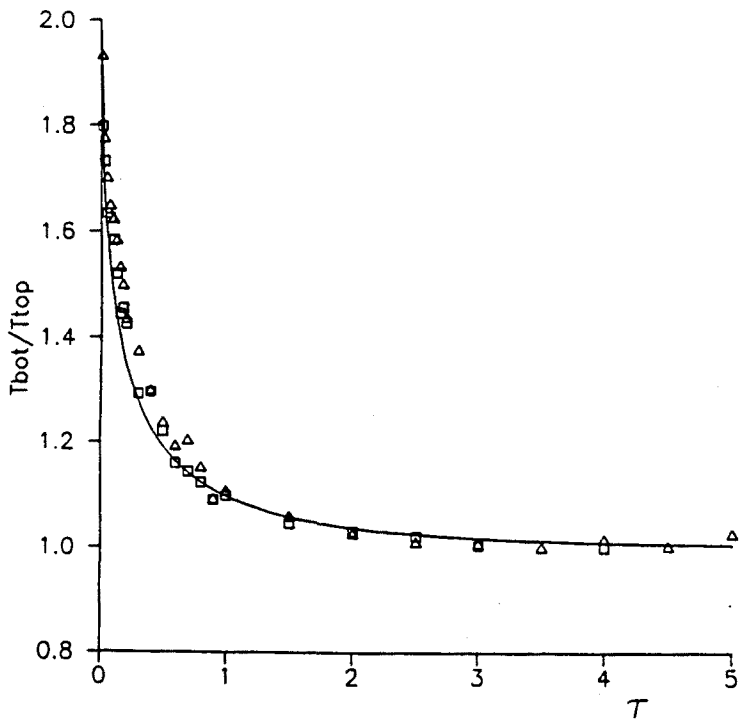


Fig.1. $T_{\text{bot}}/T_{\text{top}}$ vs τ . Squares, $D = 0.083$; triangles, $D = 0.114$.
Solid line:theoretical prediction, Eq.(6).

The second aspect we want to discuss in this work is the existence of a single time scale, characterizing the long-time evolution of the system, even for large values of τ .

If the evolution equation for the probability density P characterizing the system is written as $dP/dt = \mathcal{L}P$ where \mathcal{L} is an operator, then the temporal behavior of the system is determined by the spectrum of \mathcal{L} . If the lowest eigenvalue of \mathcal{L} is isolated (call it λ_1) then the characteristic time scale at long times is $1/\lambda_1$ (if there is no isolated lowest eigenvalue then the evolution is not characterized by a single time scale). An example of an operator \mathcal{L} that leads to isolated eigenvalues is the Fokker-Planck operator.

If such an isolated lowest eigenvalue exists, then the probability density of the first passage time to reach the well at $q = +1$ (under weak noise conditions) may be written as [6,7]

$$p(t) = T_{\text{bot}}^{-1} \exp(-t/T_{\text{bot}}) \quad (7)$$

the mean first passage time is

$$T_1 = \int_0^\infty t p(t) dt = T_{\text{bot}} \quad (8)$$

and is related to the lowest eigenvalue through [2]

$$T_{\text{bot}} = 2\lambda_1^{-1} \quad (9)$$

The second moment (giving the variance of first passage times) is given by

$$T_2 = \int_0^\infty t^2 p(t) dt = 2T_1 \quad (10)$$

and therefore

$$\frac{\Delta T}{T_1} \equiv \frac{\sqrt{T_2 - T_1^2}}{T_1} = 1 \quad (11)$$

In Fig.2 we depict the results of our numerical simulation. The agreement between the numerical data and the relation (11) is manifest, indicating for our system the existence of a well defined time scale, given by the first eigenvalue, even for large τ

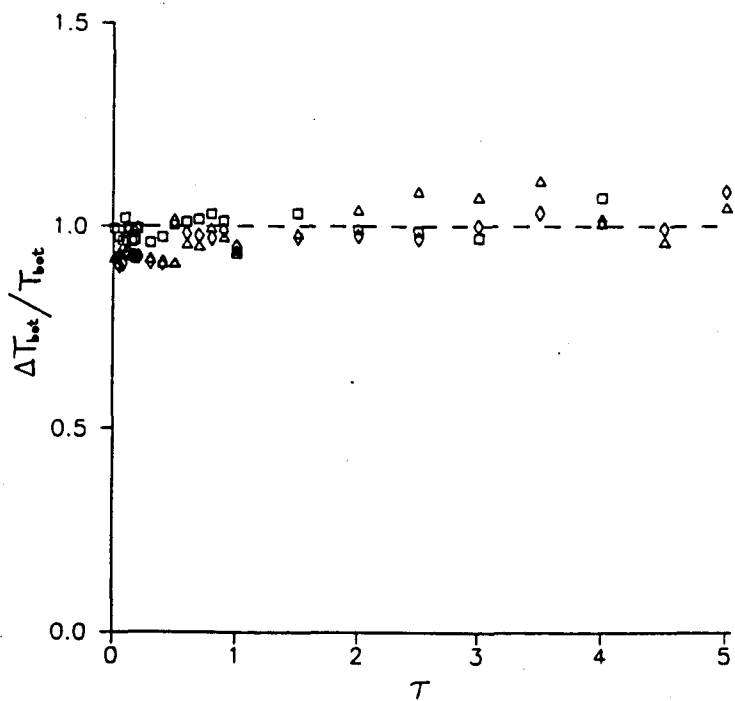


Fig.2. Simulation results for $\Delta T_{\text{bot}}/T_{\text{bot}}$ vs τ . Squares, $D = 0.083$; triangles, $D = 0.114$; rhombuses, $D = 0.153$.

REFERENCES

1. K. Lindenberg and B.J. West, Bistable systems driven by colored noise, in Reviews of Solid State Science, World Scientific, Singapore, 1989, in press.
2. L. Ramírez Piscina, J.M. Sancho, F.J. de la Rubia, K. Lindenberg and G.P. Tsironis, First-passage time in a bistable potential with colored noise, Phys. Rev. A 40, 1989, in press.
3. K. Lindenberg, L. Ramírez-Piscina, J.M. Sancho and F.J. de la Rubia, New insight towards the first-passage time in a bistable potential with highly colored noise, submitted for publication.
4. G.P. Tsironis and P. Grigolini, Color-induced transition to a nonconventional diffusion regime, Phys. Rev. Lett. 61, 7-10, 1988.
5. C.R. Doering, P.S. Hagan and C.D. Levermore, Bistability driven by weakly colored gaussian noise: the Fokker-Planck boundary layer and mean first-passage times, Phys.Rev.Lett. 59, 2129-2132, 1987.
6. K. Lindenberg, K.E. Shuler, J. Freeman and T.J. Lie, First passage time and extremum properties of Markov and independent processes, J.Stat.Phys. 12, 217-251, 1975.
7. P. Talkner, Mean first-passage time and the lifetime of a metastable state, Z.Phys. B. 68, 201-207, 1987.

**III. FIRST PASSAGE TIME FOR A MARGINAL STATE
DRIVEN BY COLORED NOISE**

III.1

I. INTRODUCTION

The behavior of physical systems under the influence of stochastic forces or noises has been a subject of study since long time ago. Recently the study of dynamical aspects of this subject has received special attention¹. One of the studied dynamical aspects is the influence of the noise in the relaxation process of a system from an initial state to the final steady state. Different quantities can be used to describe this dynamics. One can look at the evolution of the probability density of the dynamical variable of interest, or its statistical moments and correlations, or at the stochastic trajectory itself.

The First Passage Time statistics associated to the trajectory² and the Non Linear Relaxation Time³ for the moments have been the most common tools used in the study of relaxation dynamics. In this paper we will focus on the Mean First Passage Time (MFPT) and its variance.

Although all relaxation processes can be studied by the use of the MFPT technique, only few of them have a particular importance. They are those processes in which the presence of the noise is necessary to have a different dynamics than the pure deterministic motion. We are referring to the relaxation processes from an initial unstable state,⁴⁻⁸ or through a marginal state (saddle point),⁹⁻¹² or a barrier crossing between metastable states.^{2,13} These three types of processes need fluctuations to take place and the dynamics would be very different if fluctuations were not present.

III.3

II. MODELS AND TECHNIQUES

A typical example of crossing through a saddle point bifurcation appears in Optical Bistability. In this case the output intensity q of the laser obeys the following dynamical equation¹⁴

$$\dot{q} = y - q - \frac{2cq}{1+q^2} + \xi(t) = -\phi'(q) + \xi(t) \quad (2.1)$$

where y is the input intensity and $\xi(t)$ is the noise. The potential $\phi(q)$ associated with this model has an inflection point at $q_m = (c-1-\sqrt{c^2-4c})^{1/2}$ if $c \geq 4$. The process of switching-on corresponds to changing the value of the control parameter y from zero to a value above the threshold $y_m = q_m + 2cq_m/(1+q_m^2)$. For this value, the inflection point has a horizontal slope, and corresponds to a marginal or saddle node state. The system starts in $q = 0$, pass through the marginal point q_m owing to the presence of noise, and reaches its stable state at $q_0 = 2q_m/(q_m^2-1)$.

There are two different regimes in this evolution. Outside the marginal zone the dynamics is essentially deterministic, and the noise plays a secondary role. However, near the marginal point the potential is very flat, and then the dynamics is dominated by the noise. It means that the almost entire action of the noise over the system will take place there. Then, in order to study the influence of the noise, we will only need few terms of the potential expansion around this marginal point

III.4

$$\dot{q} = -\phi'(q) + \xi(t) = \beta + a(q-q_m)^n + O((q-q_m)^{n+1}) + \xi(t) \quad (2.2)$$

which governs the dynamics in its vicinity. The point $q=q_m$ is the marginal point of the system when the control parameter β is equal to zero. For the model described by Eq. (2.1), $\beta=y-y_m$, the potential is a cubic power in the variable $x=q-q_m$ and therefore $n=2$. Different systems will have the same expansion (2.2) and then will be affected by the noise in the same way. The difference between them can be evaluated from the analysis of their deterministic equations, without considering the presence of noise, as it is explained in Ref. 12. Thus we only need to use the simplest model which is given by the potential

$$\phi(x) = -\frac{a}{3}x^3 - \beta x, \quad a>0, \quad (2.3)$$

Models defined by Eqs. (2.2) and (2.3) have already been analyzed for $\xi(t)$ being white noise.⁹⁻¹² Our aim here is to consider a gaussian colored noise, the Ornstein-Uhlenbeck noise, which has a correlation function

$$\langle \xi(t)\xi(t') \rangle = \frac{D}{\tau} \exp -\frac{|t-t'|}{\tau}, \quad (2.4)$$

where D is the intensity and τ the correlation time of the noise. Now the process $x(t)$ is non-markovian and no precise theoretical scheme to attack this problem exists. The best known approximation to deal with this non-markovian problem starts from the deduction of an effective Fokker-Planck equation for the probability density

III.5

$P(x, t)$ valid up to order τ and where transient terms are neglected:^{7,15-16}

$$\frac{\partial}{\partial t} P(x, t) = \frac{\partial}{\partial x} \phi'(x) P(x, t) + \frac{\partial^2}{\partial x^2} D(1-\tau\phi''(x)) P(x, t) \quad (2.5)$$

This is equivalent to consider the case of a gaussian white noise but with a renormalization of the diffusion coefficient D , which becomes a variable-dependent quantity. In this approximation, the MFPT, $\langle T \rangle$, for the system starting from x_0 and reaching x_f , and its variance $\Delta T^2 = \langle T^2 \rangle - \langle T \rangle^2$, are given, using general formulas of white noise,¹⁰⁻¹² by

$$\langle T \rangle = \int_{x_0}^{x_f} \frac{dx_1}{D(x_1) P_s(x_1)} \int_{-\infty}^{x_1} dx_2 P_s(x_2) \quad (2.6)$$

$$(\Delta T)^2 = \int_{x_0}^{x_f} \frac{dx_1}{D(x_1) P_s(x_1)} \int_{-\infty}^{x_1} \frac{dx_2}{D(x_2) P_s(x_2)} \int_{-\infty}^{x_2} dx_3 P_s(x_3) \int_{-\infty}^{x_3} dx_4 P_s(x_4) \quad (2.7)$$

where $P_s(x)$ and $D(x)$ are defined by

$$P_s(x) = \frac{1}{D(x)} \exp - \int^x dy \frac{\phi'(y)}{D(y)} \quad ; \quad D(x) = D(1-\tau\phi''(x)) \quad (2.8)$$

This quasi-markovian approximation make sense if the initial, x_0 , and final, x_f , values of x are far away from the marginal point, and then the non-markovian transient effects are not important. Note also that the system defined in (2.3) has no steady state, and the function $P_s(x)$ has in general no physical meaning. If it would

III.6

have a steady state (for instance, putting a reflecting barrier to prevent particles to go out to infinity), $P_s(x)$ would be the stationary probability density in this approximation.

Two important quantities can be built with the parameters a and D that will be useful to obtain some additional physical information (we will turn to that point in Sec. III). The first one is $(D/a)^{1/(n+1)}$, it has dimensions of the variable x and means the size of the region near the marginal point in which the dynamics is dominated by the noise. The other quantity is $(a^2 D^{n-1})^{-1/(n+1)}$. It has dimensions of time and is related to the MFPT (or to any other temporal scale). In particular, for the system defined in Eq. (2.3) one can calculate the MFPT from $-\infty$ to $+\infty$ in the white noise case^{11,12}

$$T_0 = \langle T(\beta=0, \tau=0) \rangle = \Gamma(1/3)^2 (3Da^2)^{-1/3} \quad (2.9)$$

For $\beta > 0$, there exist another relevant time scale. It is the deterministic time, T_{det} , that the system spends to go from $x=0$ to $x=\infty$ driven by the only action of the potential $\phi(x)$. This time scale is proportional to $(a\beta^{n-1})^{-1/n}$, which is obtained from the definition

$$T_{\text{det}} = \int_0^\infty \frac{dx}{-\phi'(x)} \quad (2.10)$$

Therefore Eq. (2.2) can be adimensionalized by the change

$$x' = \left(\frac{D}{a}\right)^{-\frac{1}{n+1}} (q - q_m), \quad t' = (a^2 D^{n-1})^{\frac{1}{n+1}} t \quad (2.11)$$

with the result

III.7

$$\frac{dx'}{dt'} = x'^n + k + \eta(t') \quad (2.12)$$

where $\eta(t')$ is a colored noise of unit intensity and scaled correlation time τ' , being τ' and k

$$\tau' = (a^2 D^{n-1})^{\frac{1}{n+1}} \tau ; \quad k = (a D^n)^{-\frac{1}{n+1}} \beta \quad (2.13)$$

The parameter k is proportional to $(T_0/T_{det})^{n/(n-1)}$. It gives information on how far the system is from pure marginality by comparing two different characteristics times. These two parameters k and τ' , are the only relevant ones in this problem, and any quantity should depend only on them through the changes given by Eqs. (2.11).

III. MFPT FOR SMALL CORRELATION TIME OF THE NOISE

Now we apply Eqs. (2.5) and (2.6) to the system defined by Eq. (2.3). Making an expansion in powers of τ' we obtain the following expression for the MFPT corresponding to the evolution from $x_0=-\infty$ to $x=\infty$:

$$(a^2 D)^{1/3} \langle T \rangle = T_0 + T_1 \tau' + O(\tau'^2) \quad (3.1)$$

where

$$T_0 = \pi^{1/2} \int_0^\infty dx x^{-1/2} \exp - \left(\frac{1}{12} x^3 + kx \right) \quad (3.2)$$

III.8

$$T_1 = \pi^{1/2} \int_0^\infty dx x^{1/2} \exp -\left(\frac{1}{12}x^3 + kx\right) \quad (3.3)$$

In a similar way, the standard deviation is, up to first order in τ'

$$(a^2 D)^{1/3} \Delta T = \Delta T_0 + \frac{1}{2} \frac{A}{\Delta T_0} \tau' + O(\tau'^2) \quad (3.4)$$

where

$$(\Delta T_0)^2 = 4 \int_{-\infty}^{+\infty} dx_1 \int_{-\infty}^{x_1} dx_2 \int_{-\infty}^{x_2} dx_3 \int_{-\infty}^{x_3} dx_4 \exp -\left(\frac{1}{3}(x_1^3 + x_2^3 - x_3^3 - x_4^3) + k(x_1 + x_2 - x_3 - x_4)\right) \quad (3.5)$$

$$A = 2 \int_{-\infty}^{+\infty} dx_1 \int_{-\infty}^{x_1} dx_2 \int_{-\infty}^{x_2} dx_3 \int_{-\infty}^{x_3} dx_4 \left\{ \exp -\left(\frac{1}{3}(x_1^3 + x_2^3 - x_3^3 - x_4^3) + k(x_1 + x_2 - x_3 - x_4)\right) \right\} \\ \times ((x_1^4 + x_2^4 - x_3^4 - x_4^4) + 2k(x_1^2 + x_2^2 - x_3^2 - x_4^2) - 4(x_3 + x_4)) \quad (3.6)$$

In Figs. 1, 2-a and 2-b these results are compared to the ones obtained from numerical simulation methods¹⁶ of the system defined by Eq. (2.3). The dependence on the parameter k , Fig. 1, is fairly good, mainly in the small- τ' regime, where Eqs. (3.1) and (3.4) would become more appropriate.

In the pure marginal case ($k=0$) these integrals can be evaluated

$$T_0 = 3^{-1/3} [\Gamma(1/3)]^2 \quad (3.7)$$

$$T_1 = 2\pi 3^{-1/2} \quad (3.8)$$

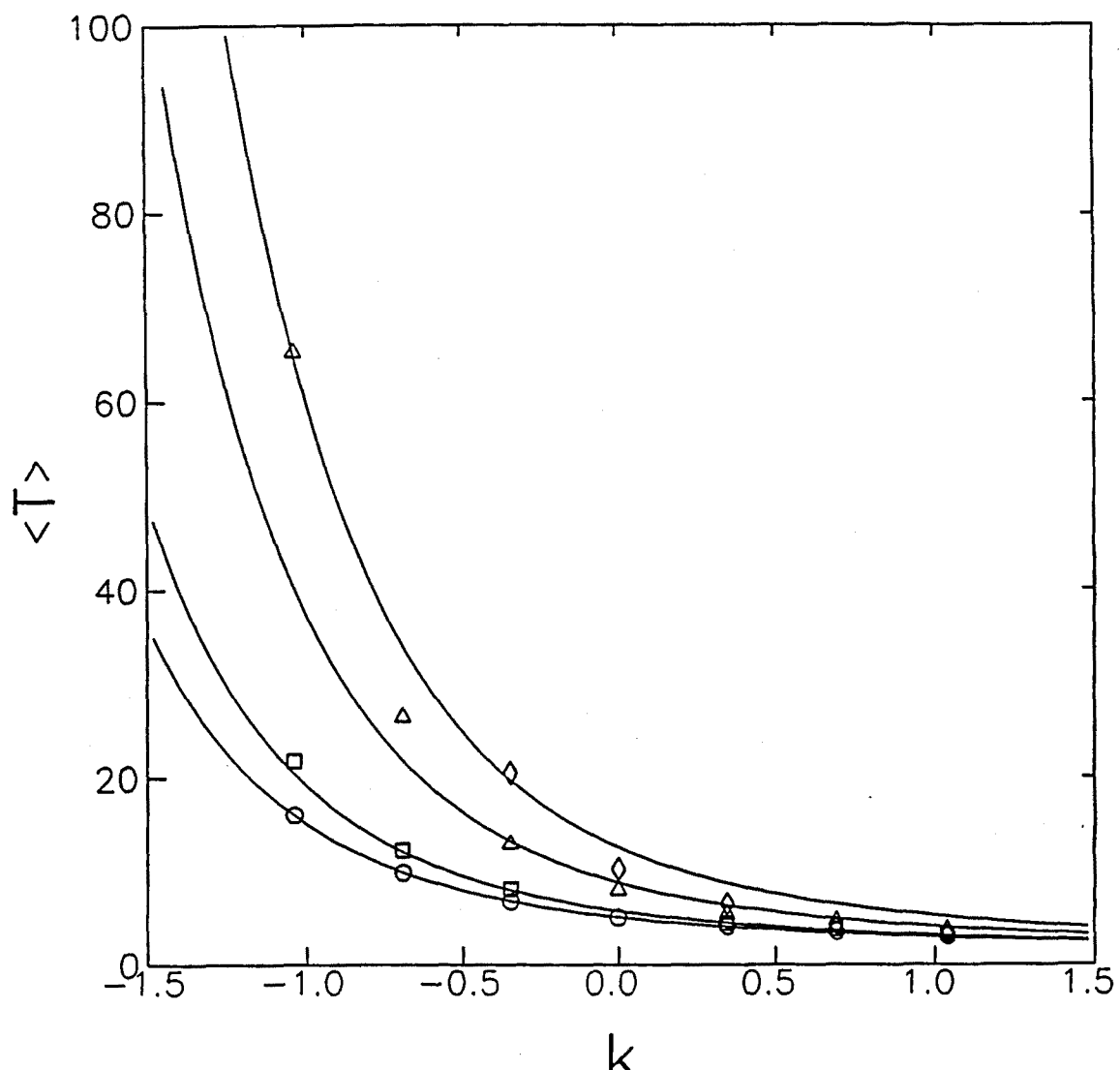


Fig. 1.- $\langle T \rangle$ versus k . Symbols are simulation results of the system defined by Eq. (1.3) with $a=3$ and $D=1$ (circles: $\tau=0.01$; squares: $\tau=0.1$; triangles: $\tau=0.5$; rombics: $\tau=1$). Solid lines: analytic results from Eq. (2.1)-(2.3)

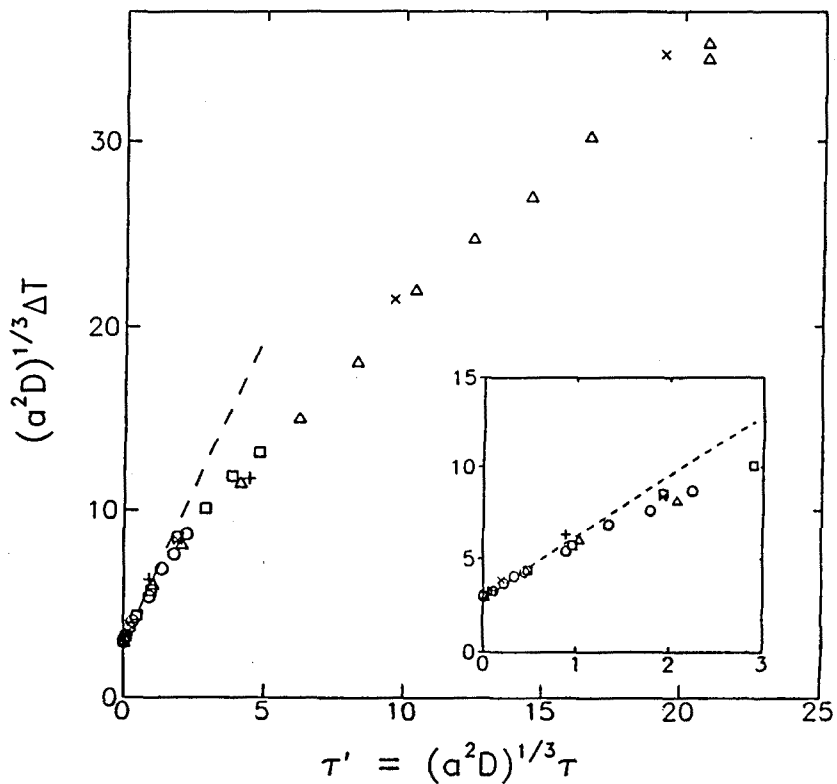
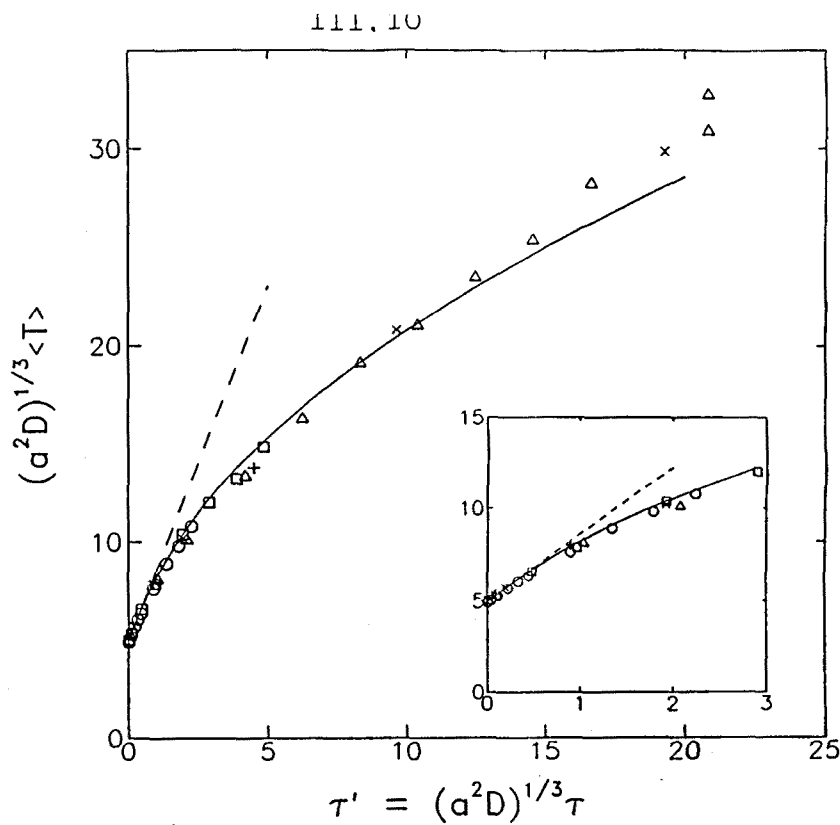


Fig. 2.- (a) Scaled MFPT vs τ' . Dashed lines are the theoretical results of Eq. (2.1), (2.7) and (2.8); Solid lines are the numerical solution of Eq. (3.13). (b) Scaled Standard Deviation vs. τ' . Dashed lines are the theoretical results of Eq. (2.4), (2.9) and (2.10). Symbols are simulation results of the system defined by Eq. (1.1) with $c=20$ (+: $D=0.01$ and x : $D=0.1$) and the system defined by Eq. (1.3) with $a=3$ and $\beta=0$ (circles: $D=0.01$; squares: $D=0.1$ and triangles: $D=1$).

III.11

$$\Delta T_0 = 3^{-5/6} [\Gamma(1/3)]^2 \quad (3.9)$$

$$A = 19.151... \quad (3.10)$$

In this case, the dependence of T and ΔT on the correlation time of the noise has been obtained from digital simulations of both of the systems defined through Eqs. (2.1) and (2.3) (with $y=y_m$ and $\beta=0$ respectively, and for different intensities of the noise), and the results can be seen in Figs. 2-a and 2-b. They confirm the dependence of the dynamical quantities scaled by Eq. (2.3) on the scaled correlation time τ' , being this dependence the same for different physical systems. This is a clear manifestation of the universal behavior near the marginal point. On the other hand, the MFPT and its variance are correctly given by Eqs. (3.1), (3.4) with (3.7)-(3.10) in the small τ region for both of the systems simulated. Moreover, a physical argument can be invoked to extend these results to finite values of τ , which is presented in the following section.

IV. MFPT FOR LARGE CORRELATION TIME OF THE NOISE

Let's start first from the standard linear model for the decay of a unstable system⁵⁻⁸

$$\dot{x}(t) = x(t) + \xi(t) \quad (4.1)$$

where the variable x is placed at $x=0$ in $t=0$, and $\xi(t)$ is an

Ornstein-Uhlenbeck noise in its steady state. For such a system, the evolution of the second moment of x is calculated exactly for all values of D and τ^7

$$\langle x^2 \rangle_t = \frac{D}{1+\tau} e^{2\tau} - \frac{D}{1-\tau} + 2D \frac{\tau}{1-\tau^2} e^{-(1-\tau)t/\tau} \quad (4.2)$$

The mean time T that the system takes to leave a region of size R should be the time needed by the distribution of x to reach a width proportional to R

$$\langle x^2 \rangle_t = \alpha R^2 \quad (4.3)$$

The proportionality constant α is evaluated easily imposing over Eqs. (4.2), (4.3) the result corresponding to $\tau=0$ (white noise) and for the limit $D \ll R^2$, which is satisfied choosing

$$\alpha = 2e^\gamma \quad (4.4)$$

being γ the Euler constant. In this way, the MFPT is given by the equation

$$\frac{1}{1+\tau} e^{2T} - \frac{1}{1-\tau} + 2 \frac{\tau}{1-\tau^2} e^{-(1-\tau)t/\tau} = \frac{2R^2}{D} e^\gamma \quad (4.5)$$

In the limit $D \ll R^2$, Eq. (4.5) is satisfied by the known result from

the Quasideterministic Theory (QDT)^{6,7}

$$T_{QDT} = \frac{1}{2} \ln \frac{R^2}{2D} + C_1 + \frac{1}{D} \ln (1+\tau) \quad (4.6)$$

with $C_1 = \gamma/2 + \ln 2$. In Fig. 3 both results are compared. They are equivalent for weak noise, but Eq. (4.5) also describes the non-weak noise situation.

For the marginal case it is no way to find a closed equation for the evolution of $\langle x^2 \rangle$. Instead, it is possible to relate this problem to the evolution of a system with a constant potential, that is to say free diffusion. Let us consider the system defined by Eq. (2.2) with $\beta=0$

$$\dot{x} = ax^n + \xi(t) \quad (4.7)$$

where $n > 1$. The dynamics outside of the marginal zone is essentially deterministic, but the noise dominates in the mentioned region of size $L \propto (D/a)^{1/(n+1)}$. Let's assume that the evolution inside this region is free

$$\dot{x} = \xi(t) \quad |x| \leq L \quad (4.8)$$

In this case, the width of the distribution is given by

$$\langle x^2 \rangle_t = 2D (t - \tau (1 - e^{-t/\tau})) \quad (4.9)$$

A similar argument that the one applied to the unstable system holds here. The MFPT for Eq. (4.7) is assumed to be proportional to the time t that $\langle x^2 \rangle$ takes to become L^2 in the free system (4.8).

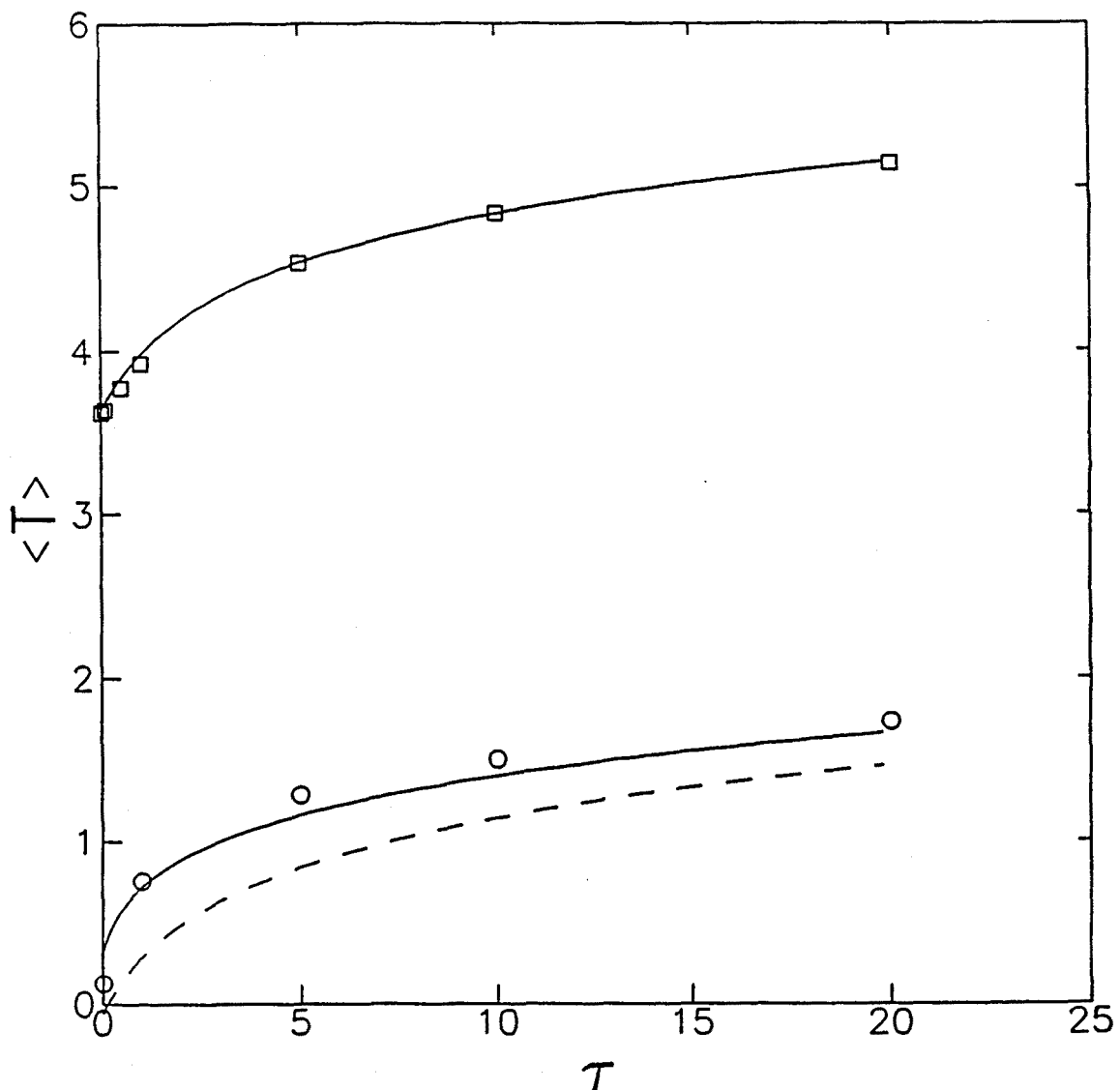


Fig. 3.- MFPT vs. τ for the unstable system (3.1). with $D=1$. Symbols are simulation results (Squares: $R=20$; circles: $R=0.5$). Dashed line is the Eq. (3.6) (QDT theory). Solid lines are the numerical solution of Eq. (3.5). The differences between both results are indistinguishable for $R=20$.

It means that

$$\langle x^2 \rangle_t \propto \left[\frac{D}{a} \right]^{\frac{2}{n+1}} \quad (4.10)$$

or, in other words,

$$t - \tau (1 - e^{-\tau/\tau}) \propto (a^2 D^{n-1})^{\frac{1}{n+1}} \propto T_0. \quad (4.11)$$

Putting $t = \mu T$, being μ the appropriate proportionality constant, the equation for the MFPT reads

$$\mu T - \tau (1 - e^{-\mu T / \tau}) = \mu T_0 \quad (4.12)$$

The parameter μ is immediately identified with the inverse of the linear term in an expansion of T in powers of τ (see Eq. (3.1)). Then Eq. (4.12) yields

$$T - T_0 = \tau T_1 \left[1 - \exp - \frac{T}{\tau T_1} \right] \quad (4.13)$$

This expression gives the passage time for the system (4.7), provided the constants T_0 , T_1 be known. These two quantities can be in general calculated by the standard methods of Sec. III.

A problem arises in this argument if n is even, which corresponds to an asymmetric potential. In that case, a system that exits from the marginal zone by its left side crossing $x = -L$, is forced by the deterministic potential to turn back, and it really

does not exit until it reaches $x=+L$. This effect becomes important when the correlation time of the noise goes to infinity. In this limit, the noise is almost constant, and the system has to wait a time of order of τ to let the noise reach a positive value, which is necessary to cross the marginal point $x=0$. This linear in τ contribution to the MFPT hides the time given by Eq. (4.13), which is asymptotically proportional to τ^2 in this limit.

For $n=2$, T_0 and T_1 are given by Eqs. (3.7), (3.8). In Fig. 2(a) the prediction of Eq. (4.13) is compared to the simulation results of the both systems (2.1) and (2.3), presenting a perfect agreement up to values of τ' as large as 10. Above that value, a linear dependence on τ' is observed, as we have commented.

V. CONCLUSIONS

We have presented an approximate theoretical scheme to calculate the dominant contributions of the colored noise on the first moments of the passage time for a relaxation process through a marginal point. This has been possible due to the fact that markovian formulas can be used because boundary effects, which are more sensitive to the nonmarkovicity, are not dominant in this case. The simple idea of substituting the real process by free diffusion in a finite interval is also profitable for large values of τ . The computer simulations have confirmed the suitability of

the approximations in a wide range of the parameters. Hence we conclude the very simple approximations presented in this paper have retained the essential physics of the dynamical process through a saddle or marginal point. They could be profitable in the study of real systems like Optical Bistability in Lasers.¹⁴

REFERENCES

- ¹ F. Moss and P.V.E. McClintock, "Noise in Nonlinear Dynamical Systems", Vols. I, II and III. (Cambridge University Press, Cambridge, England, 1989)
- ² R.L. Stratonovich, "Topics in the Theory of Random Noise" Vol.I (Gordon and Breach, New York, 1963)
- ³ M. Suzuki, Intern. J. Magnetism, 1, 123 (1971); K. Binder, Phys. Rev. B 8, 3423 (1973); J. Jimenez-Aquino, J. Casademunt, and J.M. Sancho, Phys. Lett. A 133, 364 (1988)
- ⁴ S. Zhu, A.W. Yu and R. Roy, Phys. Rev. A 34, 4333 (1986)
- ⁵ M. James, F. Moss, P. Hänggi and C. Van den Broeck, Phys. Rev. A 38, 4690 (1988);
- ⁶ J.M. Sancho and M. San Miguel, Phys. Rev. A 39, 2722 (1989);
- ⁷ J.M. Sancho and M. San Miguel, in Vol.I of Ref.1.
- ⁸ J. Casademunt, J.I. Jimenez- Aquino, and J.M. Sancho, Phys. Rev. A 40, 5905 (1989)
- ⁹ B. Caroli, C. Caroli, and B. Roulet, Physica 101 A, 581 (1980)
- ¹⁰ F.T. Arecchi, A. Politi and L. Ulivi, Nuovo Cimento 71B, 119 (1982)
- ¹¹ D. Sigeti and W. Horsthemke, J. Stat. Phys. 54, 1217 (1989); D. Sigeti, Dissertation, University of Texas at Austin (1988)
- ¹² P. Colet, M. San Miguel, J. Casademunt and J.M. Sancho, Phys. Rev. A 39, 149 (1989)
- ¹³ P. Hänggi, T.J. Mroczkowski, F. Moss, and P.V.E. McClintock, Phys. Rev. A 32, 695 (1985); C. R. Doering, P.S. Hagan, and C.D. Levermore, Phys. Rev. Lett. 59, 2129 (1987); R. Fox, Phys. Rev. A 37, 911 (1988); M.M. Klosek-Dygas, B.J. Matkowsky,

III.19

and Z. Schuss, Phys. Rev. A 38, 2605 (1988); G.P. Tsironis and P. Grigolini, Phys. Rev. Lett. 61, 7 (1988); J. F. Luciani and A.D. Verga, J. Stat. Phys. 50, 567 (1988); L. Ramirez-Piscina, J.M. Sancho, F.J. de la Rubia, K. Lindenberg and G.P. Tsironis, Phys. Rev. A 40, 2120 (1989)

¹⁴ R. Bonifacio and L.A. Lugiato, Phys. Rev. A 18, 1129 (1978); G. Broggi, L.A. Lugiato and A. Colombo, Phys. Rev. A 32, 2803 (1985); W. Lange, in "Dynamics of Non-Linear Optical Systems", Eds. L. Pesquera and F.J. Bermejo, World Scientific. Singapore (1989)

¹⁵ K. Lindenberg, B.J. West and J. Masoliver, in Vol. I of Ref. 1

¹⁶ J.M. Sancho, M. San Miguel, S.L. Katz, and J.D. Gunton, Phys. Rev. A 26, 1589(1982)

IV. STOCHASTIC DYNAMICS OF THE CHLORITE-IODIDE REACTION

I. INTRODUCTION

Features of irreproducibility have been very recently observed^{1,2} in kinetic experiments performed on several well-known chemical reactions. In a previous and very preliminary paper³ devoted to this question, we proposed a theoretical scheme based on the use of a Langevin equation aimed at modelling this random chemical behavior. Fluctuations entered into the dynamics there considered in a multiplicative way, and without scaling with the inverse of the volume, as would be the case if they were to account for some sort of thermal, dynamics independent, noise. Here we will adopt the same theoretical framework, but we will formulate it in relation with a particular reaction which has been much more studied from a chemical kinetics point of view.

Although fluctuations, or more familiarly dispersion of results, are always present in any experimental procedure, their impact on the measurements is mitigated and kept under control if one uses appropriately designed and carefully operated experimental techniques. In contrast, two striking features of the experimental observations on the chemical reactions here investigated seem to us specially intriguing. First, the irreproducibility in the reaction times is far from being negligable, with standard deviations that may be as large as a 40% of the mean values. Additionally, this randomness turns out to be largely dependent on experimental conditions such as sample volumes or stirring rates. It is precisely this mixing sensitivity which

supports the belief¹⁻³ that the observed stochasticity is caused by local inhomogeneities of the reaction volume that are largely, and somewhat surprisingly, amplified by highly nonlinear kinetics. As a matter of fact this sort of behavior is by no means unique to redox reactions as those referred here, since they were already theoretically discussed by Nicolis and collaborators⁴ for thermally explosive reactions or experimentally studied by Hofrichter and coworkers for the polymerization of sickle cell hemoglobin.⁵

According to what we have just mentioned, we tend to think that in these particular chemical reactions purely kinetic effects may be strongly affected by transport phenomena mediated by stirring. Therefore a proper dynamical description would probably require the consideration of spatial degrees of freedom to account for either microscopic or macroscopic transport of reactants or intermediates of the reaction. Here, we adopt a much more modest approach, trying to model this sort of effect in a much more 'ad hoc' way. More specifically we incorporate the effects that the mixing may have on the kinetic constants by letting them fluctuate around "mean field"-like averaged values. The intensities of such fluctuations will be further inversely correlated with the stirring rate. Proceeding in this way the set of deterministic rate laws transform into a set of Langevin stochastic differential equations. The statistics of the reaction time distribution is then analyzed in terms of the standard theory of first passage time distributions.

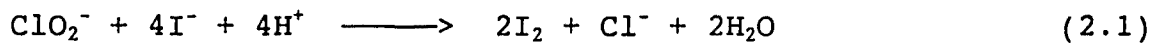
The particular chemical system here considered consists of the autocatalytic reaction between chlorite and iodide ions in an acidic medium. The experiments² were performed in batch at concentration ratios where it features a clock reaction behavior displayed by the sudden appearance of brown I₂ which is followed by the rapid disappearance of the color.

The paper is organized as follows. The chemistry of the reaction is reviewed in Section II. The stochastic model is introduced in Section III. The results, either analytical or obtained from computer simulations, are summarized and compared with those of the experiments in Section IV, and finally a last section is devoted to conclusions.

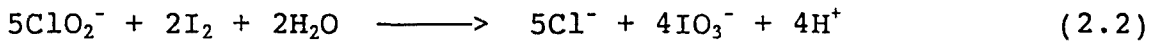
II. CHEMICAL FRAMEWORK

A. Kinetic model and rate constants

The chlorite-iodide reaction has been extensively studied from a mechanistic point of view. Although these studies have generated several controversies in the past,⁶ there does not seem to be many disputes over the stoichiometry of the major overall compound reactions. These can be essentially summarized in two determining steps². An initial process producing iodine through the oxidation of iodide by chlorite



is followed by the further oxidation of iodine to iodate with any excess of chlorite



Reaction (2.1) is autocatalytic in iodine with an experimental rate law given by

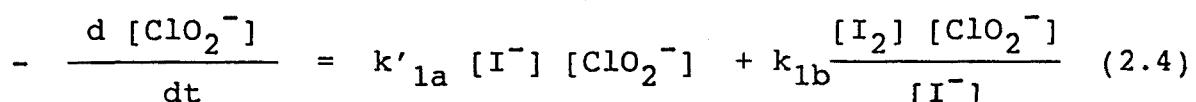
$$-\frac{d[\text{ClO}_2^-]}{dt} = k_{1a} [\text{H}^+] [\text{I}^-] [\text{ClO}_2^-] + k_{1b} \frac{[\text{I}_2] [\text{ClO}_2^-]}{[\text{I}^-]} + k_{1c} [\text{I}_2] [\text{ClO}_2^-] \quad (2.3)$$

Reaction (2.2) has been investigated by stopped-flow techniques. The conclusion is that iodide inhibits this particular phase of the chemical reaction so that it does not play a significant role until practically all the iodide of the medium has disappeared through process (2.1).² In what follows we will essentially concentrate on the initial reaction (2.1). In doing so, we follow the arguments proposed by Nagypál and Epstein² who suggested that one could qualitatively understand the observed stochasticity of the chlorite-iodide reaction as originated in local inhomogeneities of the non-ideally mixed medium. These inhomogeneities would correspond to very low iodide levels that might in turn trigger the subsequent fast consumption of iodine through step (2.2). According

to this mechanistic interpretation of the behavior of the reaction, it seems reasonable to limit our considerations here to the analysis of the random effects occurring during the initial step (2.1), when it is more likely they can significatively affect the course of the reaction. In addition, reaction (2.1) deserves special attention since, as clearly shown by the rate law (2.3), the initial reaction between ClO_2^- and I^- , apart from being autocatalytic in iodine, is inhibited by the reactant iodide. Consequently, this step supposes a sort of chemical supercatalysis, at least for not extremely low iodide concentrations.⁷ Actually, the presence of chemical mechanisms with highly autocatalytic pathways was already identified¹ as a possible essential ingredient when trying to qualitatively explain the observed stochastic behavior of these chemical systems.

The last point we want to address in relation to the chemistry of the chlorite-iodide reaction concerns the values of the rate constant appearing in the kinetic equation (2.3). There is no agreement in the literature on the experimental values of these constants. They were first evaluated from experiments in the 1960's. More recent values found in the literature are those of the Brandeis group^{6a,8}, or the set used by Boissonade and De Kepper⁹ in their theoretical study of the mixing effects on the bistability of this reaction in CSTR. With respect to the k_{1c} term it seems to be generally accepted that it is of little significance compared with the k_{1b} term.

In our approach here we have thus adopted a simplified version of the rate law (2.3) in which the k_{1c} contribution was neglected. In addition the experiments of the Brandeis group² were conducted in an acidic buffered medium so that a constant value $[H^+]$, $[H^+] = 9.3 \cdot 10^{-5} M$ for most of the experiments, can be included in the rate constant k_{1a} resulting in an effective value k'_{1a} : $k'_{1a} = k_{1a}[H^+]$. The final kinetic equation we are then led to consider is



The results that will be presented later on correspond to the set of constants proposed in Ref. 6a: $k_{1a} = 1 \cdot 10^3 M^{-2}s^{-1}$, $k_{1b} = 1 \cdot 10^{-2}s^{-1}$, although we have explicitly checked that similar conclusions to those reported here would apply irrespectively of the particular set of rate constants adopted.

B. Deterministic results

Let us denote by α and β the respective initial concentrations of ClO_2^- and I^- . The time dependent concentrations of the set of chemical species appearing in (2.4) can then be simply expressed in terms of a variable $x(t)$ by using the stoichiometric relations appropriate to reaction (2.1)

$$\begin{aligned} [\text{ClO}_2^-] &= \alpha - x \\ [\text{I}^-] &= \beta - 4x \\ [\text{I}_2] &= 2x \end{aligned} \quad (2.5)$$

Using the rate law (2.4) we then obtain the deterministic evolution equation for the single variable $x(t)$:

$$\frac{dx}{dt} = k'_{1a}(\alpha-x)(\beta-4x) + k'_{1b} \frac{x(\alpha-x)}{(\beta-4x)} \quad (2.6)$$

where $k'_{1b} \equiv 2k_{1b}$. Equation (2.6) is written in terms of four parameters: the initial concentrations α and β , and the two rate constants k'_{1a} and k'_{1b} . To simplify the following analysis it is more convenient to transform the concentration and time variables into dimensionless quantities according to

$$\begin{aligned} x &\equiv \frac{\beta}{4} q, \quad 0 \leq q \leq 1 \\ t &\equiv \frac{\theta}{4k'_{1a}\alpha} \end{aligned} \quad (2.7)$$

The equation (2.6) now reduces to

$$\frac{dq}{d\theta} = (1-\beta'q)(1-q) + k'/\beta' \frac{q(1-\beta'q)}{(1-q)} \equiv f(q) \quad (2.8)$$

written in terms of a reduced number of independent kinetic parameters, β' and k' , defined as

$$\begin{aligned}\beta' &\equiv \frac{\beta}{4\alpha} \\ k' &\equiv \frac{k'_{1b}}{k'_{1a}} - \frac{1}{16\alpha}\end{aligned}\tag{2.9}$$

The experimental concentrations used by Nagypál and Epstein² correspond to a fixed initial chlorite concentration, $\alpha=5.10^{-3}\text{M}$, whereas the iodide concentrations range from a value $\beta_{\min}=3.333.10^{-4}\text{M}$ to $\beta_{\max}=2.5.10^{-2}\text{M}$. However a noticeable stochastic behavior was only found for values of β smaller than β_{\max} by nearly an order of magnitude. Consequently, we will restrict the range of studied β values to $\beta \leq 4\alpha=2.10^{-2}\text{M}$, or in other words to $\beta' \leq 1$. This means in particular that the deterministic force $f(q)$ is always positive and drives the system from the initial condition $q=0$, in absence of iodine, towards a somewhat artificial completion of reaction (2.1) represented by $q=1$.

According to the considerations made in section II.A relative to the chemistry of the $\text{ClO}_2^-/\text{I}^-$ reaction, the kinetic law (2.4) essentially governs an initial stage of the overall reaction. We can estimate the time scale corresponding to this initial phase of the reaction by simply integrating Eq. (2.8). In addition we can obtain in this way a well defined characteristic time in absence of any stochasticity. This deterministic time will be of further utility when comparing it with its stochastic counterpart, the mean first passage time (MFPT), to be introduced in the next section.

From (2.8) and in the dimensionless time scale introduced in (2.7) it will be

$$\theta_{\text{det}} = \int_0^1 \frac{dq}{f(q)} \quad (2.10)$$

so that in the original time units $T_{\text{det}} = \theta_{\text{det}} / 4k'_{1a}\alpha$.

From a comparison of this theoretical result with what would be its experimental counterpart, $T_{\text{det}}|_{\text{exp}}$, one can estimate the existing relation between the time scale associated with the dynamics of our model equation (2.8) and the experimental time scale. This is done here by assuming that the appropriate experimental quantity to be compared with the deterministic value θ_{det} is the measured reaction time in the limit of very high stirring rates. In doing so, and without any other reference to more elaborated arguments, we simply invoke the fact that both, the deterministic limit in our theoretical scheme and the limit of very rapid stirring, should be comparable since both are expected to predict a negligible random behavior of the chemical process. This time scale normalization will become indispensable whenever we want to compare our results with the experimental ones. This is not completely surprising in view of the inherent limitations of a description based on the dynamical equation (2.8). First of all, we must keep in mind that we are only considering a very initial phase of the overall chemical reaction, whereas in the real experiments the reaction times correspond to the subsequent disappearance of iodine formed during this first step of the process.

Secondly, at very low iodide concentrations, i.e. for $q \rightarrow 1$, the inverse dependence of the k_{1b} term on $[I^-]$ should be certainly questioned.⁷ Finally, let us mention that in much more refined studies of the reaction mechanism,^{6a} some discrepancies between the observed and calculated time scales were also found, indicating that probably some details of the chemical mechanism of this reaction still remain to be completely clarified.

III. STOCHASTIC MODEL

In this section we essentially follow the ideas already introduced in Ref. 3. There our position was that stirring effects would probably be the main responsible for the observed randomness in the behavior of these chemical systems. In other words, our idea was that purely chemical effects and transport phenomena mediated by stirring should no longer be considered as independent in systems non ideally mixed, but rather stirring effects could influence the set of the somewhat averaged rate constants regulating the successive steps of the global chemical process. This in turn led us to propose the use of a Langevin dynamics with a multiplicative noise as an appropriate framework to model this sort of chemical irreproducibility. Here we will adapt this argument to the much more realistic kinetic law given by (2.4).

In absence of initial iodine concentration the kinetics specified by (2.4) is initially dominated by the mass action-like

contribution specified by the rate constant k_{1a} . However, the most important nonlinearity of the model, and, as stated in section II.A, the term that seems to be more directly related to the observed peculiar behavior of the reaction, is the autocatalytic contribution regulated by the rate constant k_{1b} . In this sense, we will assume that a stochastic force is introduced in our deterministic scheme (2.6) by letting k'_{1b} fluctuate around a prescribed mean value, according to

$$k'_{1b} \longrightarrow k'_{1b} + \mu(t) \quad (3.1)$$

Certainly the arguments we presented at the beginning of this section, in order to explain the possible origins of noise sources as the combined effect of both chemical and transport processes, would apply irrespectively to either one of two rate constants in (2.4). However, for the sake of simplicity of the model we discriminate the k_{1a} term as a noise source on the basis of the higher nonlinearity associated with the k_{1b} supercatalytic contribution to the initial kinetics of the chemical reaction. In addition we just point out that preliminary calculations performed on an earlier version of the model that incorporated noise terms through k_{1a} predicted results that from a quantitative point of view were far less significant than those that will be presented in section IV based on the hypothesis (3.1).

Introducing (3.1) into (2.6) the concentration variable $x(t)$ no longer evolves deterministically but rather in a stochastic way, according to a Langevin equation given by

$$\frac{dx}{dt} = k'_{1a}(\alpha-x)(\beta-4x) + k'_{1b}\frac{x(\alpha-x)}{(\beta-4x)} + \frac{x(\alpha-x)}{(\beta-4x)} \mu(t) \quad (3.2)$$

As was done in Ref. 3 we prescribe a Gaussian δ -time correlated statistics for the noise term $\mu(t)$

$$\langle \mu(t)\mu(t') \rangle = 2D \delta(t-t') \quad (3.3)$$

The dimensionless version of Eqs. (3.2) and (3.3) are

$$\frac{dq}{d\theta} = f(q) + \frac{q(1-\beta'q)}{\beta'(1-q)} \phi(\theta) \quad (3.4)$$

and

$$\langle \phi(\theta)\phi(\theta') \rangle = 2D' \delta(\theta-\theta') ; \quad D' \equiv \frac{D}{64k'_{1a}\alpha} \quad (3.5)$$

Equation (3.4), written in terms of the multiplicative noise $\phi(\theta)$, is the central equation we will use in the remainder of this paper. Let us express it in a much more generic way as

$$\frac{dq}{d\theta} = f(q) + g(q)\phi(\theta) ; \quad g(q) \equiv \frac{q(1-\beta'q)}{\beta'(1-q)} \quad (3.6)$$

The analysis that follows is mainly devoted to the evaluation of two basic dynamical quantities which to our understanding are the most relevant ones when trying to compare the results predicted in our model with those of the experiments. First of all, we calculate the mean first passage time (MFPT), T_1 (θ_1 in the dimensionless version). This will be directly compared with the averaged reaction time for the experiments with the chlorite-iodide reaction. In addition, and in order to better represent the actual degree of irreproducibility of the chemical process, we will evaluate the second moment of the distribution of passage times, noted T_2 (θ_2 in the dimensionless version). This will enable us to readily evaluate the variance of this distribution, easily compared with its experimental counterpart extracted from the reaction time records. Obviously, the distribution of reaction times, and its corresponding moments, are defined in relation to a particular choice of the starting and exit points of the stochastic trajectories evolving according to Eq. (3.6). In our treatment here, the starting point will correspond to the initial condition for the chemical kinetics, i.e. $q=0$, in absence of any initial iodine concentration. On the other hand, the escape value will be arbitrarily chosen here as $q=1$ corresponding to the previously identified condition for the completion of the initial kinetics (2.1). We believe that this arbitrariness, actually hard to circumvent, may be however properly compensated with the previously introduced time scale normalization procedure.

The equations satisfied by the first two moments of the distribution of passage times for stochastic trajectories starting at an arbitrary point q are respectively¹⁰ ($g'(q) \equiv dg/dq$)

$$D'g^2(q) \frac{d^2}{dq^2} \theta_1(q) + [f(q) + D'g(q)g'(q)] \frac{d}{dq} \theta_1(q) = -1 \quad (3.7)$$

$$D'g^2(q) \frac{d^2}{dq^2} \theta_2(q) + [f(q) + D'g(q)g'(q)] \frac{d}{dq} \theta_2(q) = -2\theta_1(q) \quad (3.8)$$

According to our prescriptions, they will be solved for $q=0$ with boundary conditions $\theta_1(q=1)=\theta_2(q=1)=0$. The last equation is readily transformed using (3.7) to an equation for the variance $(\Delta\theta)^2(q) = \theta_2(q) - \theta_1^2(q)$,

$$\begin{aligned} D'g^2(q) \frac{d^2}{dq^2} (\Delta\theta)^2(q) + [f(q) + D'g(q)g'(q)] \frac{d}{dq} (\Delta\theta)^2(q) \\ = -2D'g^2(q) \left[\frac{d\theta_1(q)}{dq} \right]^2 \end{aligned} \quad (3.9)$$

A particular solution for $\theta_1(q)$ and $(\Delta\theta)^2(q)$ is obtained integrating formally (3.7) and (3.9). When specialized to $q=0$ these solutions read

$$\theta_1 \equiv \theta_1(q=0) = \int_0^1 dq \left[1 + \frac{D'g^2 d/dq}{f + D'gg'} \right]^{-1} \left[\frac{1}{f + D'gg'} \right] \quad (3.10)$$

$$\begin{aligned}
 (\Delta\theta)^2 &\equiv (\Delta\theta)^2(q=0) = \\
 &= \int_0^1 dq \left[1 + \frac{D'g^2d/dq}{f + D'gg'} \right]^{-1} \left[\frac{g^2(d\theta_1/dq)^2}{f + D'gg'} \right]
 \end{aligned} \tag{3.11}$$

An exact solution of equations (3.10) and (3.11) is out of our reach. Consequently we have adopted the same strategy already proposed in our previous paper³. It consists in converting (3.10) and (3.11) into a series development in powers of the assumed small parameter D' . In addition we determine θ_1 and $(\Delta\theta)^2$ via computer simulations¹¹ of the stochastic dynamics specified by (3.6). Obviously, both the analytical and computer evaluated results have to coincide in the limit of very small values of D' . The lowest orders contributions to θ_1 and $(\Delta\theta)^2$ respectively read

$$\begin{aligned}
 \theta_1 &= \int_0^1 dq \frac{1}{f(q)} - \frac{1}{2} D' \int_0^1 dq \frac{d}{dq} \left(\frac{g}{f} \right)^2 + O(D'^2) \\
 &= \theta_{\text{det}} - \frac{1}{2} \frac{D'}{k'^2} + O(D'^2)
 \end{aligned} \tag{3.12}$$

and

$$(\Delta\theta)^2 = 2D' \int_0^1 dq \frac{g^2(q)}{f^3(q)} + O(D'^2) \tag{3.13}$$

The integrals left in (3.12) and (3.13), and those corresponding to higher orders in D' , may be solved using standard numerical integration routines.

IV. ANALYTICAL AND SIMULATION RESULTS

In this section results will be obtained corresponding to our stochastic model of the kinetics of the chlorite-iodide reaction and they will be further compared with those obtained by Nagypál and Epstein.² Essentially, three different parameters were tested in those experiments: volume of the reaction mixture, stirring rate, and initial iodide concentration. In this way several series of approximately 50 repeated measurements were obtained by keeping fixed two of the previous parameters and varying the remaining one.

In our formulation here we do not consider as completely independent parameters those corresponding to the sample volume and the stirring rate. Indeed, we believe that the intensity of the stochastic forces, or in other words the degree of randomness, should be actually related to some sort of mixing efficiency that would eventually depend on both stirring rates and volume of the reaction vessel. Thus, in all what follows we will essentially concentrate in analyzing the results corresponding to measurements performed with a fixed volume, $V=9\text{cm}^3$, and initial chlorite concentration, $[\text{ClO}_2^-]=5 \cdot 10^{-3}\text{M}$, whereas the stirring rate and the initial iodide concentration are viewed as variable parameters.

A. Dependence on stirring rates

The first set of presented results are those corresponding to different stirring rates. Values of T_1 and ΔT are obtained for different values of D while keeping fixed the initial iodide concentration to the experimental value $[I^-] = 6.666 \cdot 10^{-4} M$. The dimensionless results obtained either analytically or via simulations are summarized in Fig.1. Before going to a more explicit comparison with the experiments, let us note that according to Fig.1, the averages of the first passage times increase in going to smaller values of the noise intensity, whereas their variances, contrarily, decrease. Both behaviors are easily understood. The variances $(\Delta T)^2$ directly measure the degree of randomness, here introduced through the noise terms of intensity D . On the other hand, the presence of a multiplicative noise, results, as was mentioned in Ref. 3, in a positive modification of the deterministic rate constant k' . This in turn leads to negative contributions to the first passage times with respect to their deterministic values.

The central question that yet remains to be solved consists in relating our model parameter D with the experimental stirring rate. To this end, and since we do not have available more fundamental arguments, we can only aim at directly comparing our theoretical results with those of the experiments. This procedure is here carried out in terms of the relative quantity $\Delta\theta/\theta_1$ instead of using separately either one of the two computed moments θ_1 or $\Delta\theta$. In passing we note that by referring to this relative quantity, we do not need to use any time scale normalization. In Fig. 2 we

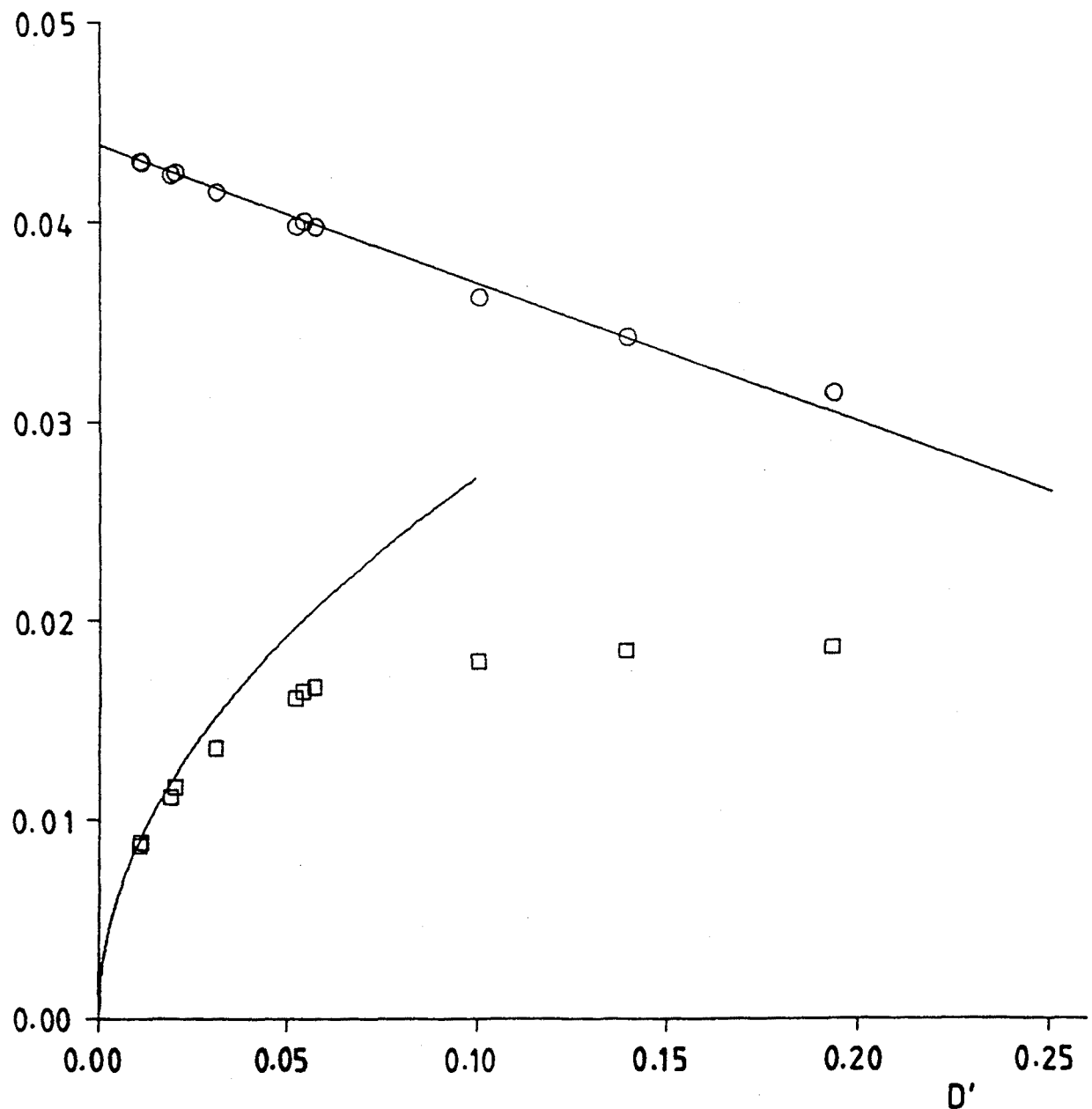


Fig. 1.: Theoretical results for θ_1 and $\Delta\theta$ versus noise intensity D' for a fixed initial concentration $[I^-] = 6.666 \cdot 10^{-4} M$ ($\beta' = 0.03333$). Solid lines correspond to the analytical approximations given by (3.12) and (3.13). Simulation results of the Langevin dynamics (3.4,5) are represented by circles for θ_1 and squares for $\Delta\theta$.

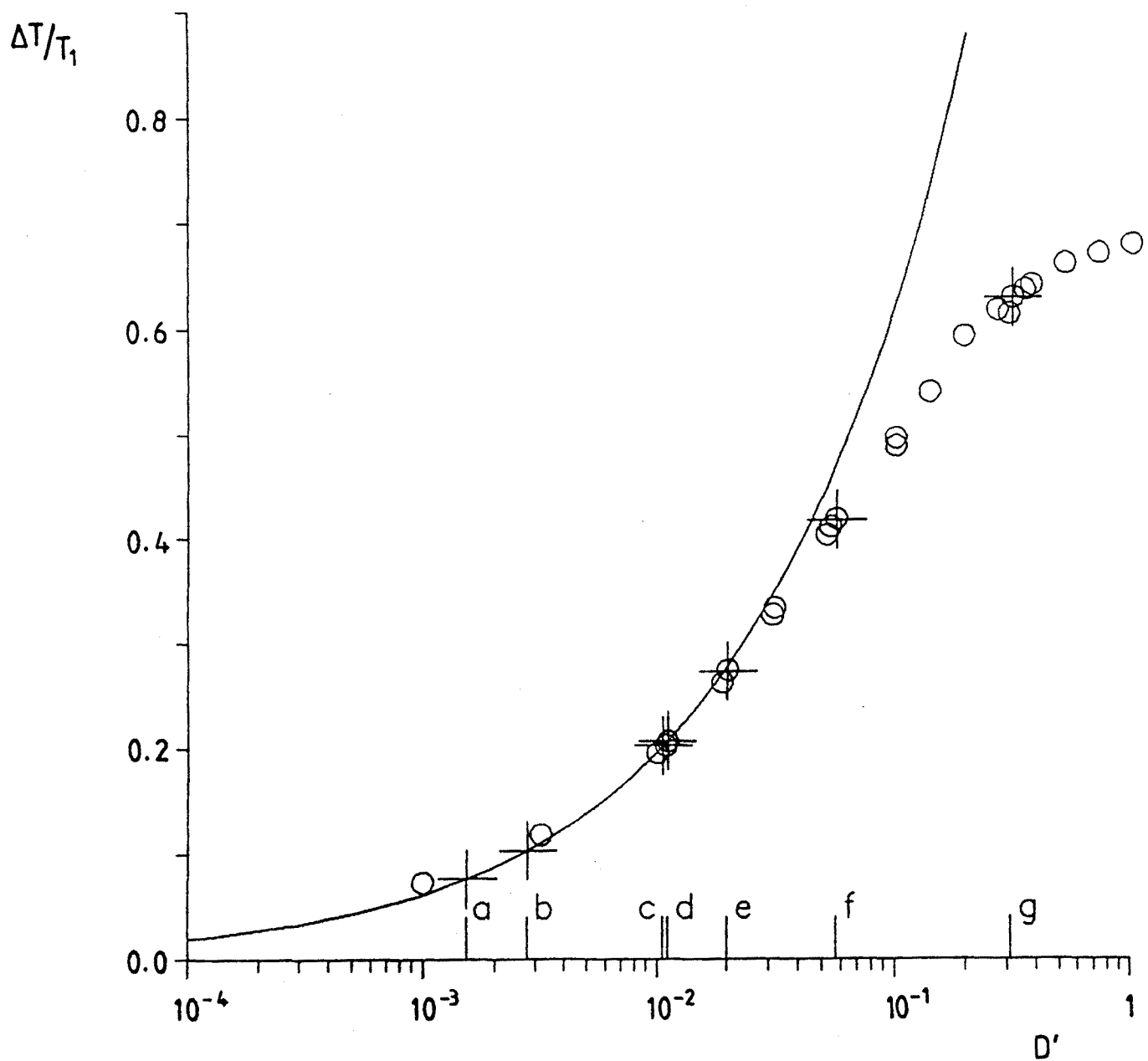


Fig. 2.: Results for $\Delta T/T_1$ versus the noise intensity D' for a fixed initial concentration $[I^-] = 6.666 \cdot 10^{-4} M$ ($\beta' = 0.03333$). The solid line correspond to analytical results. Circles stand for simulation results. The crosses correspond to experimental data for different stirring rates (rpm): a=1450, b=1100, c=850, d=750, e=650, f=570 and g=500.

plot in a semilogarithmic scale both analytical and simulation results for $\Delta\theta/\theta_1$ corresponding to different values of D' . The experimental data for stirring rates comprised between 500 rpm and 1450 rpm, are also shown. By directly looking at this figure we can estimate the actual values of D' corresponding to the set of experimental stirring rates. Once this procedure has been completed, individual values of θ_1 and $\Delta\theta$ are easily evaluated. By finally converting them into the experimental time scale through the normalization factor $T_{det}|_{exp}/\theta_{det}$, we can directly compare our predictions with laboratory measurements as is done in Table I. The results corresponding to the four first rows correspond to simulation results whereas those corresponding to the last three ones were obtained with the small D' expansion.

We notice that theoretical and experimental results compare better in the limit of high stirring rates or equivalently low D' values, but even in the opposite limit of considerably large values of D' , the discrepancies for either the averaged reaction times or their standard deviations are at most of the order of a 20%. At this point it is worth noting that the statistics provided by the experimental measurements is rather poor obviously due to the limited set of data available. With fifty exactly replicated experiments the statistical errors in the averaged values of T_1 or ΔT may be as large as a 10%. On the contrary, these statistical errors are minimized in our simulation procedure by performing our statistics over sets of up to 10^4 stochastic trajectories. This

results in statistical errors with an upper bound of a 0.6% in T_1 and 1% in ΔT .

Finally we deduce from Fig.2 that, as expected, the intensity of the noise terms in our model and the stirring rate are inversely correlated. Speculative fits suggest an inverse power relation $D' \sim (\text{stirring rate})^{-\alpha}$, although this can only be viewed, at this point, as a mere conjecture that should be tested for other systems and experimental conditions.

B. Dependence on iodide concentration

Once the estimation of the values of the noise intensity corresponding to the different stirring rates has been completed, the model does not have any other adjustable parameter. Therefore, the consistency of our whole theoretical scheme may be further checked by analyzing the results obtained for different initial iodide concentrations at a fixed stirring rate. To compare with experimental data we refer to series of measurements performed with the stirring fixed at 850 rpm and initial iodide concentration ranging from $3.333 \cdot 10^{-4} M$ to $2.5 \cdot 10^{-2} M$. Experimental and analytical results ($D' = 1.06 \cdot 10^{-2}$) are summarized in Table II.

From these results we can immediately see that the theoretical and experimental estimations of T_1 and ΔT agree in predicting larger values of both quantities when β' increases. However in order to better see the effect of the iodide concentration on the randomness of the reaction, we refer again to the relative quantity $\Delta T/T_1$. Both the experimental and theoretical results predict the

Table 1.- Theoretical and experimental values for T_1 and ΔT corresponding to a fixed initial iodide concentration $[I^-] = 6.666 \cdot 10^{-4} M$ ($\beta' = 0.03333$) for different stirring rates. Times are expressed in seconds.

St. (rpm)	D'	$T_1(s)$	$\Delta T(s)$	$T_1 _{exp}(s)$	$\Delta T _{exp}(s)$
500	$3.1 \cdot 10^{-1}$	103.7	65.3	80.1	50.4
570	$5.70 \cdot 10^{-2}$	154.2	64.6	112.3	46.9
650	$2.00 \cdot 10^{-2}$	164.7	45.2	143.2	39.2
750	$1.11 \cdot 10^{-2}$	167.0	35.3	145.8	30.3
850	$1.06 \cdot 10^{-2}$	167.1	34.5	148.3	30.1
1100	$2.77 \cdot 10^{-3}$	169.3	17.6	169.0	17.5
1450	$1.53 \cdot 10^{-3}$	169.6	13.1	170.4	13.1

Table 2.- Theoretical and experimental results for T_1 and ΔT corresponding to a fixed stirring rate of 850 rpm ($D' = 1.06 \cdot 10^{-2}$) for different initial iodide concentrations.

$[I^-](M)$	β'	$T_1(s)$	$\Delta T(s)$	$T_1 _{exp}(s)$	$T _{exp}(s)$
$3.333 \cdot 10^{-4}$	0.01667	97.9	26.7	81.7	9.1
$6.666 \cdot 10^{-4}$	0.03333	167.1	34.5	148.3	30.1
$1.333 \cdot 10^{-3}$	0.06667	279.5	43.1	298.4	45.9
$3.333 \cdot 10^{-3}$	0.16667	533.6	55.8	572.0	77.8

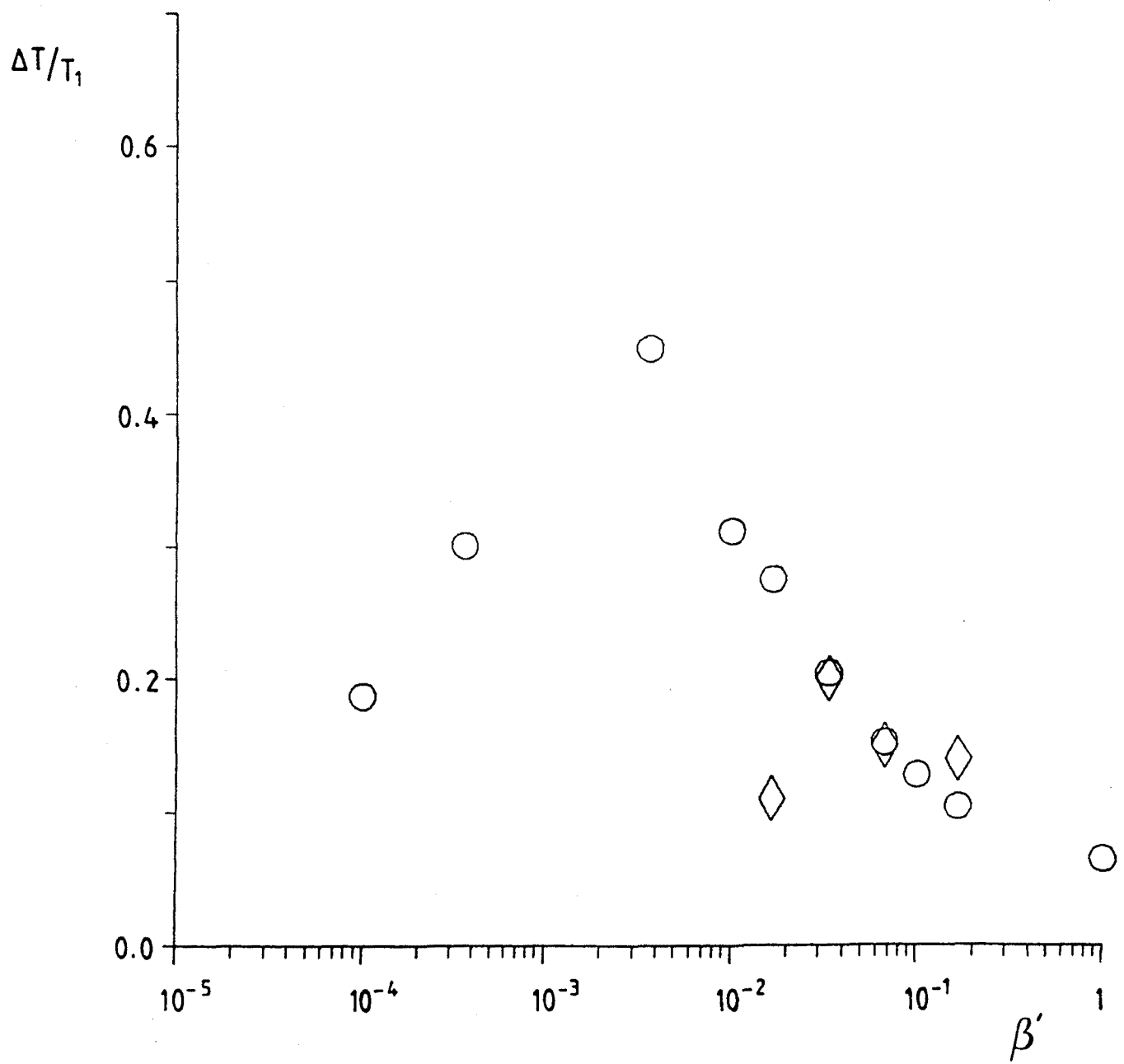


Fig. 3.: Results for $\Delta T/T_1$ versus initial iodide concentration β' for a fixed stirring rate of 850 rpm ($D' = 1.06 \cdot 10^{-2}$). Circles stand for theoretical results and diamonds correspond to experimental date.

appearance of a maximum at an intermediate value of β' , as it is shown in Fig. 3. The position of such a maximum differs however by nearly an order of magnitude in comparing our theoretical predictions with the results of the experiments.

V. CONCLUSIONS

The experimental observed randomness of the chlorite-iodide reaction has been analyzed in terms of a theoretical model based on the use of a stochastic differential equation with multiplicative noise. Results for both the averaged reaction times and their standard deviations are computed and analyzed in terms of two basic experimental parameters: the stirring rate and the initial iodide concentration. With respect to the influence of stirring, our results predict, in accordance with experiments, larger reaction times and smaller variances as the stirring rates increase. In regard to the dependence on the initial iodide, a maximum of the relative standard deviation at an intermediate value is found in the experiments that is also predicted in our model. From a quantitative point of view the comparison between theoretical and experimental results would certainly improve if we could overcome the present limitations either due to the reduced set of experimental data available or coming from the simplified version of the chemical kinetics here used. In any case the use of Langevin

equations appear to be a promising step further to analyze this sort of random chemical behavior.

REFERENCES

- 1 I. Nagypál and I.R. Epstein, J. Phys. Chem. 90, 6285 (1986).
- 2 I. Nagypál and I.R. Epstein, J. Chem. Phys. 89, 6925 (1988).
- 3 F. Sagués and J.M. Sancho, J. Chem. Phys. 89, 3793 (1988).
- 4 G. Nicolis and F. Baras, J. Stat. Phys. 48, 1071 (1987).
- 5 J. Hofrichter, J. Mol. Biol. 189 553 (1986).
- 6 a) I.R. Epstein and K. Kustin, J. Phys. Chem. 89, 2275 (1985).
 b) Gy. Rabai and M.T. Beck, J. Phys. Chem. 90, 2204 (1986).
 c) O. Citri and J.R. Epstein, J. Phys. Chem. 91, 6034 (1987).
- 7 As is discussed in Ref. 2 the rate law (3) should be slightly modified with respect to the $[I^-]$ dependence, since the k_{1b} term would indefinitely increase as $[I^-]$ decreases. The minimal modification commonly proposed in the literature consists in replacing $1/[I^-]$ by $1/([I^-]+c)$, so that the I^- inverse catalysis is only significant for iodide concentrations larger than c .
- 8 D.M. Weitz and I.R. Epstein, J. Phys. Chem. 88, 5300 (1984).
- 9 J. Boissonade and P. de Kepper, J. Chem. Phys. 87, 210 (1987).
- 10 N.G. Van Kampen, Stochastic Processes in Physics and Chemistry (North Holland, Amsterdam, 1981); C.W. Gardiner, Handbook of Stochastic Methods for Physics, Chemistry and the Natural Sciences, Springer Series in Synergetics, vol.13 (Springer Verlag, Berlin, 1983).
- 11 J.M. Sancho, M. San Miguel, S.L. Katz and J.D. Gunton, Phys. Rev. A 26, 1589 (1982).



UNIVERSITAT DE BARCELONA



Biblioteca de Física i Química
